NASA

Technical Memorandum 79612

Greenbelt Community Project: Solar Energy Retrofit for a Multi-Family Dwelling

E. W. Hymowitz, R. J. Hannemann, L. L. Millman, and J. E. Pownell

JUNE 1978

National Aeronautics and Space Administration

Goddard Space Flight Center
Greenbelt, Maryland 20771

TM 79612

GREENBELT COMMUNITY PROJECT:

SOLAR ENERGY RETROFIT

FOR A

MULTI-FAMILY DWELLING

by

E. W. Hymowitz, R. J. Hannemann,*

L. L. Millman, and J. E. Pownell

June 1978

GODDARD SPACE FLIGHT CENTER
Greenbelt, Maryland

*Hannemann Engineering Services
Upper Marlboro, Maryland 20870

GREENBELT COMMUNITY PROJECT: SOLAR ENERGY RETROFIT FOR A MULTI-FAMILY DWELLING

E. W. Hymowitz, R. J. Hannemann,

L. L. Millman, and J. E. Pownell

ABSTRACT

As a result of the energy crisis of 1973-74 a cooperative project was initiated between Goddard Space Flight Center and the nearby community of Greenbelt, Maryland. The purpose was to design, install and operate an experimental solar heating system on a group of four tandem town houses. The system was successfully developed and is now operating. This report describes the design, installation, system operation and performance as well as the important consideration's for judging the economic feasibility of solar heating systems.

GREENBELT COMMUNITY PROJECT:

SOLAR ENERGY RETROFIT FOR

A MULTI-FAMILY DWELLING

E. W. Hymowitz, R. J. Hannemann,

L. L. Millman, and J. E. Pownell

FOREWORD

Federal agencies have missions assigned to them. Mission boundaries are usually quite sharply defined, and they are rarely traversed. But it does happen—sometimes events and conditions combine to create a situation which represents an irresistable opportunity. That is what happened in the winter of 1973-74. The energy crisis, available technology, Goddard's professional and community interests, Greenbelt's expressed needs and nearness to Goddard Space Flight Center—put them all together and you have an opportunity for action which was appropriate, but non-traditional, for GSFC. Fortunately, the opportunity was not wasted—hence, the origin of the Greenbelt Community Project.

The success of a project depends in large measure on the quality of leadership it enjoys. The Greenbelt Project—of unaccustomed origin, non-space in nature, community-service oriented—put a particular premium on dedicated, enlightened leadership. And that is what Emil Hymowitz, Project Manager, provided. He, like those whose help he enlisted, took on the project in addition to regular duties, donated many hours of uncompensated effort, and successfully fought numerous difficult administrative and technical battles. The successful

completion of the Greenbelt Project is largely the result of Emil's commitment of mind and heart.

H. J. Peake

There were numerous participants in the Greenbelt Project in addition to the authors. They represented Greenbelt Homes, Inc., University of Maryland, and Goddard Space Flight Center. The contributions of the following people are gratefully acknowledged:

George E. Kowalski
Stephen L. Sargent
Robert K. Collier, Jr.
James W. Smith
Royal D. Breashears
Dean D. Mulder
George E. Craft
Leslie M. Meredith
Harold J. Peake
John B. Webb
James W. Woods, Jr.
Forest H. Wainscott, 2D
Walter S. Glazar
Charles J. Falkenhan
Frederick C. Gross
Elaine R. Bobbitt
Carol A. Sigler
Laura Schallmo
Donald E. Witten
Henry O. Obler
Charles G. Dan, Jr.
William A. Leary
Samuel E. Willis
Hugh B. O'Donnell
Joseph A. Muller
Norman Ackerman
James J. Webb
Paul S. Caruso, Jr.
Curtis E. Cullison

E. W. Hymowitz

Table of Contents

List of Tables and Figures

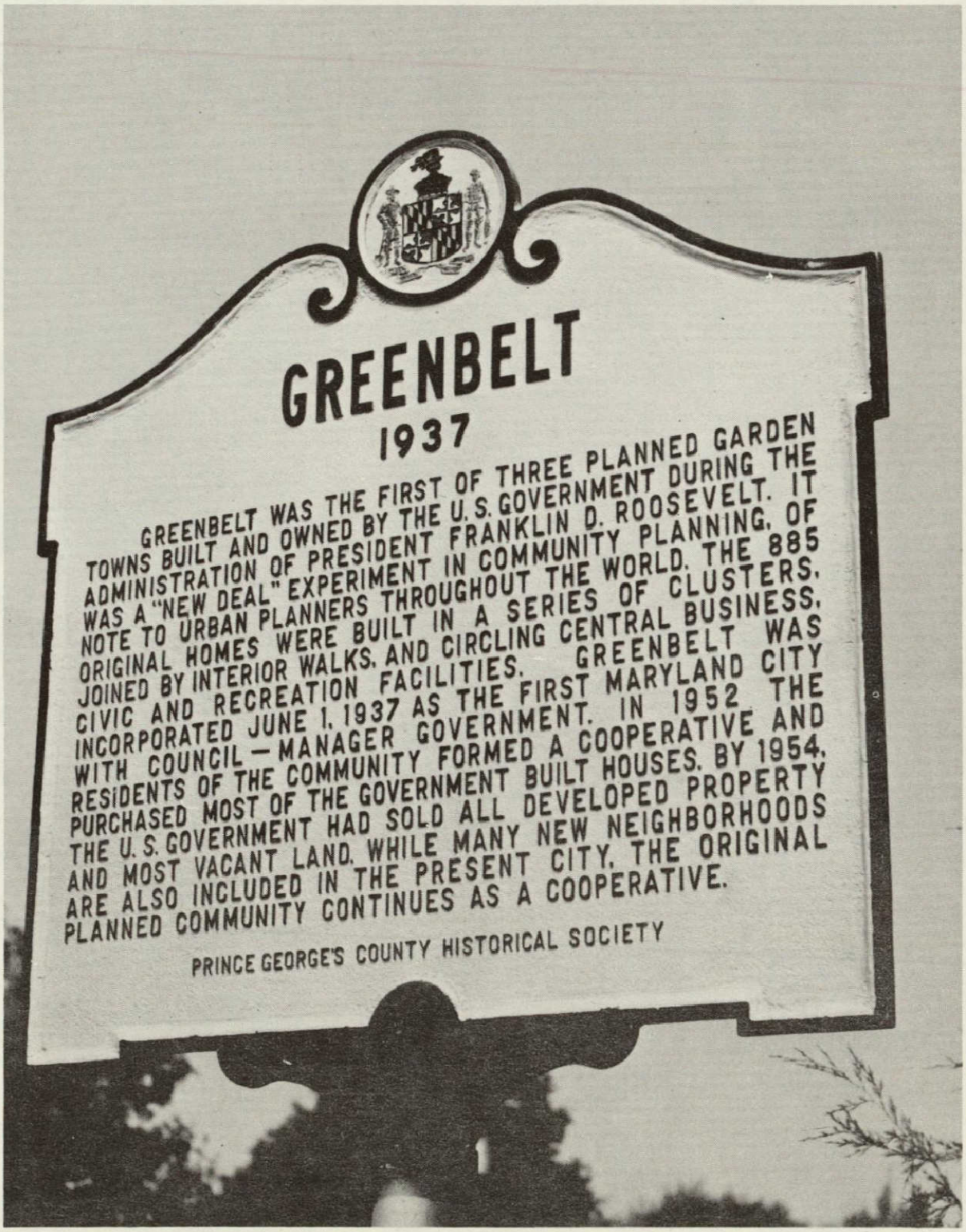

GREENBELT COMMUNITY PROJECT:
SOLAR ENERGY RETROFIT FOR
A MULTI-FAMILY DWELLING

I. Introduction

A. The Greenbelt Community

In 1935 during the first administration of Franklin D. Roosevelt the Congress authorized the Resettlement Administration to design and build three new American towns. They were planned to achieve the age-old concept of a total community, with added emphasis on sufficient green space and community facilities. In addition to Greenbelt, Maryland, the other towns authorized were Greendale, Wisconsin, and Greenhills, Ohio.

The original Greenbelt community of brick and masonry homes totaled 574 and was opened for occupancy in 1937. An additional 1000 frame homes were authorized during World War II. The plan of the community is shown in Figure 1. The Government sold the homes, all facilities, and 700 acres of land to Greenbelt Homes, Inc. (GHI) in 1953. GHI is a cooperatively managed corporation, which owns the homes jointly with the occupant-owners and provides maintenance and heating on a pro-rata basis. GHI is managed by a President and Board of Directors elected by the owner-members.

The conceptual realization of this planned community, now over 40 years old, has been recognized from the beginning. Greenbelt has been visited frequently through the years by architects and urban planners.

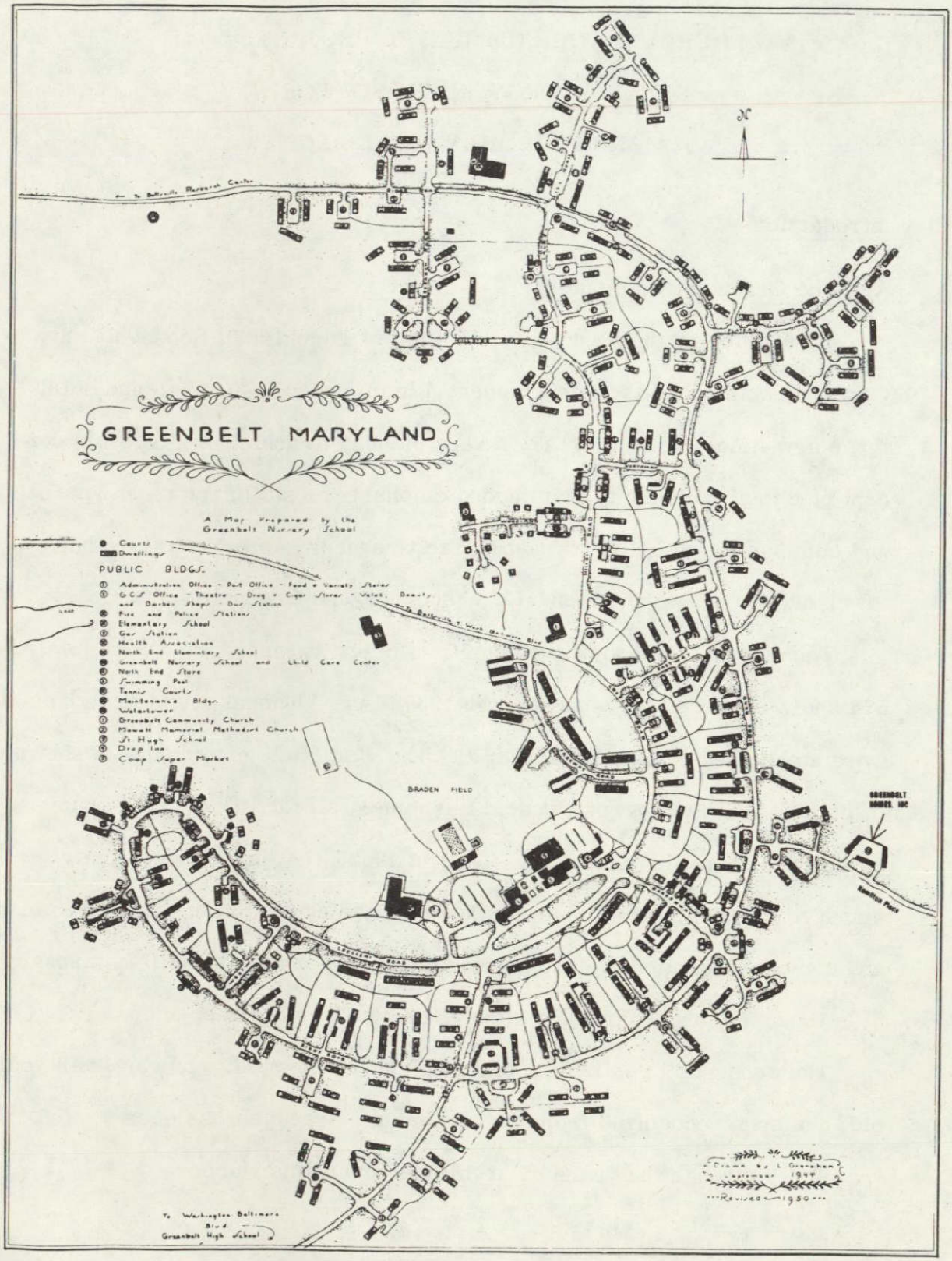

Figure 1. Plan Sketch of Greenbelt Community

energy source for the existing oil-fired hot water heating system. The analysis indicated that here also savings of the order of 20 percent to 25 percent were possible for an overall savings of 40 percent to 50 percent when using both added insulation and solar augmentation.

A proposal in the form of a project plan was issued by the committee in August 1974. This served as the basis for further discussion and in February 1975 resulted in the signing of an agreement between Greenbelt Homes, Inc. and the Goddard Space Flight Center to initiate a project which would have two phases, the first phase consisting of two tasks:

(1) The instrumentation of two selected masonry and two brick four-unit dwellings to measure heat loss and fuel consumption, and,

(2) The installation of selected non-solar related fuel conservation measures to the above dwellings (i.e. storm windows and doors).

Assuming Phase I was completed satisfactorily, the project participants might then undertake a second phase that would carry through the installation of solar energy systems.

It was also considered that because of the similarity of the original Greenbelt homes, which are basically of two types, economies of scale could be realized if it were decided to install the same solar energy system on additional homes.

C. Project Implementation

The active phase of the project began on February 11, 1975, with the signing of a Cooperative Agreement between the Director of the Goddard Space Flight Center (GSFC) and the President of Greenbelt Homes Incorporated (GHI). The NASA Project Manager then formed a Working Group

of GSFC and GHI engineers and undertook the solar energy system design and development.

By May the design had progressed sufficiently to conduct a design review which was attended by specialists from Goddard and outside. Some suggestions made during the review were incorporated into the system design.

The procurement of system components was carried out during the summer of 1975. Custom-made casement type storm windows and storm doors were installed on one masonry and one brick type building during the summer. At this time the decision was made to proceed with the installation of a solar energy system on the masonry building only rather than on both masonry and brick buildings. This somewhat reduced the scope, cost and complexity of the task. In addition, the masonry building was easier to work with because of the flat roof (as opposed to the pitched roof of the brick building).

During the fall the roof trusses were installed and the collector panels mounted and coupled together. It was then necessary to join together the various system components (valves, pumps, tanks, etc.). These were installed in the mechanical room containing the central heating system for the building. Due to a shortage of labor available to the project this task completion was delayed until late spring of 1976.

Through the summer of 1976 project engineers experimented with the complete installation and developed a breadboard control system. During this time almost all hot water needs of the four-family building were met by the solar system. Based on the experience gained with the system during

this period, a commercial grade control system was designed, built and installed during late 1976 and early 1977.

By the end of February 1977 the system was fully operational. In parallel with the above development and installation, a data acquisition system, consisting of thermocouples and other sensors was installed at key points throughout the solar energy system, the solar energy building living space, and the identical unmodified control building. In all, approximately 65 temperatures, valve or motor state conditions, and solar insolation can be continuously monitored and recorded.

II. System Design

A. Environmental Description

Greenbelt, location 39° 00.3' N, 76° 52.6' W, is subject to a temperate continental climate, warm summer subtype DCA according to the Trewartha classification system [1]. This climate is characterized by warm to hot summers with relatively cold winters.

Temperature extremes show a definite seasonal symmetry. Mean daily maximum summer temperatures reach 30.6°C (87°F) while mean daily minimum winter temperatures may be as low as -1.4°C (29.4°F). On the average, there are 176 days between the last freeze of the spring and the first freeze of the fall. Temperature data is given in Table 1 and illustrated in Figure 2. A pertinent indication of winter climatic severity is the average number of heating degree days; monthly data is shown in Figure 3. (Note that the data is presented in the conventional fashion: °F-days referenced to 65°F.) The average annual heating degree day total is about 4400.

Table 1. Environmental Temperature Data

(Mean daily maximum and minimum temperatures)

Month	Mean Daily Maximum		Mean Daily Minimum	
	F	C	F	C
January	44.3	6.8	29.5	-1.4
February	46.1	7.8	29.4	-1.4
March	53.8	12.1	35.8	2.1
April	65.8	18.8	45.6	7.6
May	75.5	24.2	56.0	13.3
June	83.4	28.6	64.9	18.3
July	87.0	30.6	69.3	20.7
August	85.0	29.4	67.9	19.9
September	78.6	25.9	60.7	15.9
October	68.3	20.2	49.6	9.8
November	56.5	13.6	38.9	3.8
December	45.6	7.6	30.5	-0.8

Monthly wind speed and direction are shown as Figure 4. Winds are generally moderate and show limited seasonal variation. Prevailing winds are 9.5 mph from a southerly direction.

No significant seasonal concentration of precipitation can be noted. Mean annual precipitation is 43.5 inches; snowfall is moderate, with an average of 18.7 inches per year. Detailed precipitation data is given in Figure 5.

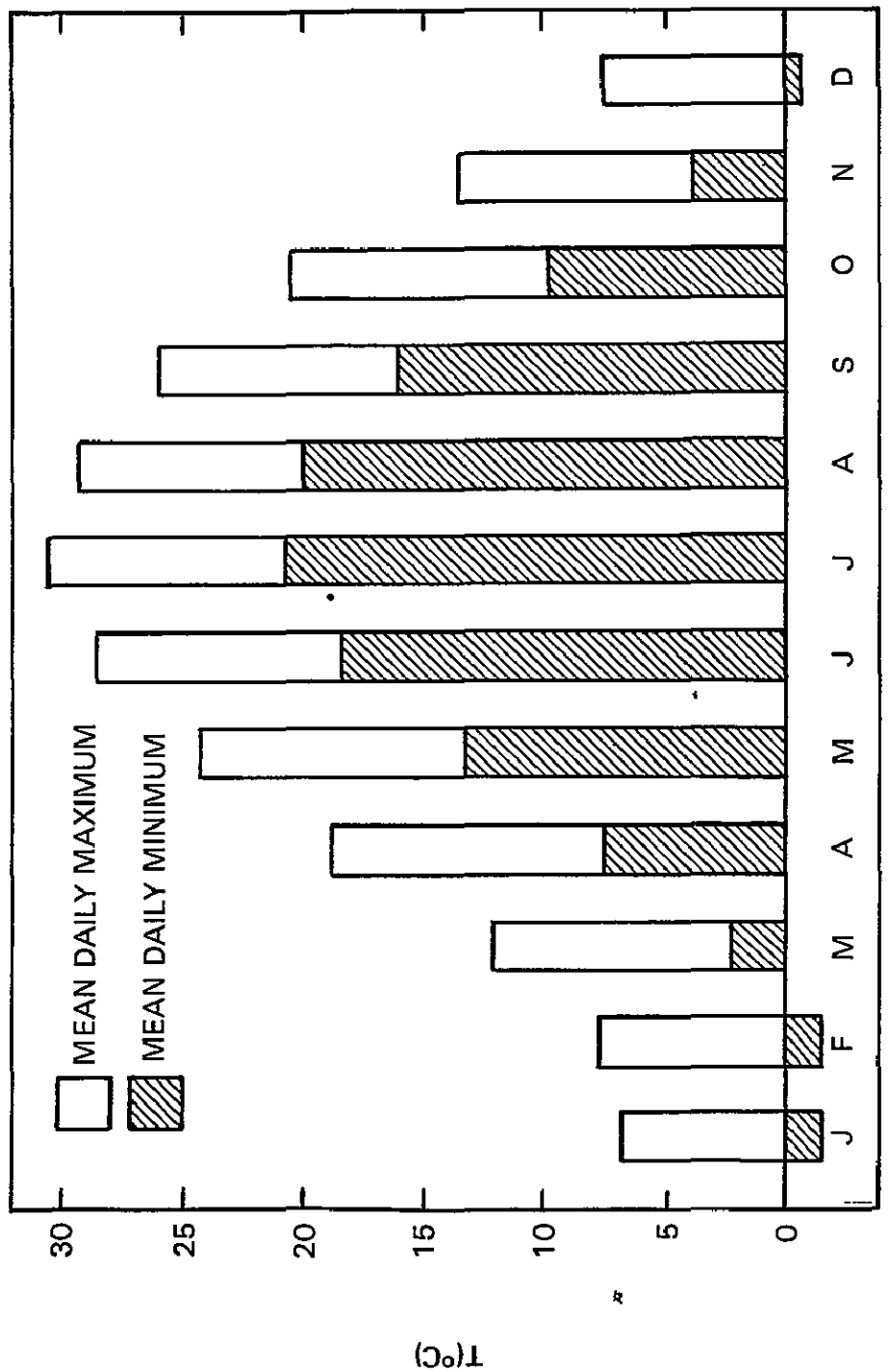

Figure 2. Mean Daily Maximum and Minimum Temperatures (Wash. Nat. Airport) [2]

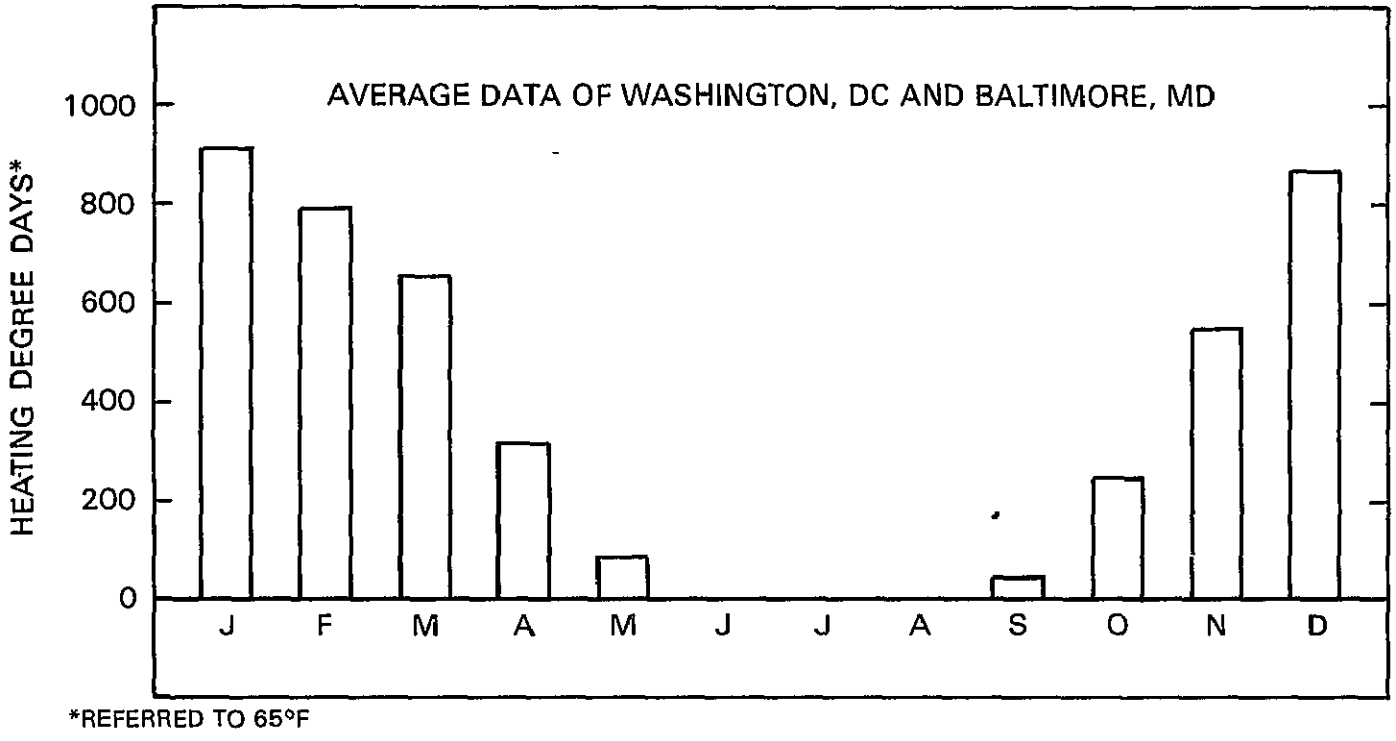

Figure 3. Mean Monthly Heating Degrees Days [3]

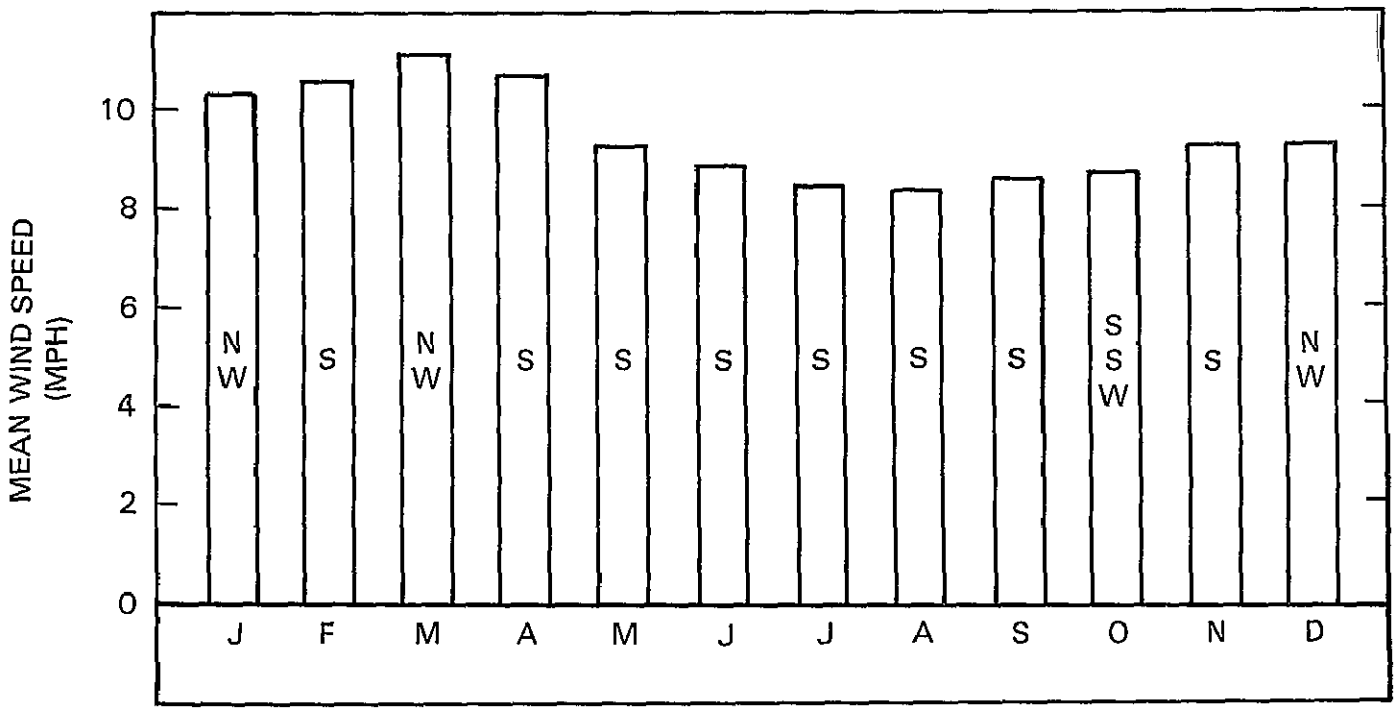

Figure 4. Mean Wind Environment [4]

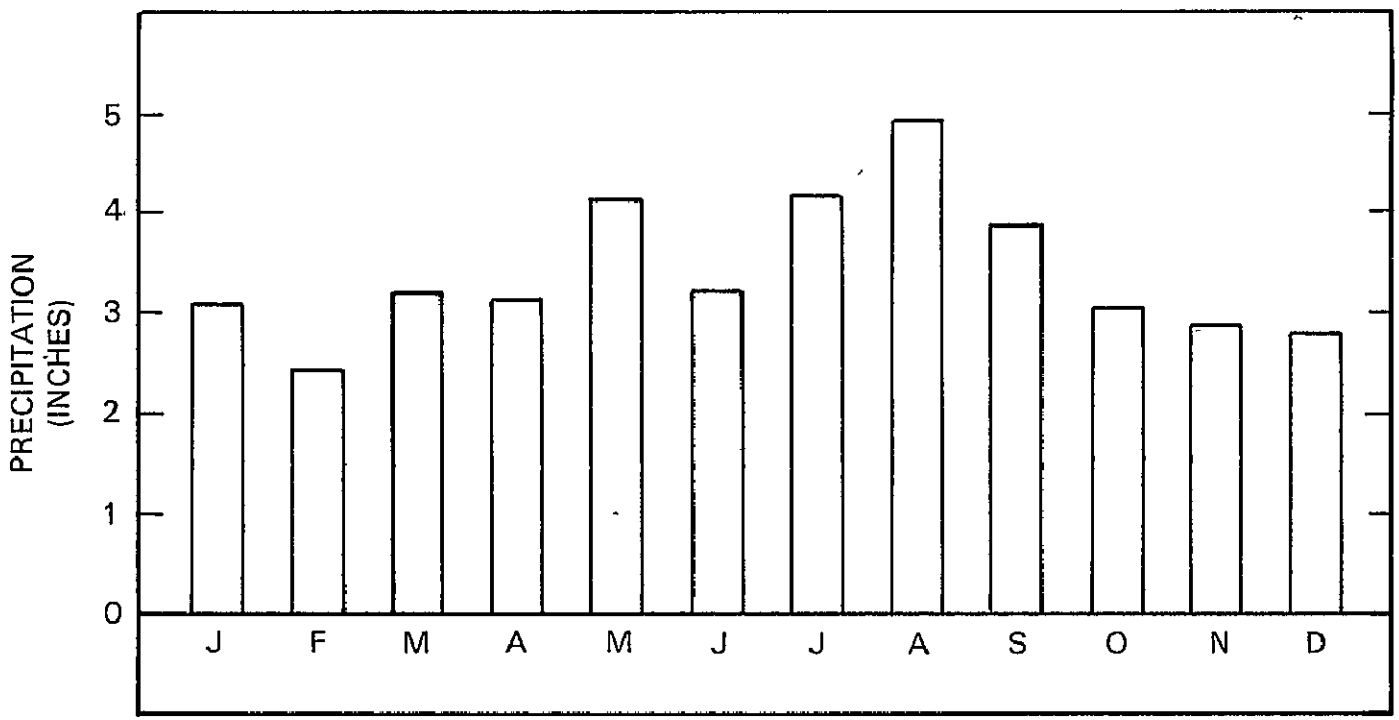

Figure 5. Precipitation Data [2]

The average solar radiation (incident on a horizontal surface) for the Greenbelt area is 14.7 MJ/m^2day (350 Langleys/day). The mean sky cover (sunrise to sunset) is 6.0 hours; 57 percent of the total possible sunshine is received. In a typical year, 105 days will be "clear", 105 will be "partly cloudy", and 155 days will be overcast. Average insolation data is given in Table 2 and Figure 6, for both horizontal surfaces and 54° tilt angle surfaces (appropriate for the Greenbelt project solar collectors). Observed solar

Table 2. Solar Radiation Data

(Smithsonian/NOAA Data for Washington, DC)

Month	Horizontal Surface		54° Tilt Angle Surface	
	MJ / m^2 day	Langleys / day	MJ / m^2 day	Langleys / day
January	8.25	197	16.8	400
February	11.4	272	17.7	422
March	14.1	337	17.1	408
April	16.2	387	14.9	356
May	21.9	522	16.6	397
June	22.7	541	15.9	379
July	22.1	528	16.6	396
August	19.1	457	17.2	411
September	16.3	389	19.6	467
October	14.0	333	21.6	516
November	8.84	211	17.7	422
December	6.74	161	15.2	362

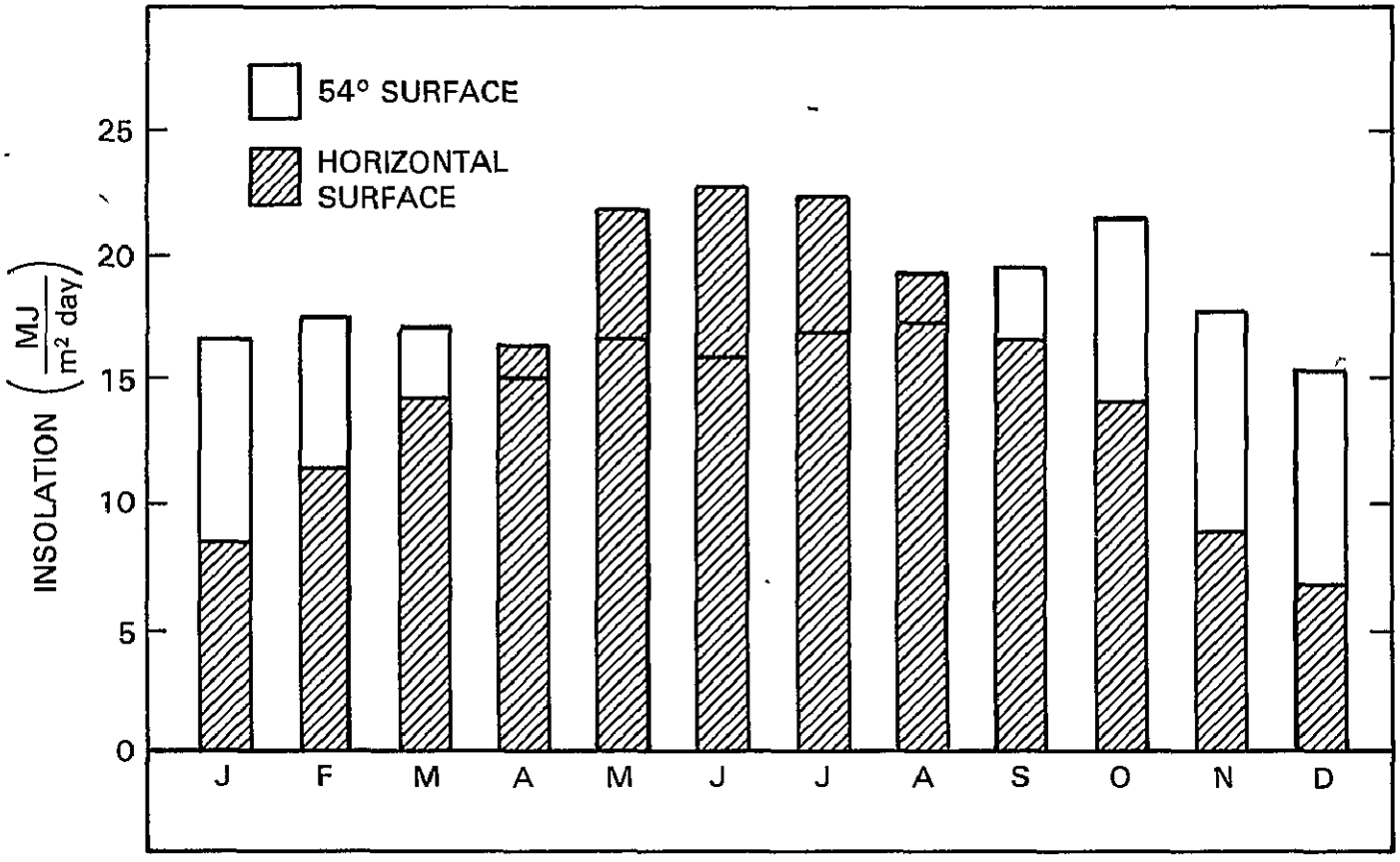

Figure 6. Solar Radiation Environment (Smithsonian/NOAA Data for Washington, DC)

radiation data during the period covered by this report will be presented in Section IV.

Of significance to the interpretation of solar performance data is the micro-environment of the system. The rooftop collectors are oriented in a south-facing direction at a 54° tilt. Approximately 12m (40 ft.) directly south of the test building is an identical flat-roofed building, the top of which is below the collector line-of-sight. To the east and west of the building are large (12m to 15m (40 to 50 ft.)) deciduous shade trees which have essentially no effect on direct solar radiation to the collectors and a minimal effect on diffuse radiation during the heating season. The building is located 8m (25 ft.) from a north-south street and approximately 15m (50 ft.) from an east-west thoroughfare with moderate vehicular traffic

B. System Design Parameters

Preliminary system design is concerned with determination of system size and selection of major components. It is therefore necessary to perform initial calculations to predict performance of such a system. The principal design parameters of interest are:

1. Solar collector characteristics
2. Collectable solar energy
3. Seasonal temperatures
4. Building heat loss summary
5. Building heat input requirements

The following discussion examines briefly how these parameters were treated in the initial design of the Greenbelt system. A first estimate of

Table 3. Solar Collector Characteristics

Manufacturer	Sunsource, Incorporated Los Angeles, CA
Model	Miromit Model 110
Absorber area	1.51 m^2 (16.2 ft^2) (steel)
Selective coating	Black nickel (Tabor)
Quoted absorptivity	0.92
Quoted emissivity	0.094
Glazing	Single, 0.397 cm (5/32 inch) water-white crystal glass
Flow arrangement	Seven parallel 1.27 cm (1/2 inch) steel pipe flow channels, 2.54 cm (1 inch) leaders
Insulation	Sides: 1.27 cm (1/2 inch) celotex boards Back: 7.62 cm (3 inch) fiberglass Frame is 24 gauge galvanized steel
Number of collectors installed	56
Total active collector area	84.3 m^2 (907.2 ft^2)
Dry weight	79.4 kg (175 lb) per collector

system capability is given in terms of predicted percentage of building heat input that might be supplied by solar energy.

1. Solar Collector Characteristics

The solar collectors used in the Greenbelt project are commercially available units whose significant characteristics are noted in Table 3. Figure 7 is taken from a NASA publication and illustrates operating efficiency for this collector [4]. Typical flow rates in this system are of the order of 18 gals./minute (1.14 l/s). This produces a flow rate of 9.94 lb/hr

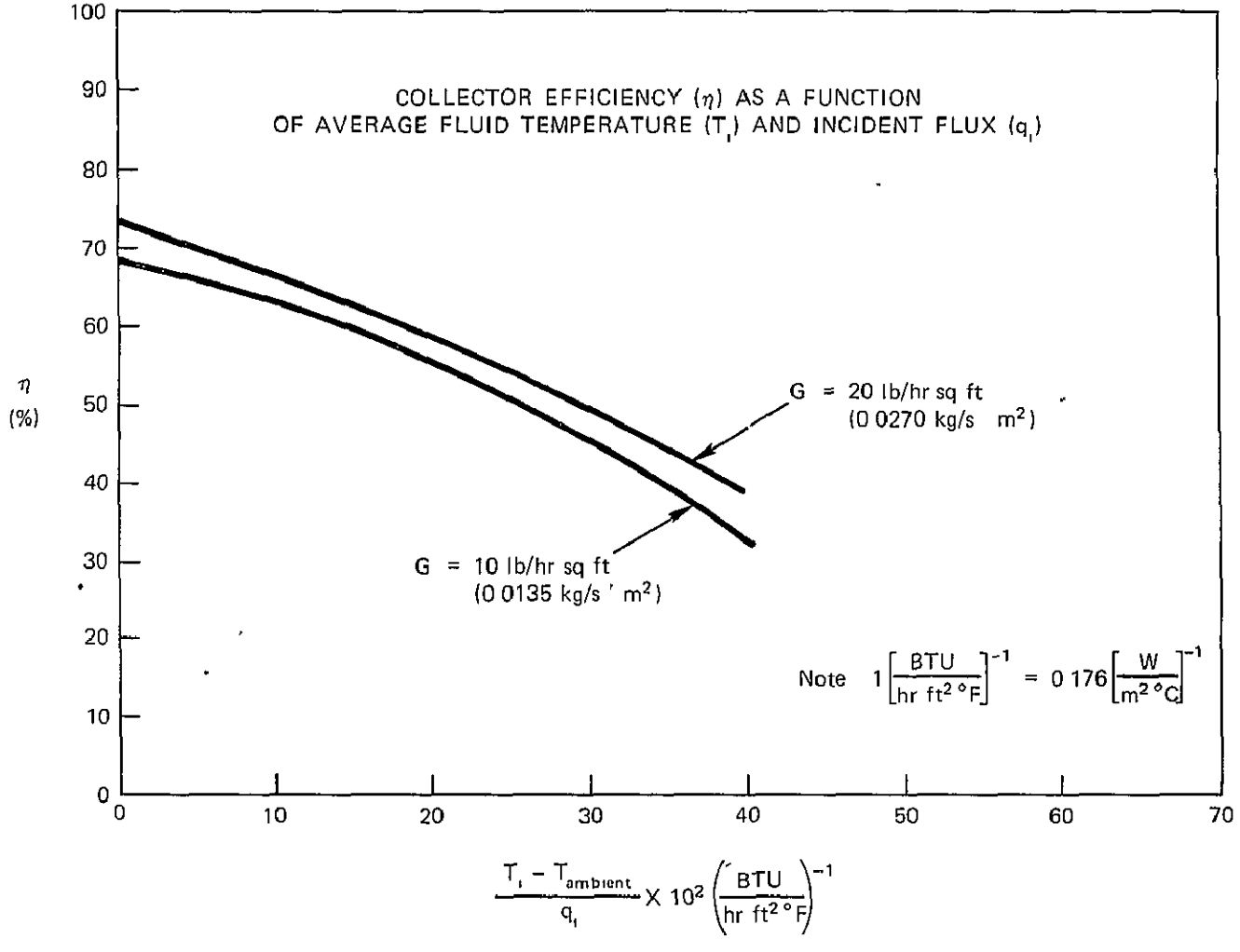

Figure 7. Collector Performance Correlation

sq. ft. (0.0135 kg/s.m.^{2}) and approximates the G = 10 lb/hr sq. ft. curve of the graph.

2. Collectable Solar Energy

Table 2 (Solar Radiation Data) shows the average available solar energy for the Greenbelt location. Because many of the calculations performed with heating systems in the U.S. are still done using English units, the table is repeated here in BTU/ft^2 day, as Table 4. The amount of energy collected from the incident energy is a function of the efficiency of the

Table 4. Collectable Solar Energy

BTU/ft^2 day

	Horizontal Insolation	54° Collector Angle Insolation	Collectable Energy (50%)
January	727	1476	738
February	1004	1556	778
March	1244	1505	753
April	1428	1314	657
May	1926	1464	732
June	1996	1397	699
July	1948	1461	731
August	1686	1517	759
September	1435	1722	861
October	1229	1905	953
November	779	1558	779
December	594	1337	699

Note: Each collector has 16.2 ft^2 area. 56 collectors are roof mounted.

collector and total system. An initial estimate was made of 50 percent for average collector efficiency only and the resultant is called the collectable energy. This is also given in Table 4.

The collectors face south, although a change in azimuth of 10° to 20° does not greatly affect the amount of energy collected. However, the angle of the collector to the horizontal is optimized for maximum energy collection during the heating months. This value is approximately the latitude plus 15° giving 54° as the tilt angle. A system optimized for potable hot water heating only or air conditioning would have smaller angles designed to match the energy collected to the energy required. A good discussion of these factors is available in the referenced publication [5].

3. Seasonal Temperatures

Figures 2 and 3 present data on maximum and minimum temperatures and heating degree days per month. For design calculation purposes it is necessary to use average daily heating degree days for each month. These are given in Table 5, upon which Figure 3 was based.

4. Building Heat Loss Summary

The loss characteristics of the Greenbelt homes were computed using the construction blueprints to examine dimensions, wall and ceiling materials and methods of assembly. Values of the overall coefficient of heat transfer (U) were obtained from available handbook data on thermal conductivity of the construction materials. In addition to wall and ceiling conduction losses, estimates were made of air infiltration. This refers primarily to door and window air leakage and door openings. The U values given in Table 6 include the effect of the newly installed storm doors and windows.

Table 5. Heating Degree Days

	Baltimore	Washington	Average	Daily
January	936	871	904	29.0
February	820	762	791	28.0
March	679	626	653	21.2
April	327	288	308	10.3
May	90	74	82	2.6
June	0	0	0	0
July	0	0	0	0
August	0	0	0	0
September	48	33	41	1.4
October	264	217	241	7.8
November	585	519	552	18.4
December	905	834	870	28.0

Above degree days referred to 65°F.

5. Building Heat Input Requirements

In assessing the building requirements, use was made of the Heat Loss Summary, Table 6 and the Heating Degree Days table, Table 5. Calculations were carried out for each month and these were compared with the amount of collectable solar energy for that month, Table 4.

The following typical calculation is for December:

Q_A = Building heat requirement

Q_{H_2O} = Heat required for potable hot water

Table 6. Building Heat Loss Summary

	A ft^2 area	U Value BTU/HR ft^2 °F	UA BTU/HR °F
Walls	3658	0.241	882
Ceiling	2243	0.134	301
Foundation	2243	0.331	742
Windows	688	0.40	275
Doors	120	0.25	30
			2230

H_C = 2230 BTU/HR °F

H_I = 266 BTU/HR °F

H_A = 2496 BTU/HR °F

H_C = Heat loss by conduction

H_I = Heat loss by infiltration estimated as UA = 0.4 × 66 = 266 from Greenbelt Project Plan

H_A = Total heat loss

$Q_A = H_A \times$ Degree Days

= 2496 BTU/HR °F × 28°F

= 69,888 BTU/HR

69,888 BTU/HR × 24 HR/day = 1,677,300 BTU/day

$Q^*_{H_2O} = 70 \times 10^6$ BTU/year = 192,000 BTU/day

Q_{Total} = 1,677,300 + 192,000 = 1,869,300 BTU/day

*From Greenbelt Project Plan

Collectable energy per December day per collector

$= 669 \text{ BTU/ft}^2 \times 16.2 \text{ ft}^2$

$= 10{,}838 \text{ BTU/day/collector}$

For 100% Q_{Total} to be supplied by solar energy

$$= \frac{1{,}869{,}300 \text{ BTU/day}}{10{,}838 \text{ BTU/day/collector}}$$

$= 172$ collectors required

However, only 56 collectors can be roof mounted. Therefore, $56 \times 10{,}838 = 606{,}928$ BTU/day from solar and $\frac{606{,}928}{1{,}869{,}300} = 32.5\%$ (assumes no system losses).

The above implies that during December, the month with the highest number of degree days and lowest insolation, a maximum of 32.5% of the building heat input requirements may be supplied by solar energy. The same calculation can be performed for each month of the year. The result is Table 7, which gives a preliminary estimate of possible amount of building energy requirement that may be supplied by the solar system.

C. System Requirements

At the beginning of system design an attempt was made to define system requirements and constraints which would influence the system configuration. A discussion of some of the primary requirements and the mechanisms of satisfying them in the Greenbelt Project solar energy system is presented below. The reader may wish to refer to Figure 9 (Energy System Schematic) in following the discussion. In each case, the desirable feature is noted and the implementation of the requirements follows.

Table 7. Estimate of Maximum Building Energy to be Supplied by Solar System

Month	Percentage
January	34.5
February	37.3
March	46.7
April	75.6
May	100.0
June	100.0
July	100.0
August	100.0
September	100.0
October	100.0
November	56.0
December	32.5

1. The ability to switch from solar augmentation back to conventional system with minimum effort:

The switch on the "V4 differential thermostat" on the central panel can be switched from "auto" to "off". This manually closes the bypass valve on the space heat exchanges (V4), isolating the conventional furnace-radiator loops from the solar water loop. This is done automatically when on "auto".

2. The ability to use the existing 3 way valve on boiler since it lowers radiator temperature:

This requirement refers to the microtherm temperature controlled mixing valve V2. When the solar collectors or storage tank are providing enough heat (such that the radiator return is hotter than a control temperature referenced to the outside ambient temperature) the water bypasses the boiler and the oil burner stays off. For instance, if the outside temperature is 45°F, and the microtherm control is set at 90°F, a solar system water temperature of about 120°F is sufficient to open valve V4 and allow use of heat from the solar system for space heating.

3. The treatment of space heating and hot water heating as separate problems:

Solar heated water passes through the domestic hot water heat exchanger first, before going to the space heat exchanger. Preheating of domestic water occurs even when the solar water is not hot enough to provide space heating. A separate oil-fired domestic hot water tank was provided to permit the main boiler to be shut-off during the summer.

4. The circulation of solar collector water only when hotter than storage tank:

A differential temperature thermostat senses difference in temperature between solar collectors and tank. A three way valve (V1) provides bypass as necessary.

5. Isolation of boiler from heat storage tank:

A differential temperature thermostat senses the difference in temperature between the radiator return water and the solar heated water inlet to the space heat exchanger. A three way valve (V4) bypasses the space heat exchanger whenever the radiator water is hotter than the solar water.

6. Venting of solar system, with freeze protection:

The design alternatives were the use of an antifreeze solution in the collector loop, together with heat exchangers in the storage tanks, or the use of water as the collection fluid with a vented system and gravity drainage from the collectors to prevent freezing.

The latter alternative was chosen. The system uses float valves at the top of the collector array for venting, supplemented by vacuum breakers should the float valves freeze in the closed position. Solenoid valves in the boiler room open in response to low collector temperatures and drain the collector water into the storage tank.

7. The capability of storing all collectable heat on a December day:

For December the collectable energy at an efficiency of 50 percent is 669 BTU/day ft^2, resulting in a BTU potential solar energy input of 607,000 BTU/day.

With a working temperature difference in the storage medium during the day of 40°F. the capability of accumulating this thermal energy with water storage would require 15,175 lbm or 1828 gallons of fluid. The installed storage tank capacity is approximately 2500 gallons filled with about 2000 gallons of water.

D. Evolution of System Design

The design of a solar energy system is by no means a trivial exercise. In order to document the development of the Greenbelt demonstration system, the evolution of the present design will be very briefly described here. Note that the details of the control system are supplied in Section II.E.

The initial system design is first outlined; operational problems with this design are then noted. Changes in the initial configuration to ameliorate these problems are described in the final subsection.

1. Description of the Original System

A schematic of the mechanical portion of the initial solar energy system is shown in Figure 8. Water is drawn from the storage tank by the main pump (P1), then routed either through the solar collectors or directly to the boiler mixing valve (V2) and then to the radiators, domestic hot water (D.H.W.) heat exchanger, and finally returned to the storage tank. The solar collector selector valve (V1) is controlled by a differential thermostat; storage tank water is allowed to circulate through the collector when sufficient sunlight is present to add heat to the system. Another valve (V4), controlled by thermistors in the tank and radiator return line, bypasses the flow around the tank when the stored heat has been exhausted. The furnace is then used in the normal heating cycle. The throttle valve (T1) in the return line from the D.H.W. heat exchanger serves to keep the system supply pressure sufficiently high in the radiators.

2. Problems

During the initial operation of the system in April-May 1976 several problems were experienced which led to a reconfiguration of the system. The major problems were:

(a) When the solar collector selector valve (V1) was in the bypass position (collectors bypassed) and the tank valve (V4) in the supply position (water drawn from the tank), there was insufficient pressure to the radiators. Also there was insufficient pressure drop in the collector bypass mode and

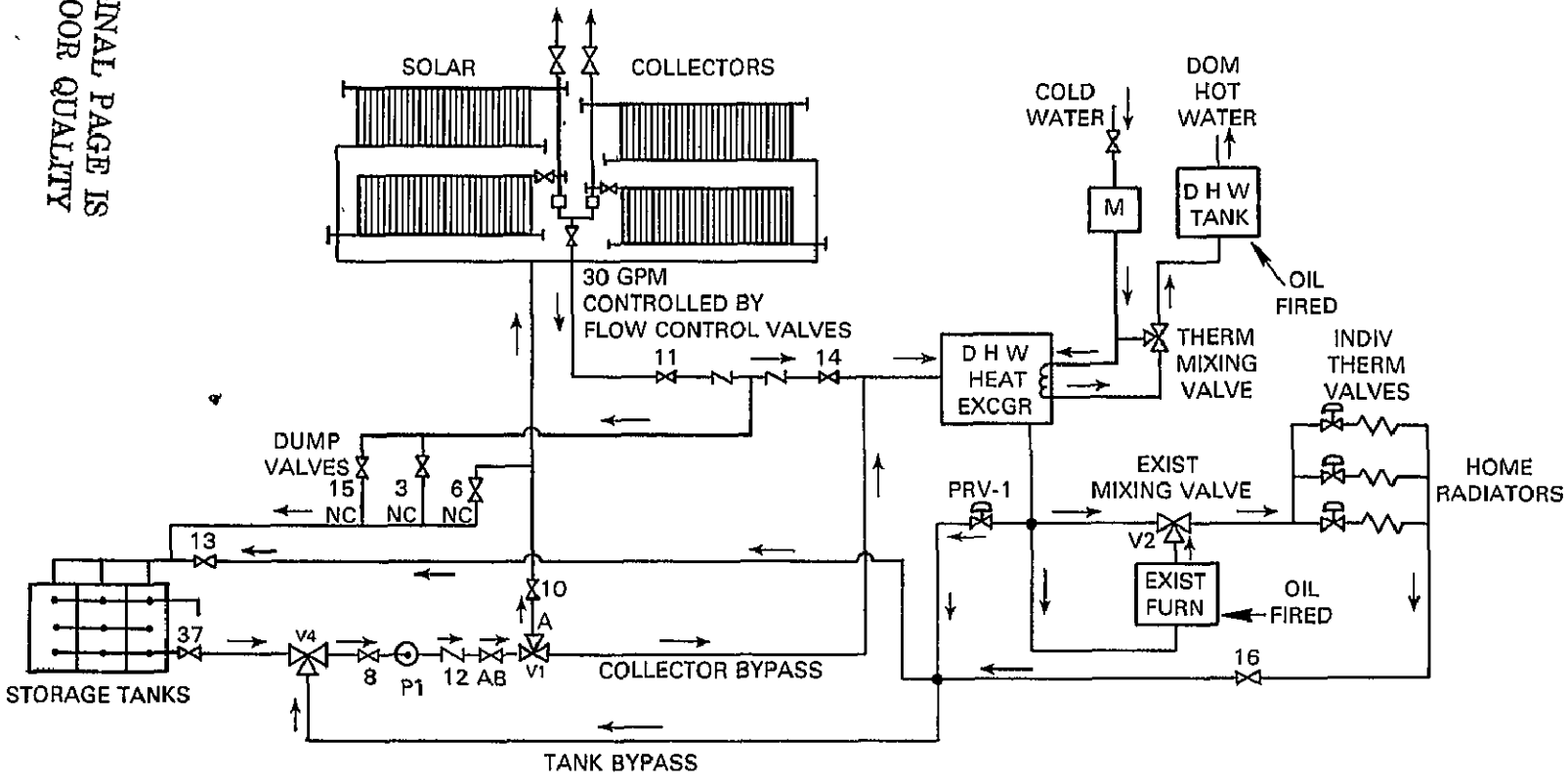

Figure 8. Initial Mechanical Subsystem

the pump motor overheated. An attempted solution was to throttle the return flow from the radiators with a hand valve to raise the back pressure. This solved the above problems but generated another (discussed next).

(b) With the solar collector valve (V1) in the collector position and the return restricted as in (a) above, less than half of the design flow circulated through the collectors. The increase in collector operating temperature resulted in reduced thermal efficiency and output.

(c) With both the storage tank valve (V4) and the collector valve (V1) in the bypass position, system pressure dropped, the system became airbound, and the pump cavitated.

The solution to these problems in the final design was the addition of a heat exchanger to isolate the pressurized radiator loop from the vented solar loop.

(d) When the solar energy system was put into operation in January 1977, freezing occurred in several collectors before the freeze dump valves opened, despite the freeze-prevention measures built into the design. The solution to this problem is described in the next subsection.

3. Final System Design

Figure 9 shows the final system configuration.

(a) Separation of Solar Heating System from Radiator Loop

The solution to the low system pressure problems discussed above was to introduce a heat exchanger to physically isolate the solar heating system (which is a vented, low pressure, high flow rate circuit) from the original heating system (which is a closed, pressurized, low flow rate circuit) while thermally coupling the two circuits. The shell side of

the added heat exchanger was inserted in series with the solar collectors, domestic hot water heat exchanger, and storage tank. The original tank bypass valve (V4) was relocated to the radiator loop to bypass fluid around the tubes of the new heat exchanger. A one-sixth horsepower pump (P2) was also provided to circulate fluid in the radiator loop. The repositioned valve (V4) serves to prevent the furnace from heating the storage tank when the radiator return water is hotter than the solar water.

(b) Collector Freezing Problem

In order to combat the freezing problem, a small pump (P4) was added to the collector circuit to recirculate water in the collectors whenever the collector system was in bypass and the outside temperature was below 35°F. This serves to equalize temperatures throughout the collectors so that the collector thermistor will sense freezing conditions in time to dump the collectors before freezing occurs in isolated locations. Also, the freeze circuit in the Model 104 differential thermostat (controlling V1 and dump valves) was readjusted internally from the factory setting of 35°F to a new value of 50°F for dumping.

(c) Domestic Hot Water Recirculation

A small pump (P3) was added to the domestic hot water loop to provide additional solar heating of the water in the domestic hot water tank when there is no demand flow of domestic water. This pump is controlled by a differential temperature thermostat with sensors in the DHW tank and DHW heat exchanger.

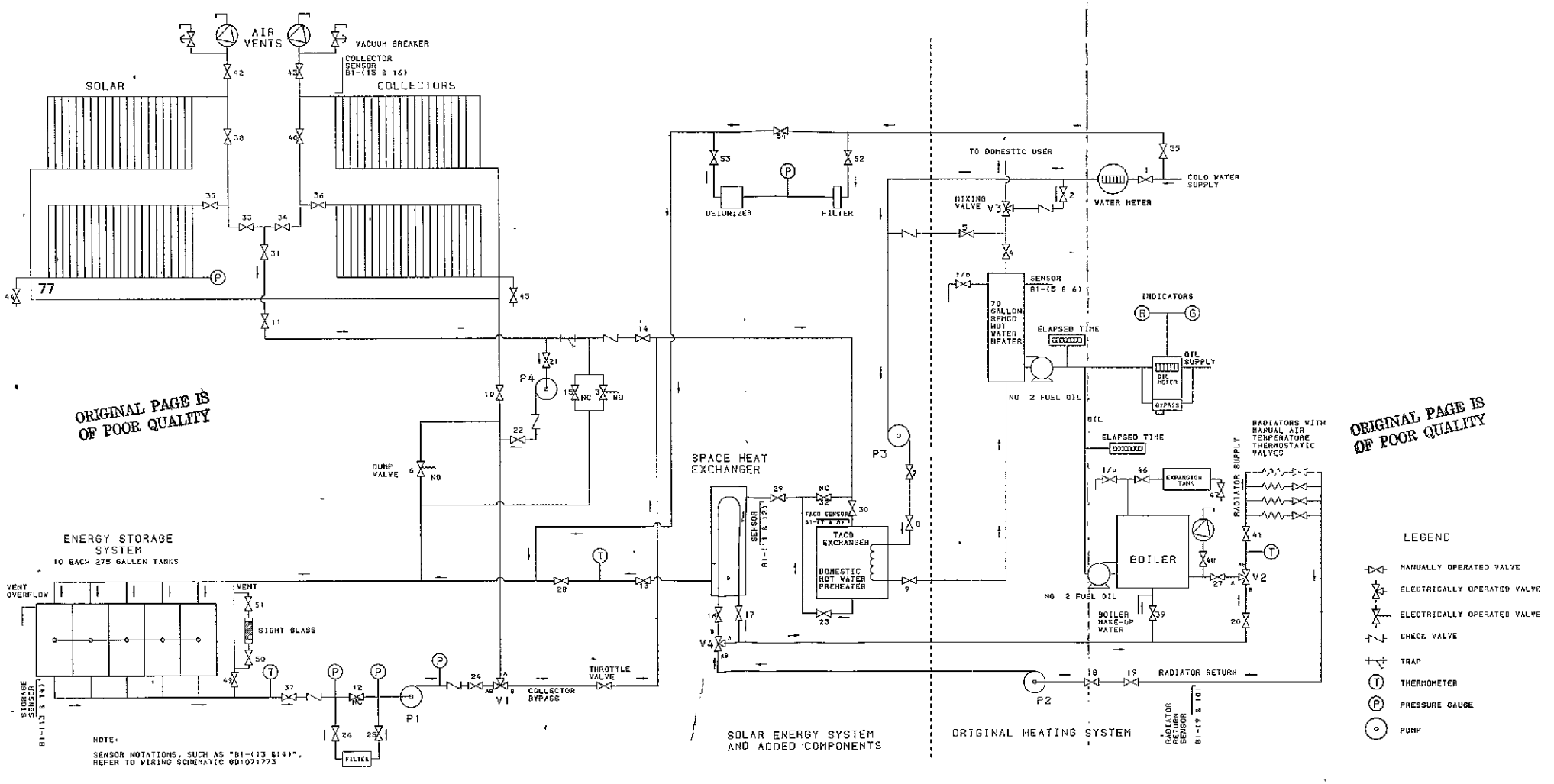

Figure 9. Heating System Schematic

FOLDOUT FRAME

FOLDOUT FRAME

E. Control System and Operating Modes

1. Electrical Power and Fluid Control

The flow control of the water in the solar heating system is accomplished with differential comparator type thermostats. Typical thermostat operational characteristics are as follows: When the temperature at point A is 10 ± 3°F higher than at point B, functions controlled by a N-O (normally open) relay contact are activated, while those controlled by the N-C (normally closed) contacts will terminate. Subsequently, when the temperature at point A returns to within 3 ± 1°F of the temperature at point B the functions controlled by the N-O relay will cease and likewise those controlled by the N-C relay will be reactivated.

The control system used in the solar project consists of 3 commercially available solid-state differential thermostats with matching thermal sensors. The sensors used are commercially supplied, and are rugged thermistor types designed to withstand the stagnation temperatures of solar collectors. Each thermistor is selected to give a thermal temperature coefficient of -4.8% per °F at 77°F (10,000 ohms nominal resistance). Figure 10 illustrates the basic control functions for the solar collection system.

The first differential temperature flow controller (DTFC) is a Rho Sigma Model 106. Its function is to provide both manual and automatic on-off control of circulating pump P3 (see Figure 9). When the collector inlet water temperature to the domestic hot water heat exchanger is 10°F greater than the temperature of the water in the oil fired domestic hot water heater, pump P3 is energized.

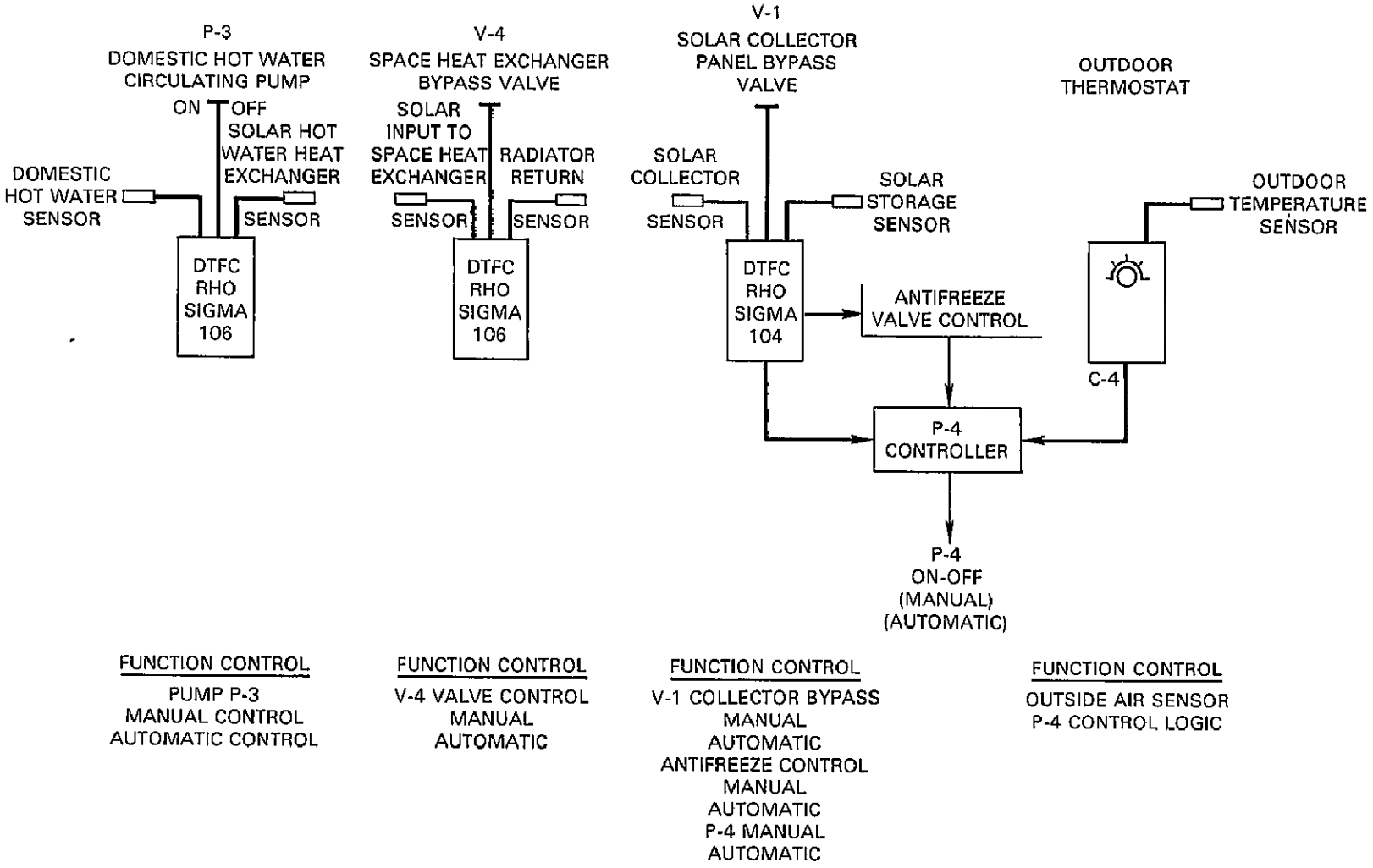

Figure 10. Basic Control Functions of Solar Heating System

The second DTFC is also a Rho Sigma Model 106 and is installed to control the flow of the radiator water through V4. It provides either direct flow through the space heat exchanger or a bypass flow path in order to prevent the boiler from heating the solar storage if the solar storage temperature is less than the radiator return water temperature.

The third DTFC unit is a Rho Sigma Model 104. Basically, it is the same as the Model 106 with the addition of a collector freeze-prevention sensor circuit. This controller senses the collector exit water temperature and compares it with the temperature of the water in the storage tank. When the collector water temperature is 10° ± 3°F greater than the storage temperature valve, V1 will be energized to place it in a collector flow position. As the collector water temperature approaches the storage tank temperature (3° ± 1°F), V1 is energized to place it in a collector bypass position to preserve the maximum energy in the storage tank, should the collector outlet water temperature continue to be below the storage tank temperature level.

In addition, the collector sensor continuously compares the collector temperature against a pre-set reference temperature. When this reference temperature is reached, a relay is energized which causes the collector fluid to drain, thereby preventing freeze-up. Presently, the pre-set reference temperature is 50°F.

This temperature may seem somewhat higher than required for freeze protection. However, temperature gradients across the collector array make a lower reference level inadequate should sudden changes in ambient temperature occur when the collectors are not in sunlight.

To minimize temperature gradients across the collector array, pump P4 provides loop circulation under certain conditions. Three conditions must be satisfied before P4 can operate: (1) the outside ambient temperature must be 35°F or below, as monitored by a separate outdoor thermostat; (2) valve V1 must be in the bypass mode; (3) the freeze protection relays must not be deenergized (i.e., in the dump mode). When the above conditions are met, P4 is automatically started to equalize the temperature of the solar collection fluid until it reaches the preset temperature of 50°F. If 50°F is reached, the fluid is drained automatically into the storage tanks.

The various system operating modes which the control subsystem is designed to manage are summarized in Table 8.

III. System Installation and Configuration

A. Roof Mounted Equipment

Fifty-six solar collectors were mounted on the rooftop in the configuration shown in Figures 11 and 12.

After the asphalt composition and insulation were removed from the roof in two lengthwise strips, 2 × 6 inch wooden runners were nailed to the concrete roof using explosively driven nails. Thirty pairs of iron corner brackets were screwed to each runner together with spacer blocks as shown in Figure 13. The wells were then covered with hot tar. Thirty triangular trusses, fabricated by a local lumber yard, were installed in the spaces formed by the corner brackets protruding from the roof (see Figure 14). Two by four inch runners were nailed between the centers of adjacent trusses at seven locations and diagonal braces were added to produce a rigid structure on which to mount the collectors as shown in Figures 15 and 16.

Table 8. System Operating Modes

Condition	Response
1) Collector temperature > storage temperature.	Valve V-1 operates in AB-A mode.
2) Collector temperature < storage temperature.	Valve V-1 operates in AB-B mode.
3) Collector temperature $\leq$ 50°F	Solenoid valves 3 & 6 open, draining the collectors.
4) Collector outlet temperature and/or storage temperature > radiator return temperature.	Valve V-4 operates in AB-B mode.
5) Collector outlet temperature and/or storage temperature < radiator return temperature.	Valve V-4 operates in AB-A mode, bypassing heat exchanger.
6) Temperature of radiator return water preheated by solar $\geq$ microtherm reference temperature.	Valve V-2 operates in B-AB mode, bypassing boiler.
7) Temperature of radiator return water preheated by solar < microtherm reference temperature.	Valve V-2 proportions solar preheated water with boiler water to achieve microtherm reference temperature.
8) Domestic hot water tank temperature < collector outlet and/or storage temperature.	Pump P-3 turns on; circulating domestic hot water through heat exchanger.
9) Domestic hot water tank temperature > collector outlet and/or storage temperature with a demand for hot water.	Make-up water for hot water tank preheated in heat exchanger.
10) Outside ambient temperature $\leq$ 35°F; V-1 in AB-B mode; solenoid drain valves are closed.	Pump P-4 turns on, circulating water through the collector array.

Note: 6 and 7 are part of existing HW heating system and operate independently of solar system. Microtherm uses outside temp. as reference.

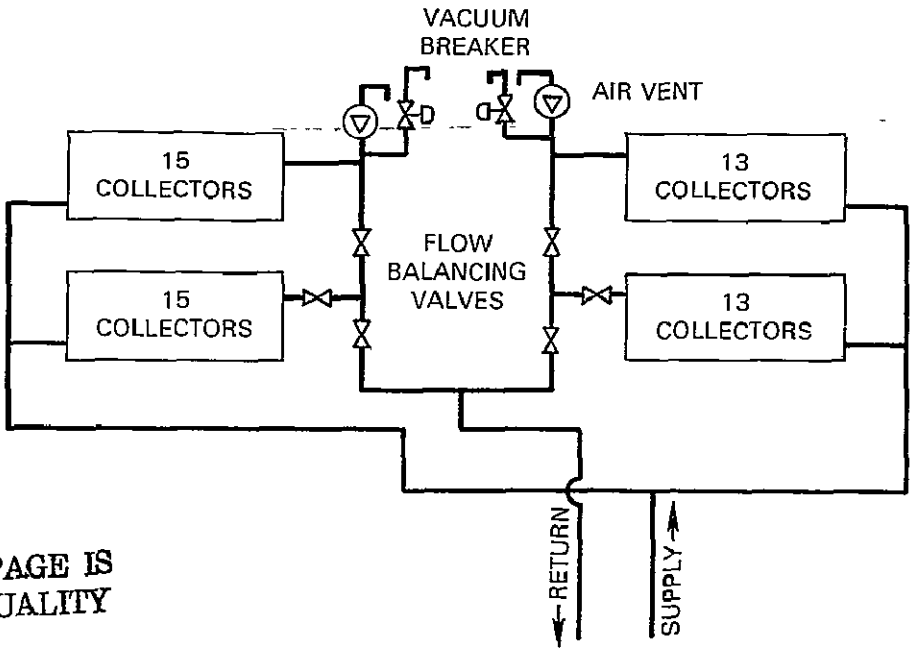

Figure 11. Collector Schematic Drawing

Two by six inch runners were nailed to the front of the truss framework, angle brackets were screwed to the corners of the collectors and the collectors were finally attached to the runners. Rubber automotive type heater hoses and clamps were used to interconnect adjacent solar collectors. The collectors themselves are described in Section II.C; more detailed information is contained in Suncource Tech Note 75023 and literature available from American Heliothermal Corporation.

The north side of the truss framework (at the rear of the collectors) was covered over with plywood and shingles to resemble a conventional pitched roof; a sheet metal extension was added to the existing chimney to exhaust furnace flue gasses above the new roof level.

The solar collectors are arranged in four parallel arrays, as seen schematically in Figure 11. Because of the difference in height between left and

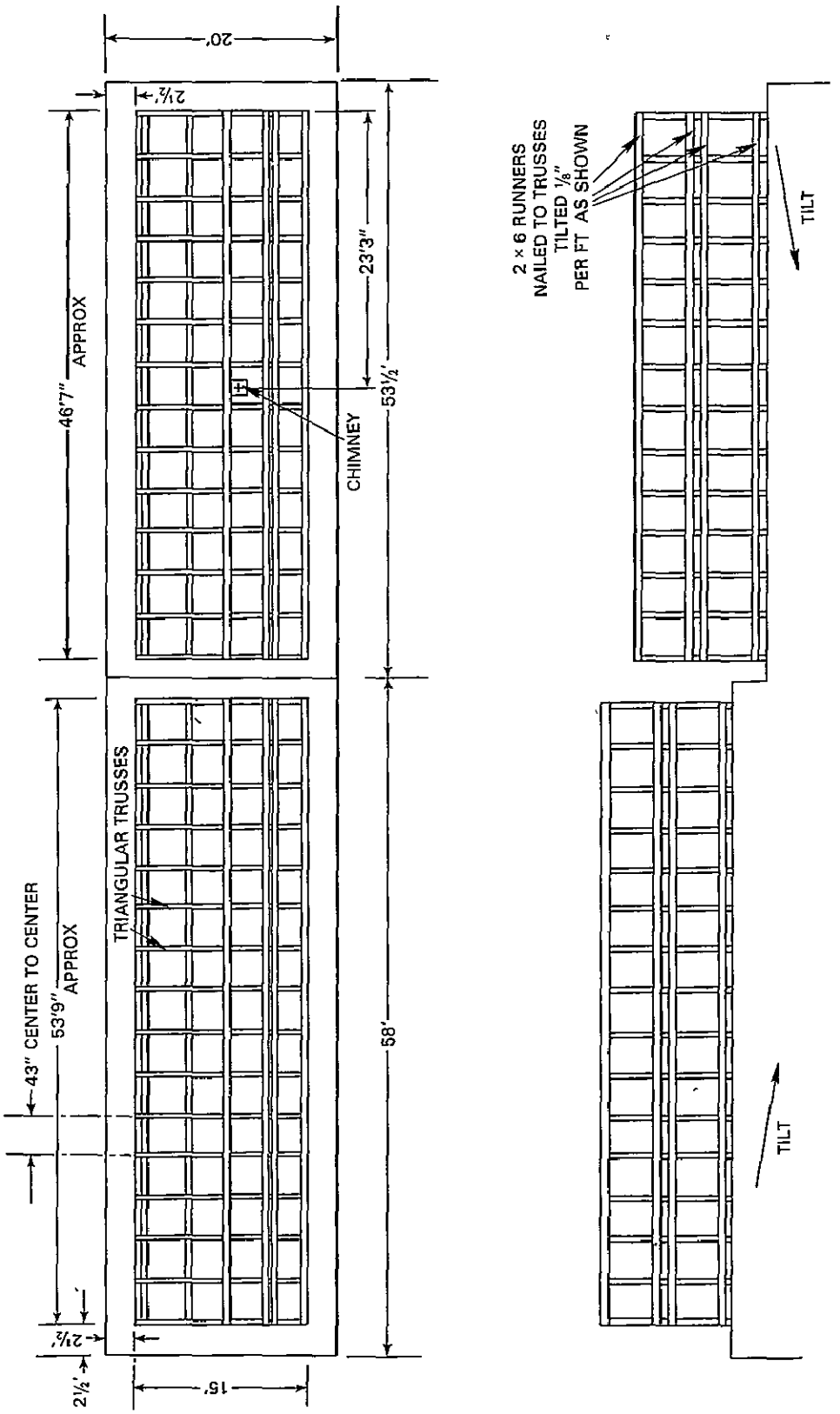

Figure 12. Flat Roof Layout

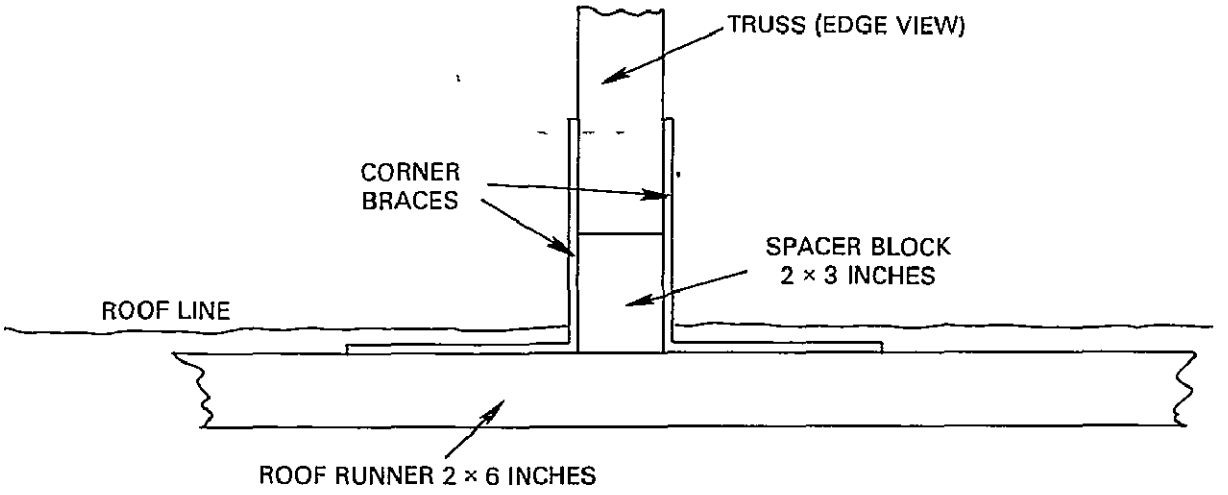

Figure 13. Roof Truss Attachment Detail

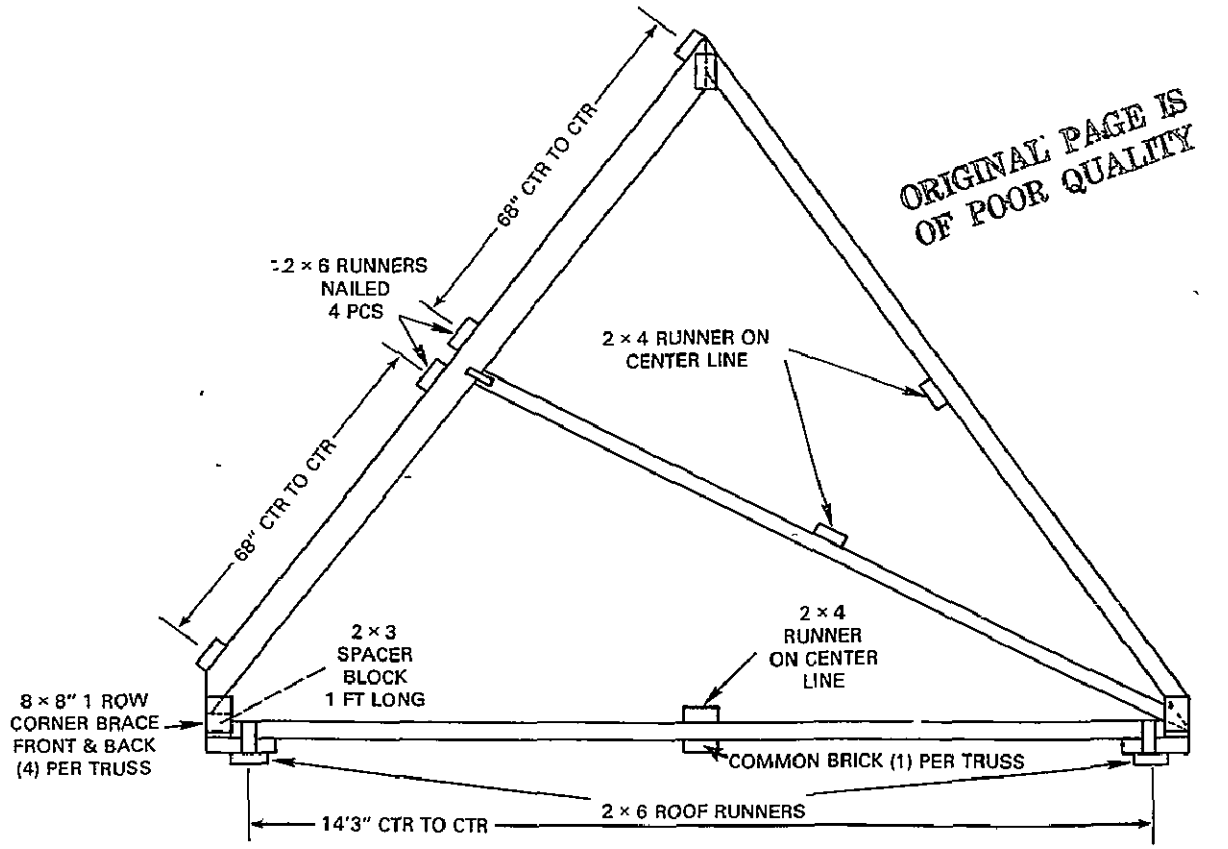

Figure 14. Collector Mounting Truss (Side View)

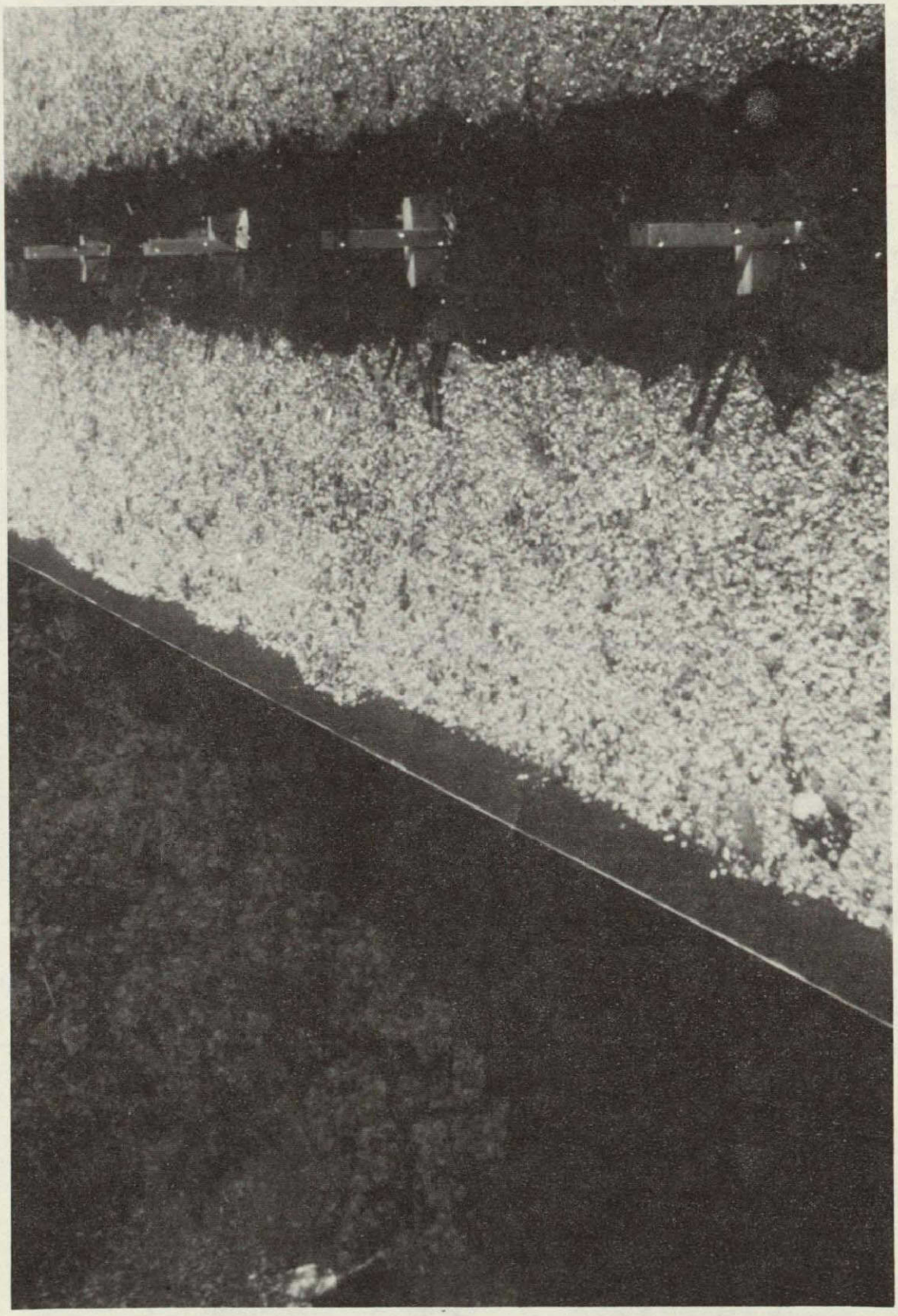

Figure 15. Mounting Detail on Roof

Figure 16. Collector Mounting

right sections and upper and lower arrays, valves in the outlet of each array were adjusted to provide equal flow rates and outlet temperatures. Float valve air vents and vacuum breakers are installed at the top of each section to allow the collectors to drain when temperatures approach freezing (see Photograph Figure 17). Photograph Figure 18 shows collectors being mounted and coupled together.

All plumbing to the rooftop system consists of cast iron pipe insulated with two inches of preformed polyurethane. An aluminum jacket was fabricated around the insulated pipe to protect it from the weather.

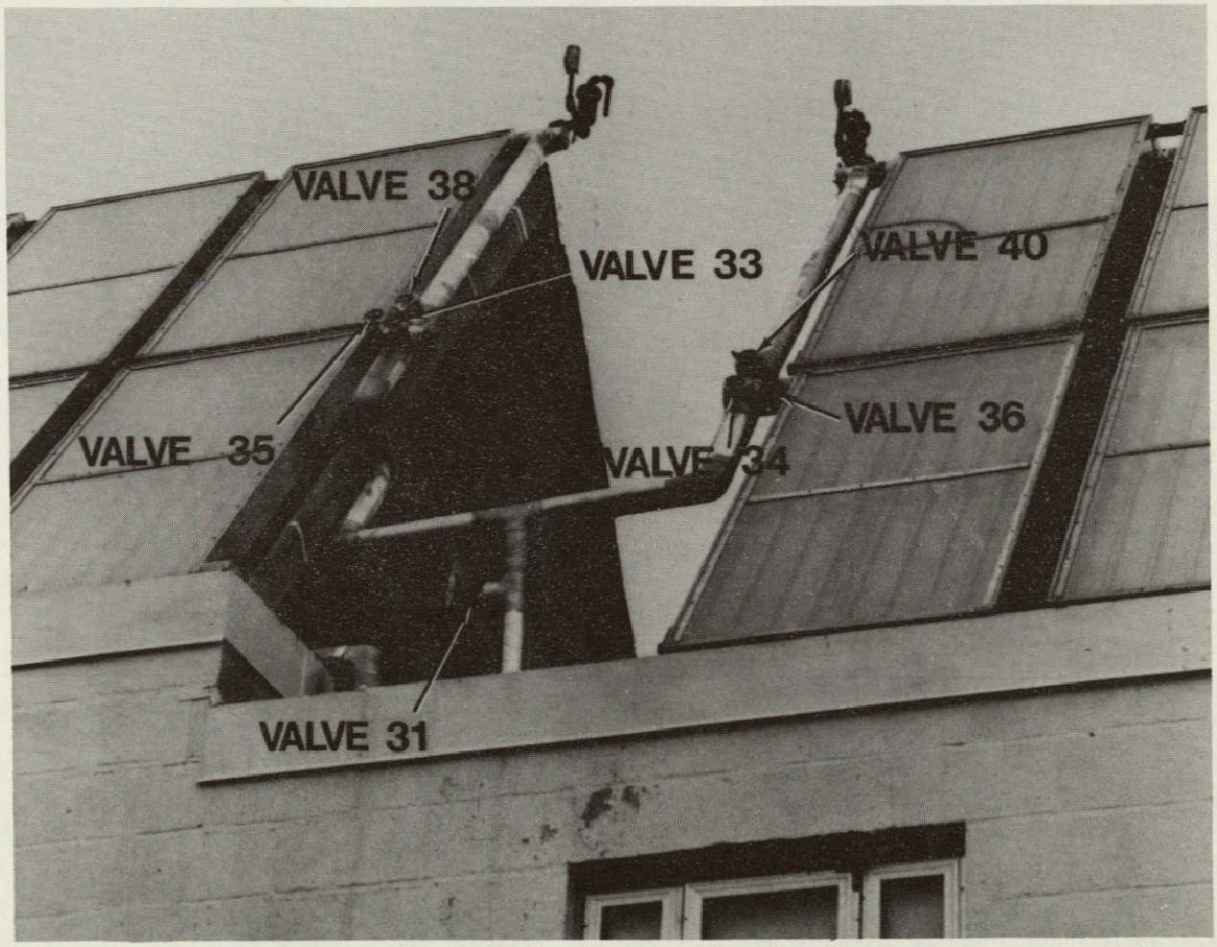

Figure 17. Collector Valve Arrangement

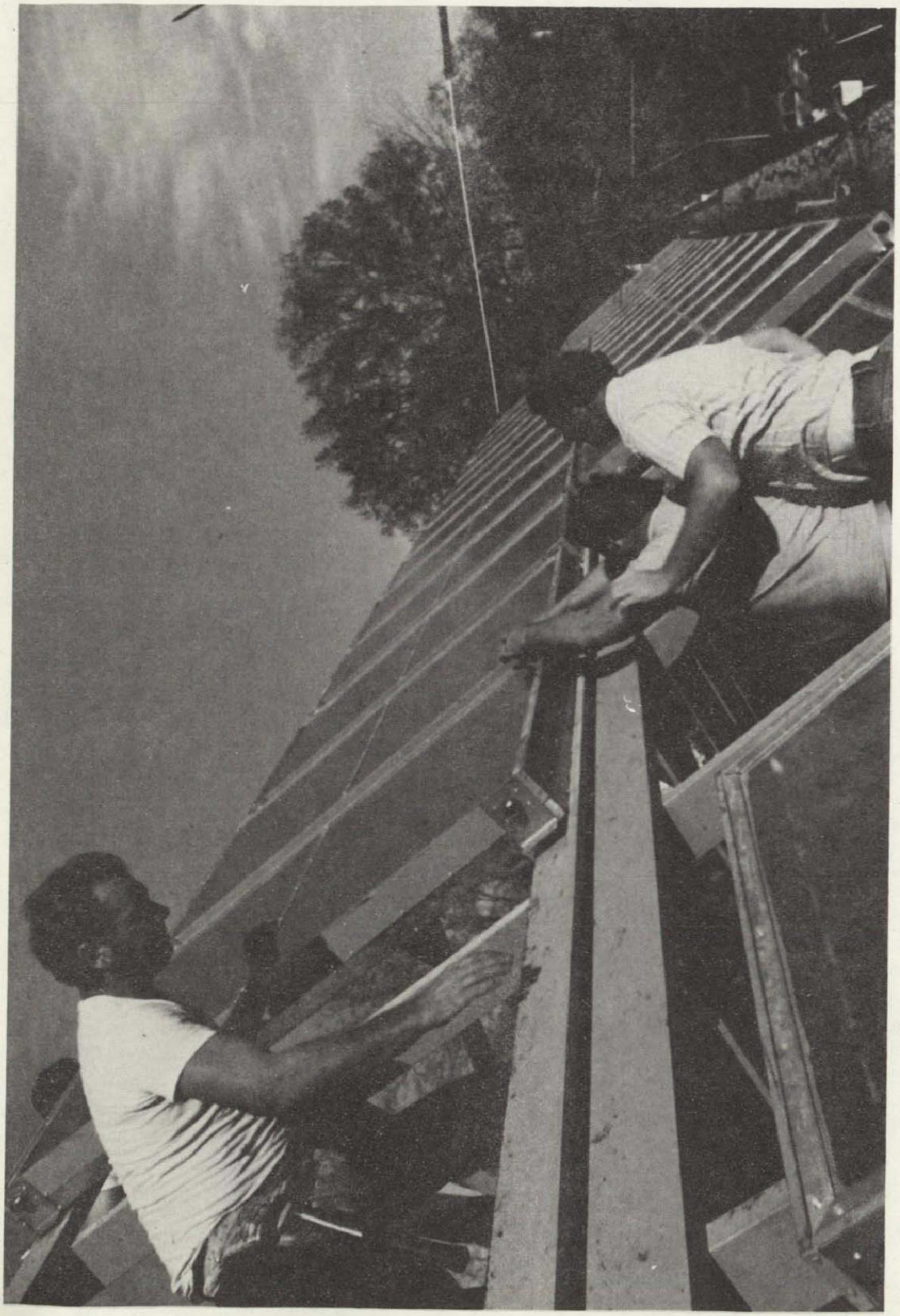

Figure 18. Collector Installation

B. Mechanical Room Equipment

The crawl space beneath the solar heated residence building varies from 3 1/2 feet to 4 1/2 feet in height except for the boiler room which is 8 feet high. The general layout is shown in Figure 19.

1. Storage Tanks

The thermal storage system consists of ten 275 gallon common oil storage tanks joined in parallel. This size was selected as the largest that could be carried down the basement stairs and through the door. The earthen floor of the higher section of the crawl space was dug out approximately one to two feet and timbers were laid to accept the tanks in two rows. Each tank was carried into the boiler room, turned on its side, slid across the lower crawl space into the higher space and erected. Polyurethane insulation was foamed around the tanks to a thickness of four inches. Figures 20 and 21 show storage tanks in place before and after application of foam insulation.

2. Mechanical Equipment

Located in the deeper, concrete floored mechanical room are the boiler, hot water heater, pumps, valves, heat exchangers, filters, and data recording instrumentation.

Before modification to include solar heating, the boiler room contained the following equipment:

a. Boiler: Kewanee Type R, Model 83R3 3X with Robot Autoheat Type DX1 oil burner (2 1/2 gallons per hour consumption.)

b. Domestic hot water heat exchanger: TACO 30 gallon "Tankless" hot water heater.

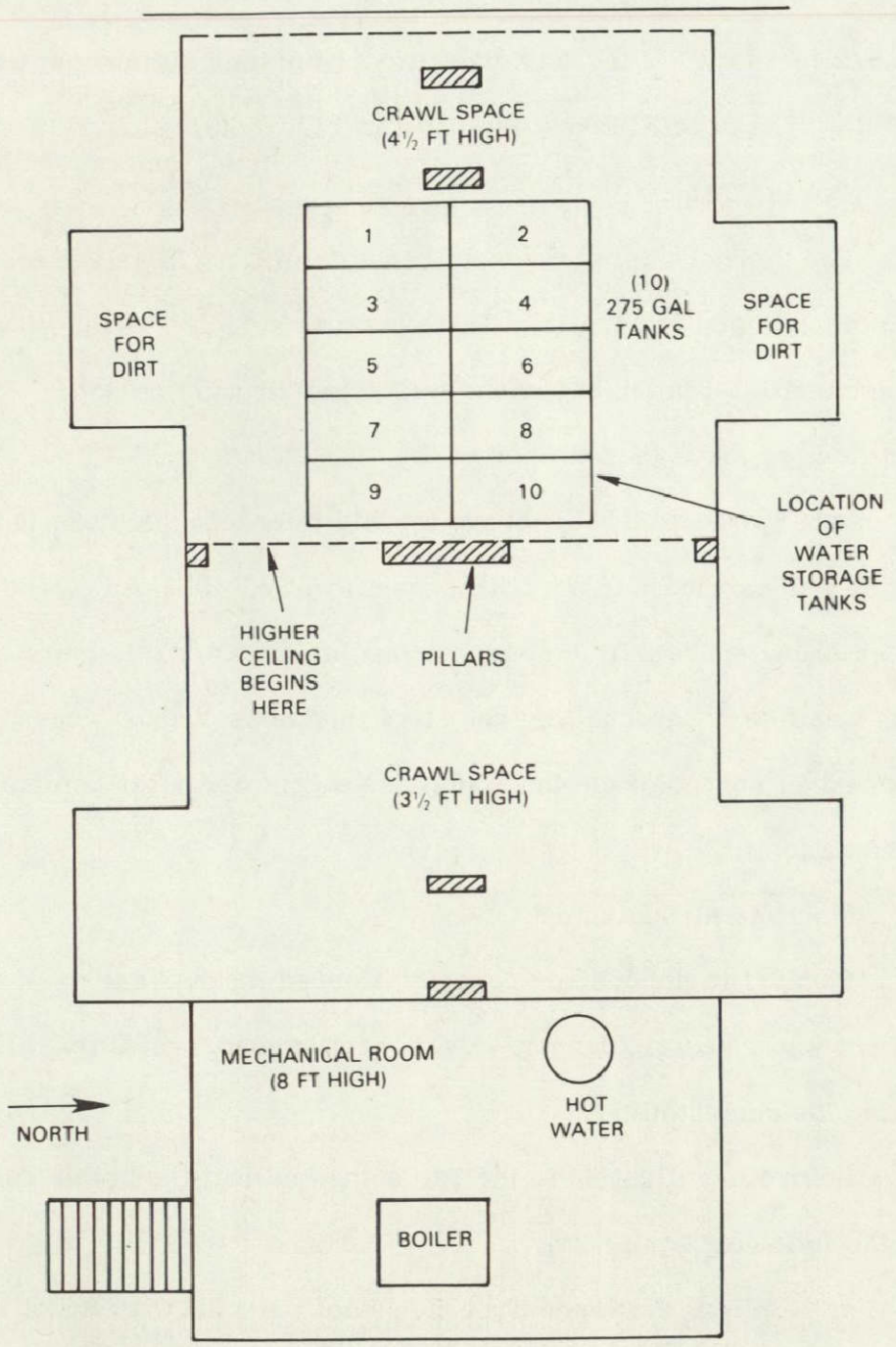

Figure 19. Schematic Diagram of Mechanical Room

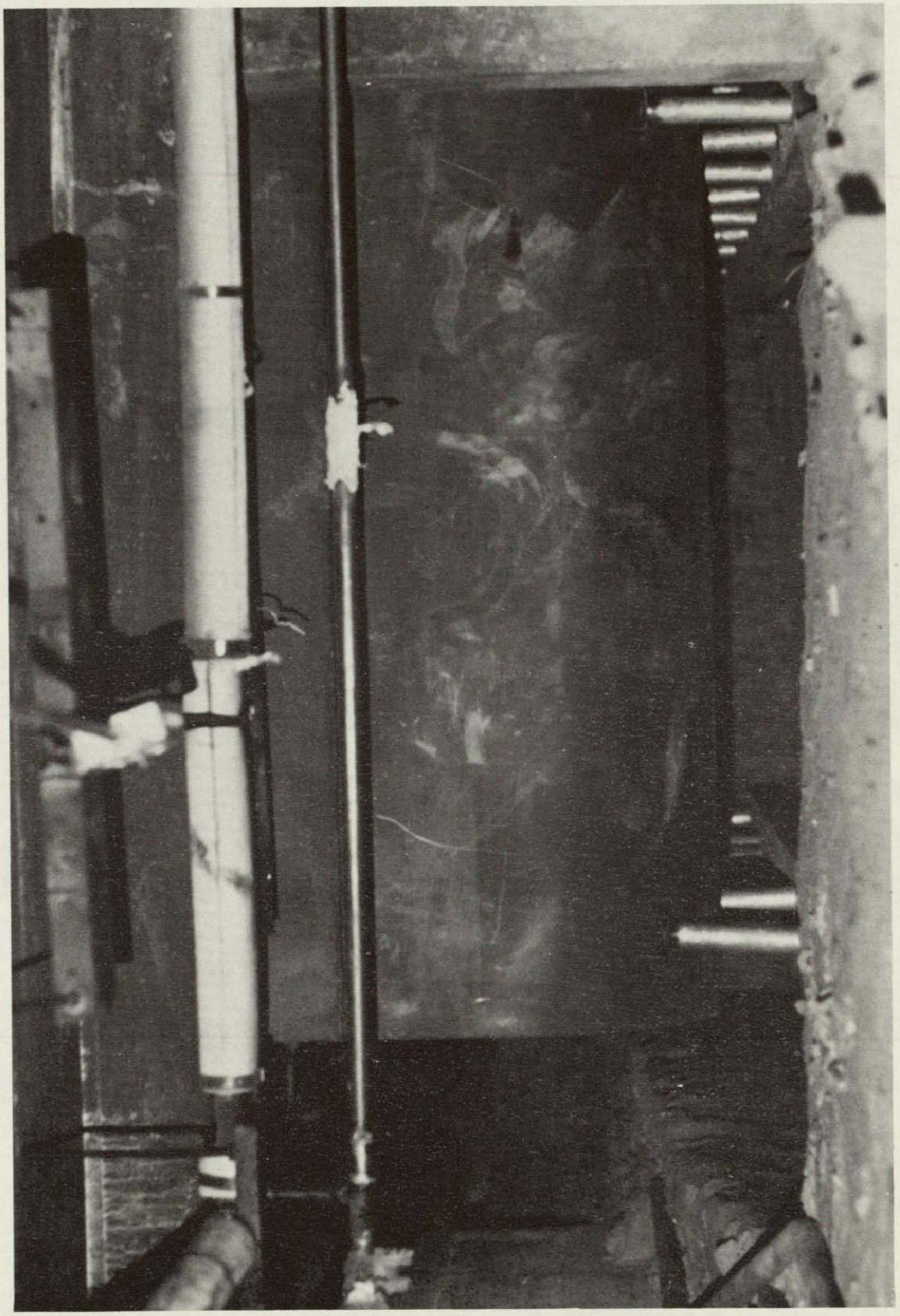

Figure 20. Storage Tanks

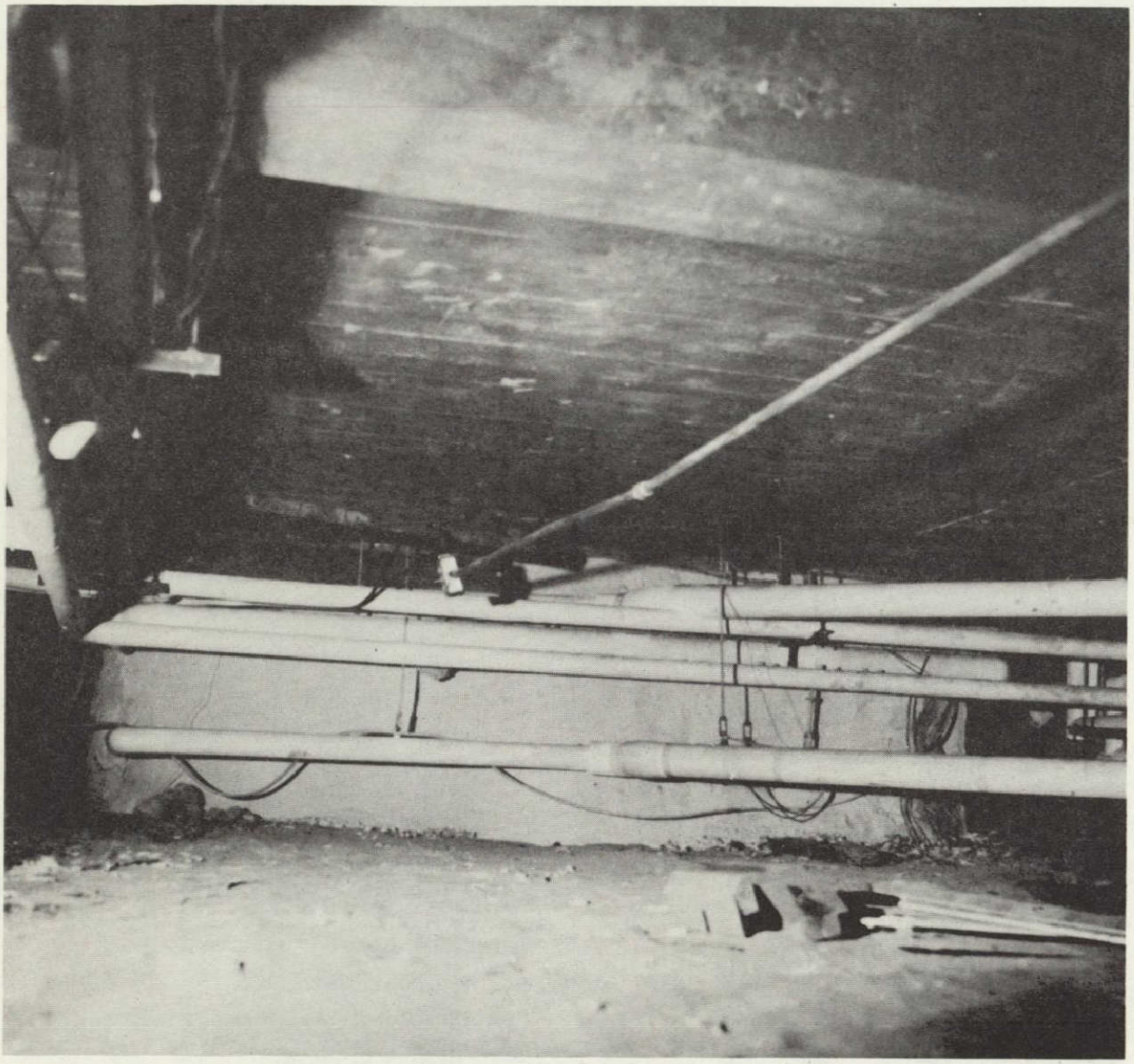

Figure 21. Storage Tanks (Insulated)

c. Space heating circulation pump, (P2): Bell and Gosset two-inch flanged, 1/6 horsepower.

d. Furnace proportional temperature control (V2): Barber-Coleman Microtherm Dual Bulb Thermostat Model TP 231. Three-way valve actuator VP-3044.

j. Fuel quantity meter: Flowtron Industries Polyfuel Monitor Model PM-100.

IV. System Performance and Operating Experience

A. Introduction

The primary impetus behind the Greenbelt Project was the desire to demonstrate the performance of retrofit solar energy systems for multi-family residential dwellings under realistic conditions. Several facets of the project make this effort noteworthy. First, the system was installed and operated in an eminently realistic atmosphere—the building was continuously occupied by tenants whose lifestyle was not disturbed by the construction or operation of the system. The building had multiple units; most solar work has been directed towards single-family homes. Finally, the existence of an identical non-solar building in close proximity to the test home provided an excellent baseline for evaluating system performance.

The control building was instrumented to provide temperature, fuel consumption, and hot water use data. Fuel savings by the solar energy equipped dwelling could thus be directly gauged. Measured temperatures indicated substantially similar heating loads for the two buildings. It should be noted that the control building used approximately 6 percent more hot water in an 11 month period during the course of the study; since hot water use is on the order of 20 percent of the total heating load of the buildings, this discrepancy does not have a significant impact on the conclusions reached. (Table 9 has corrected total fuel savings data to account for this 6 percent discrepancy.)

Table 9. Annual Performance Data — 1977

Month	Gallons of Fuel Oil Consumed		Fuel Savings	Solar Savings ($)	f
	Control Bldg.	Solar Bldg.			
JAN	937.8	733.1	204.7	87.61	0.22
FEB	574.5	417.0	157.5	67.41	0.27
MAR	472.9	258.0	214.9	91.98	0.45
APR	320.2	131.5	188.7	80.76	0.59
MAY	189.4	58.9	130.5	55.85	0.69
JUN	157.8	12.9	144.9	62.02	0.92
JUL	96.2	1.1	95.1	40.70	0.90
AUG	99.7	1.9	97.8	41.86	0.98
SEP	109.3	4.1	105.2	45.03	0.96
OCT	354.4	165.4	189.0	80.89	0.53
NOV	435.3	346.8	88.5	37.88	0.20
DEC	644.5	537.8	106.7	45.67	0.17
Total	4392.0	2668.5	1723.5	737.66	0.39
Corrected Total	4345.0	2668.5	1676.5	717.54	0.386

The Greenbelt Project solar heating system has been in operation since January 1976, but the emphasis in the initial year's activity was on system prove-in and design modifications. Data for 1977 will be discussed in this report, since the system was in its final configuration for most of the year (the instrumentation system was not fully operational during January and February). Due to measuring equipment limitations, the detailed

data gathered is insufficient to provide a thoroughgoing evaluation of each of the solar heating subsystems. The fuel use data, however, more than makes up for this deficiency, since a comparison of overall solar system performance is then possible by examination of similar information for the control building.

In order to sensibly discuss the performance of the system and to compare these results with long-term predictions, pertinent meteorological data for 1977 must be considered. Figure 22 presents observed insolation and degree-day information for 1977 and provides a comparison with the long-term averages of these quantities. It can be seen that 1977 was somewhat more favorable for solar energy collection and use than average and somewhat less severe in required energy for space heating.

In fact, on a yearly basis, the Washington, D.C. area received almost 5 percent more solar flux, required about 5 percent less heating energy than normal, and received 12 percent less rainfall than normal. Over the heating-season months, however, it should be noted that in the January-April period the area received greater-than-normal insolation, but in September, October, and November, solar radiation was less than normal. It can be concluded that the year was slightly more favorable than normal for solar energy, but the performance observed should be substantially accurate as an indicator of long-term system effectiveness.

B. Typical Daily System Performance

In Figure 23, the solar energy collection hour-by-hour during a typical sunny day is shown. The observed insolation exhibits the characteristic pattern of rising intensity during the morning hours, peaking at noon (in

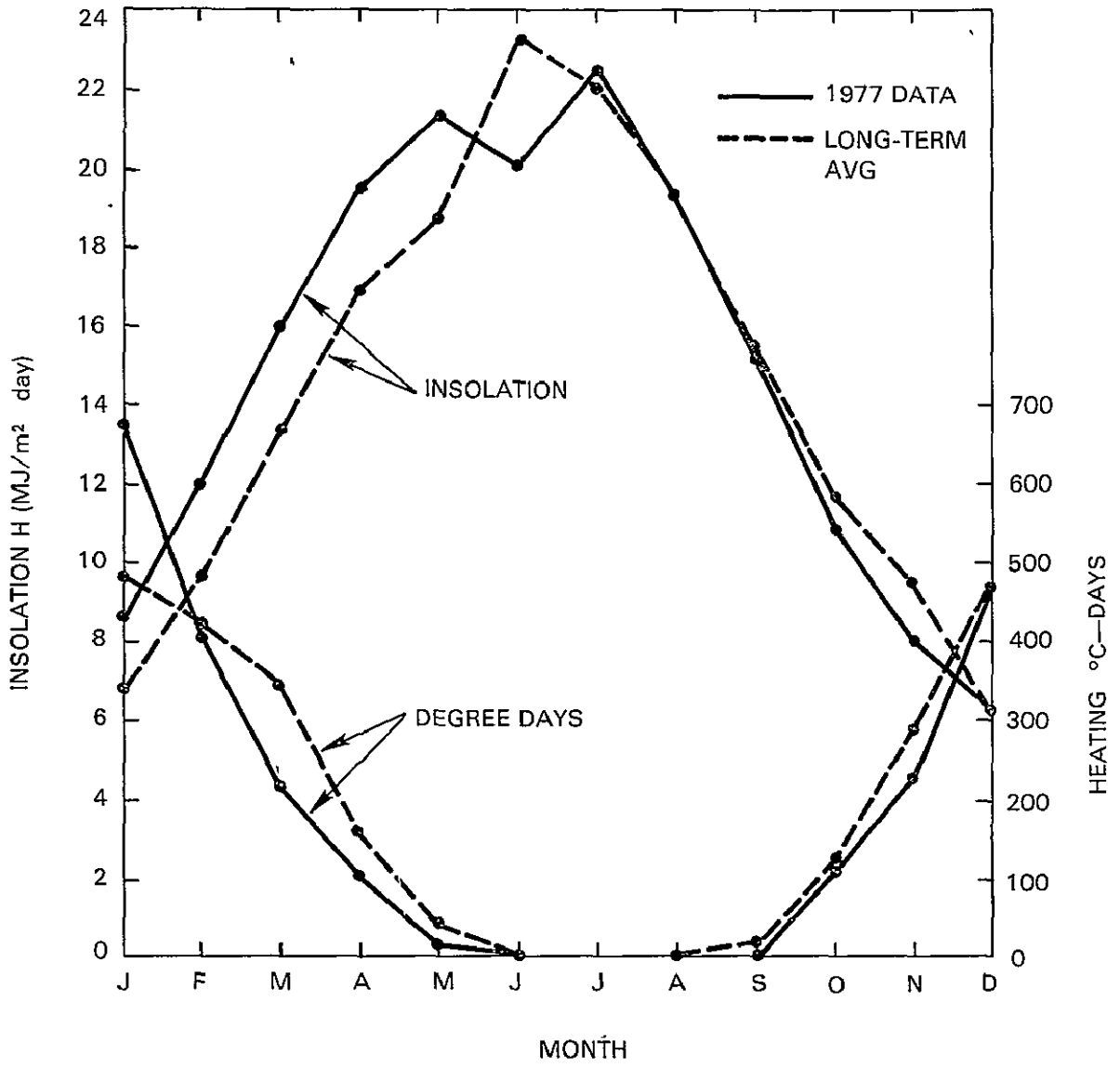

Figure 22. 1977 Weather Data

mid-December, local noon is essentially equivalent to solar noon), and declining till sunset. Solar energy is not immediately collected; rather, only when the collector temperature becomes greater than the storage temperature does collector-loop circulation begin. The two hour delay before solar energy collection begins (and the premature shutdown of the collector system 1 hour before sunset) was typical of the observed results.

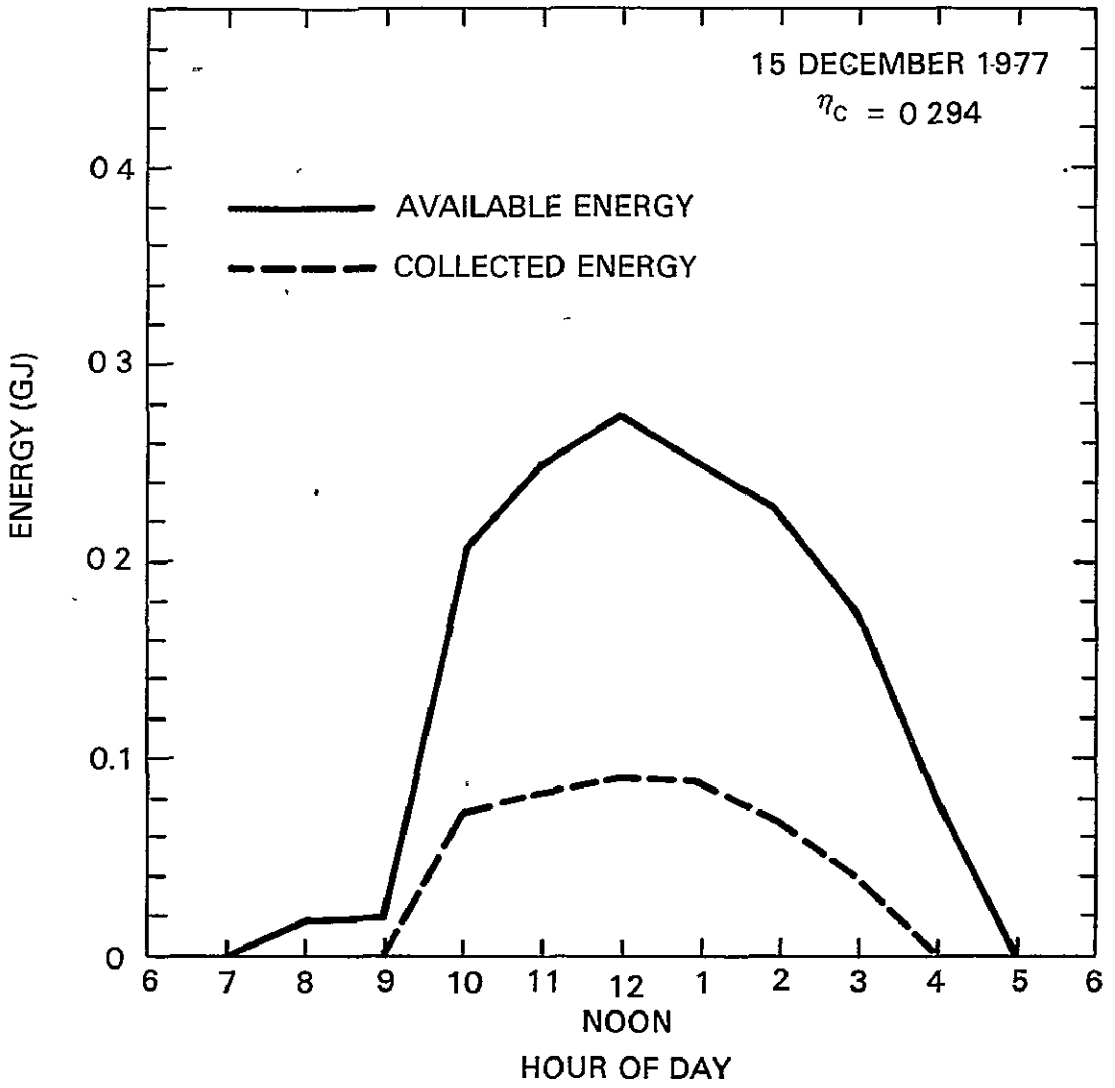

Figure 23. Typical Daily Collected Energy

The overall observed collection efficiency of 29 percent is a quite acceptable figure, particularly considering the delayed collector start-up and early shut-down (thus causing the collector efficiency to be zero during these hours). The "instantaneous" collector efficiency at noon can be seen to be about 34 percent; the observed 52°C collector inlet temperature and 9.6°C ambient temperature result in a predicted single-collector efficiency

of about 44 percent from Figure 7. This discrepancy is not surprising when comparing single module bench test data to multiple module collector system performance.

Solar energy provided almost 60 percent of the building space heating load on December 15, which is to be expected for a (rare in December!) sunny, relatively mild day (average outdoor temperature: 5°C). As we will see in Section C, the monthly space heating load fraction supplied by solar energy during December 1977 was on the order of 1 percent, which is to be expected in December and January.

C. Typical Monthly Performance Data

Monthly solar collection system performance data is presented in Figures 24, 25, 26, and 27. In each case, the available solar energy (Q_S) and the energy actually collected (Q_C) are shown plotted on a daily basis. The monthly average ambient temperature, total available solar energy, and collected solar energy, as well as the average collection efficiency, are shown for each of the monthly data summaries.

Typically, monthly average collection efficiencies for the system are on the order of 30 percent. During the summer months, (represented by Figures 24 and 25 for June and July, 1977) the system essentially functions as a domestic hot water heater, since the space heating load is negligible during these months. For June and July, the fractions of the required heating load supplied by solar energy were 92 and 99 percent, respectively.

During the spring and fall months (represented here by data for October, Figure 26), a substantial portion of the space heating load as well as much of the domestic hot water heating could be expected to be supplied by

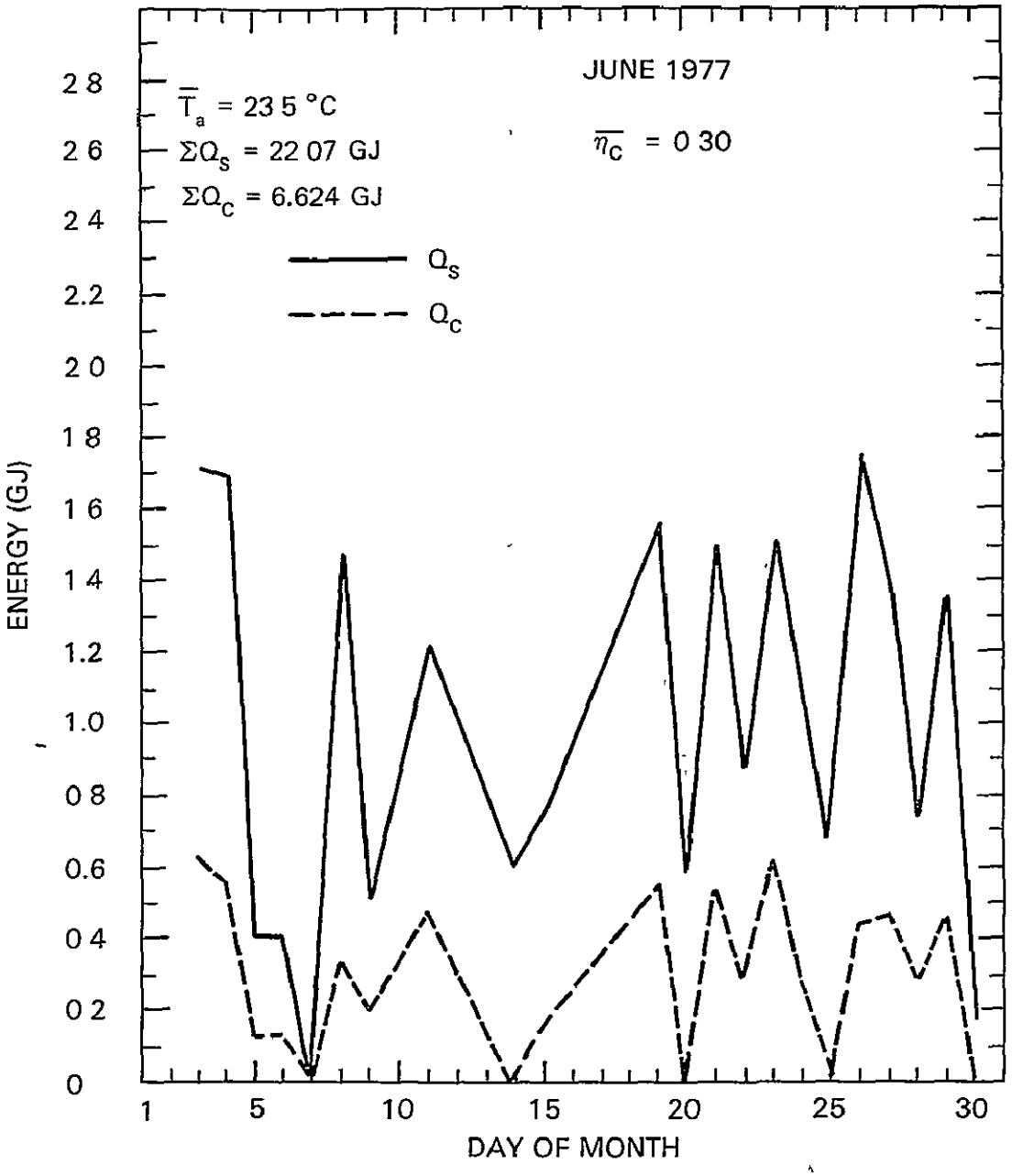

Figure 24. Monthly Collected Energy — June 1977

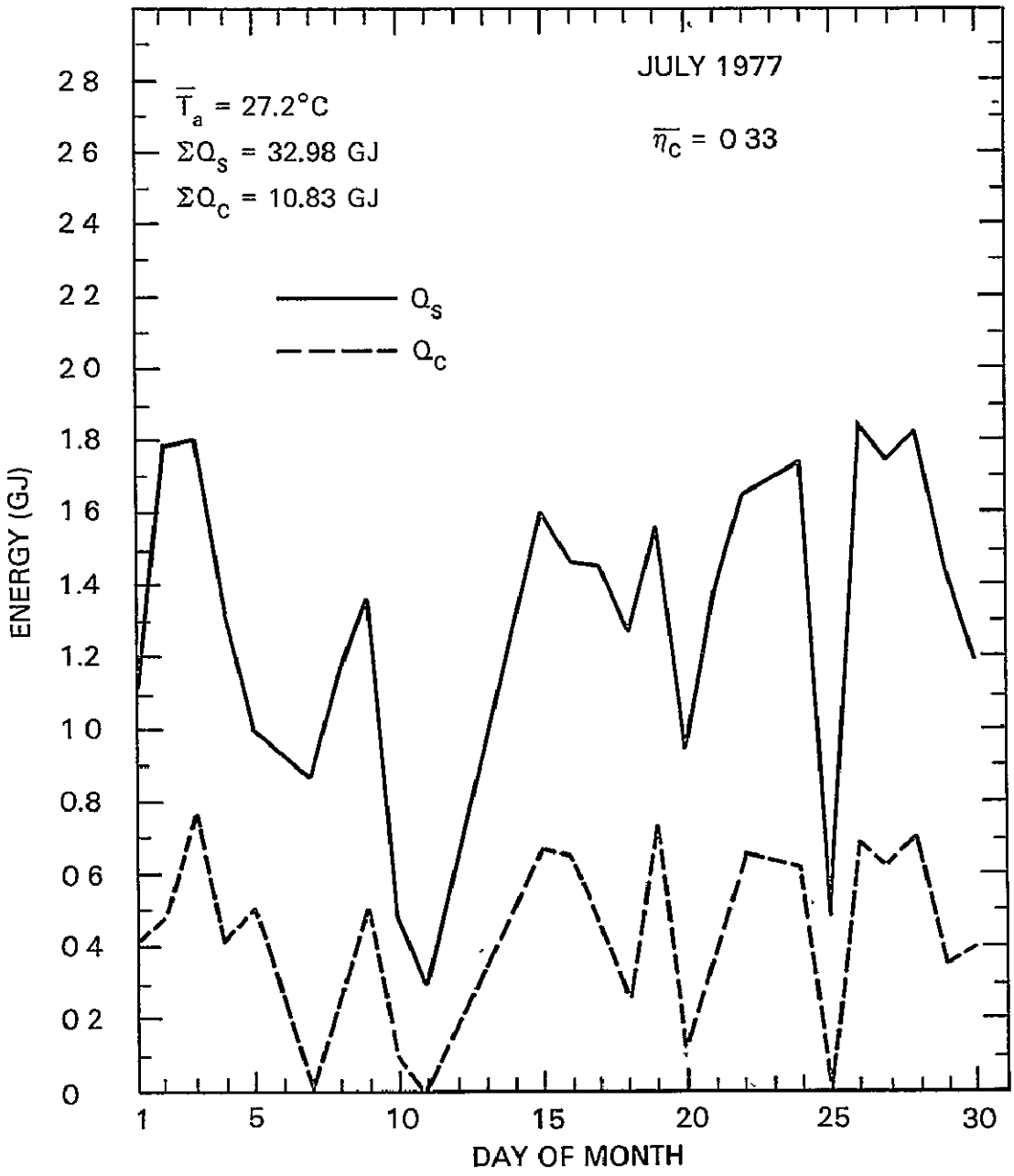

Figure 25. Monthly Collected Energy — July 1977

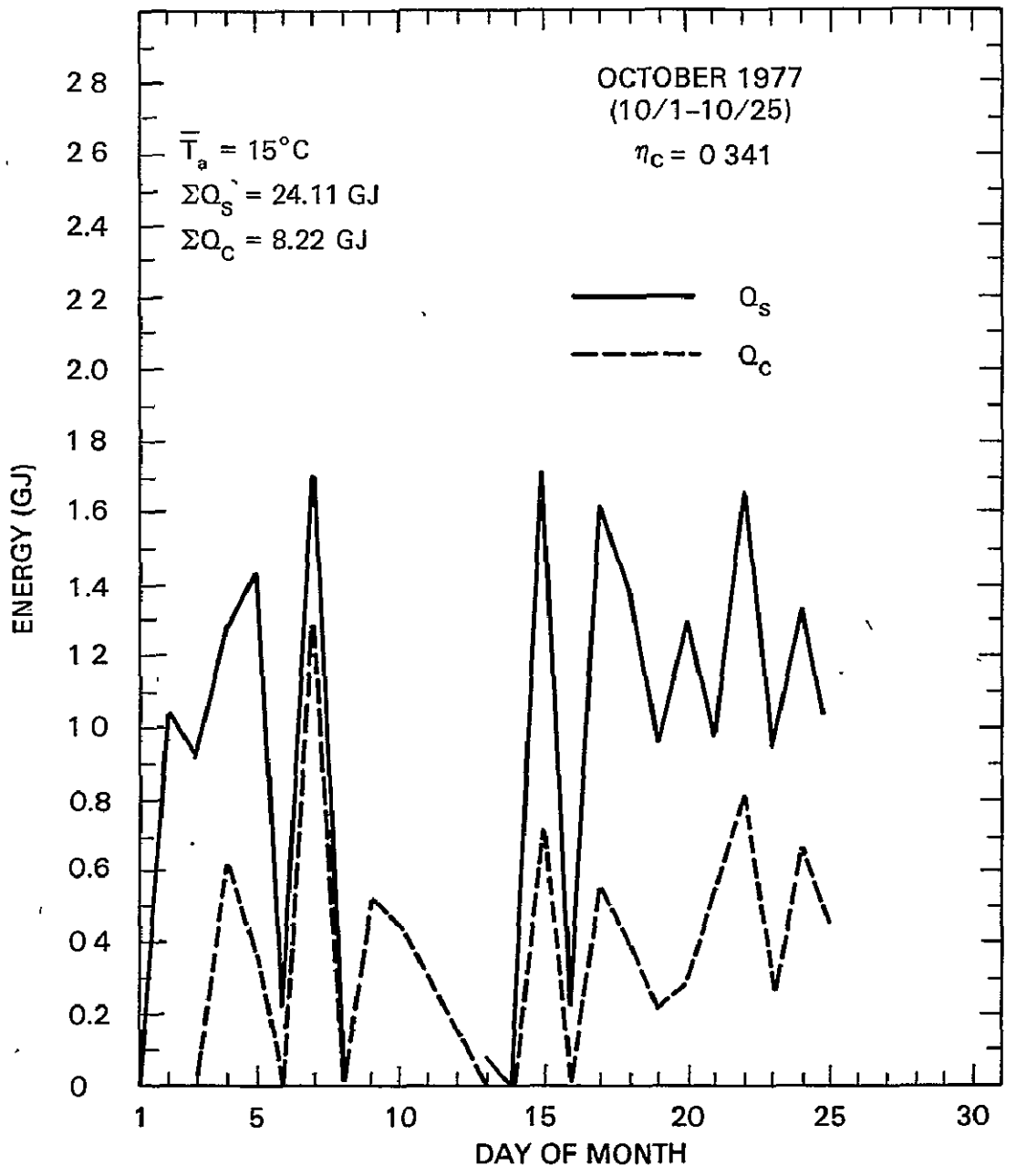

Figure 26. Monthly Collected Energy — October 1977

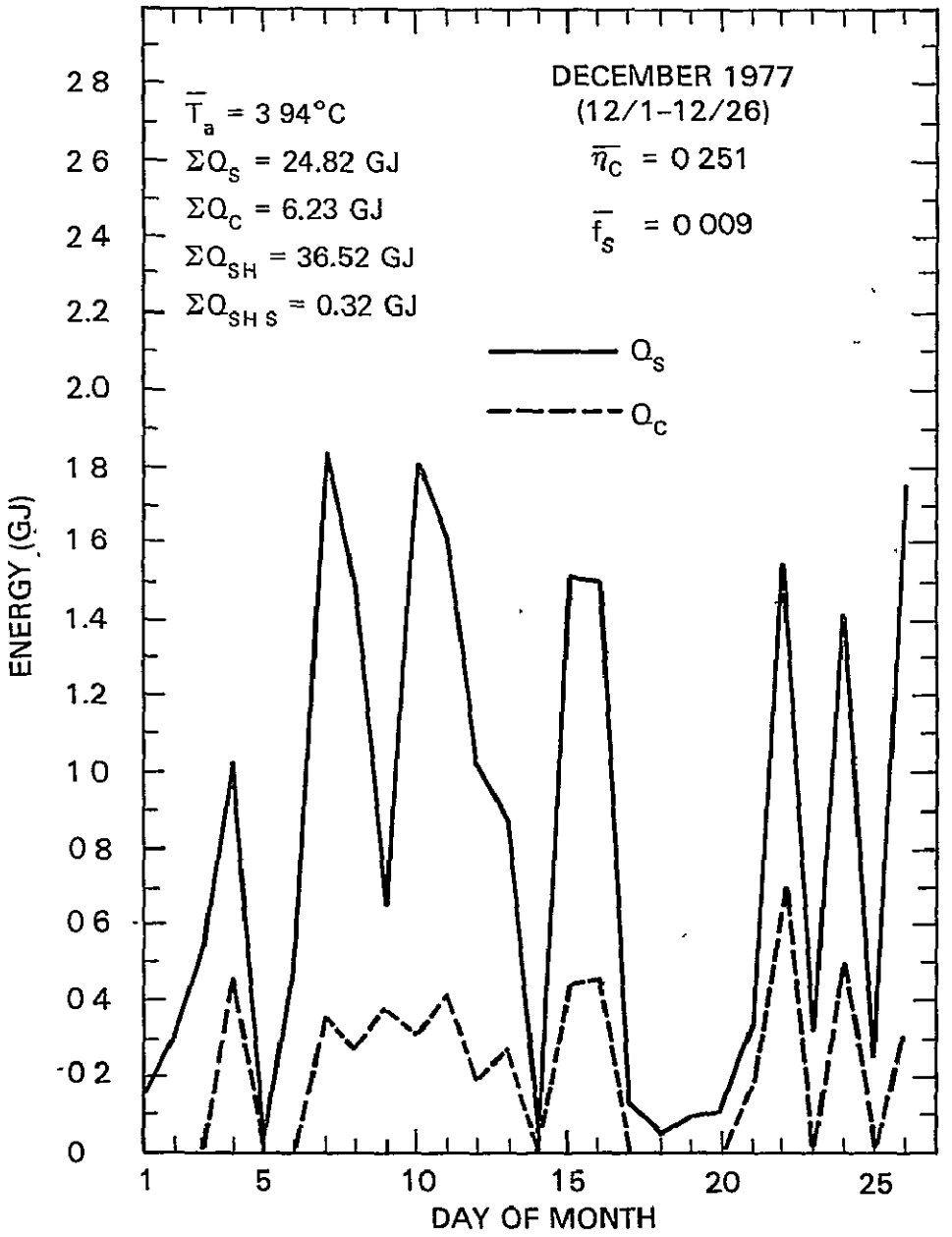

Figure 27. Monthly Collected Energy — December 1977

the solar energy system. This is in fact what is noted; 53 percent of the total heating load during October was supplied by the solar energy system. During this month about 70 percent of the heating load can be attributed to space heating.

Finally, during the winter months, the solar system once again functions as a domestic hot water heater, due to the high-temperature radiator water required to provide suitable building space heat. (Note that the solar system performance could perhaps be improved by varying (increasing) radiator flowrate in addition to calling for high radiator supply temperature when increased heating is called for by low ambient temperatures.) The monthly average collector system efficiency dropped to 25 percent during December, which can be attributed to longer collector start-up delays due to low ambient temperatures (collector loop circulation does not begin until the collector outlet temperature is higher than the storage water temperature) and to larger collector-inlet to ambient temperature differences.

D. Annual Performance by Comparison to Control Building Data

The data described in Sections B and C above was primarily derived from detailed temperature, insolation, and flowrate data gathered by the installed Data Acquisition System. In this section, system performance is examined by considering the ultimate arbiter of solar system effectiveness: economic savings accrued by use of the system.

Detailed fuel use data for both the solar energy research home and the control building were obtained throughout the year. These data are displayed in Table 9, along with the resulting fuel savings, solar savings in dollars, and the inferred fraction of total energy provided by the solar subsystem.

As might be expected, these fractional values are on the order of 20 percent during the winter months, rising to almost 100 percent in the summer when the system is called upon to provide domestic hot water only. The overall yearly fraction of heating load supplied with solar energy was 39 percent. Also shown are corrected total values accounting for the observed 6 percent discrepancy in hot water use between the control building and the solar residence. As previously mentioned, the correction is small.

The data is presented in graphical form in Figure 28. As can be seen, although fuel use varies dramatically through the year, the solar system savings is less variable. This is because the system functions very effectively as a domestic hot water heater, adding space heating to this baseline load when conditions permit.

E. Comparison of Results to Expected Thermal Performance

The primary output of the f-chart design procedure (carried out for the Greenbelt Project and described in Appendix C) is the expected long-term-average fraction of the total heating load which can be expected to be supplied by solar energy (f). Figure 29 presents the observed f values as compared to those generated by the f-chart correlation.

The agreement is seen to be surprisingly good; the annual fraction of the heating load supplied by solar energy as predicted by the correlation is 40 percent as compared to the observed 39 percent. This good agreement can be regarded as being purely fortuitous, since many years of data are needed to predict long-term-average performance. Further, it will be recalled that the weather conditions for 1977 were actually more conducive than normal for solar energy use, so that one can conclude that the Greenbelt

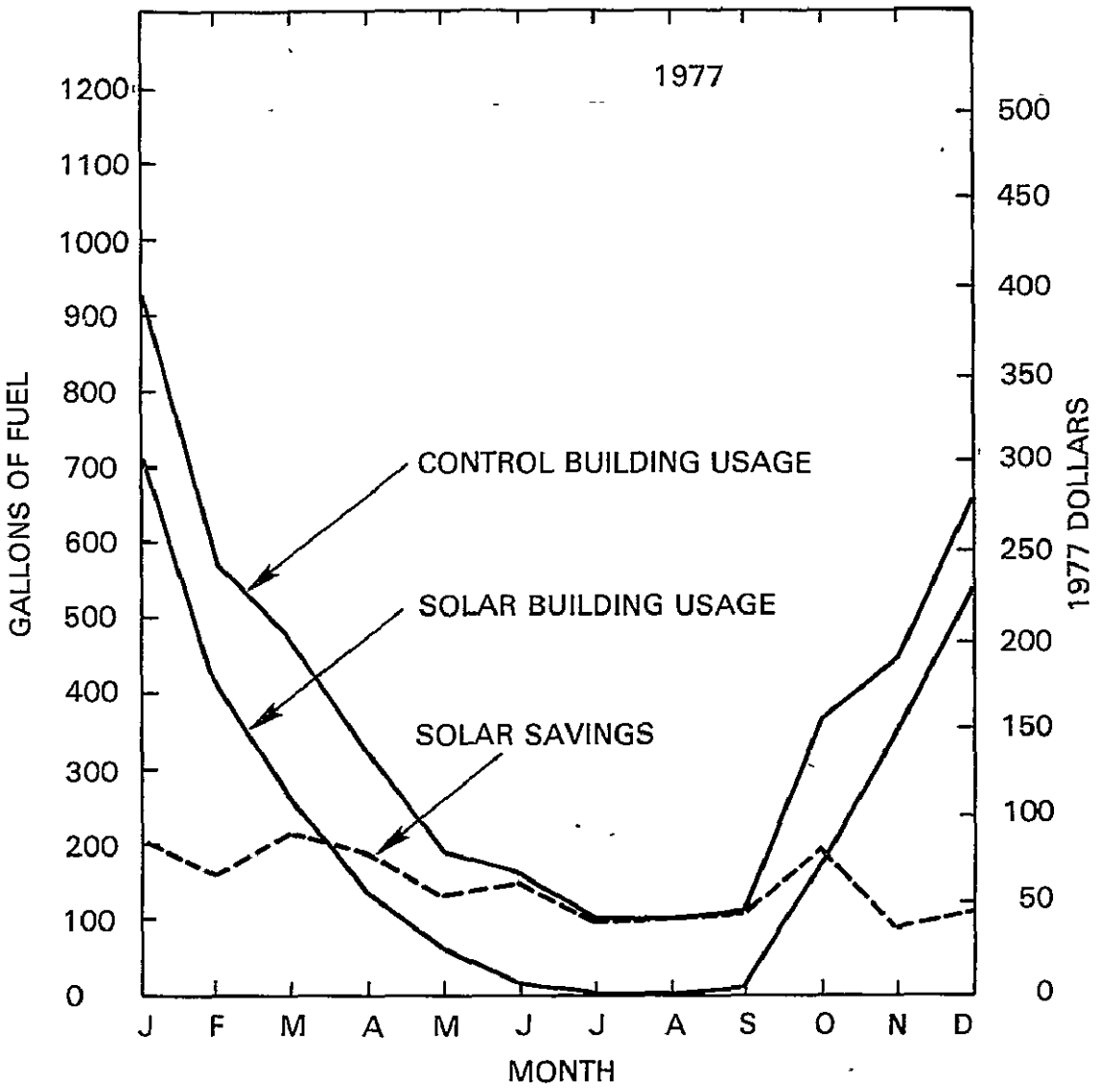

Figure 28. Performance of Solar System

Project solar system is somewhat less efficient than might be expected. Two factors are suspected to be the cause of this behavior: (1) the space heat exchangers used are probably undersized for solar energy applications, and (2) the control system can perhaps be adjusted to allow solar heating at lower storage temperatures.

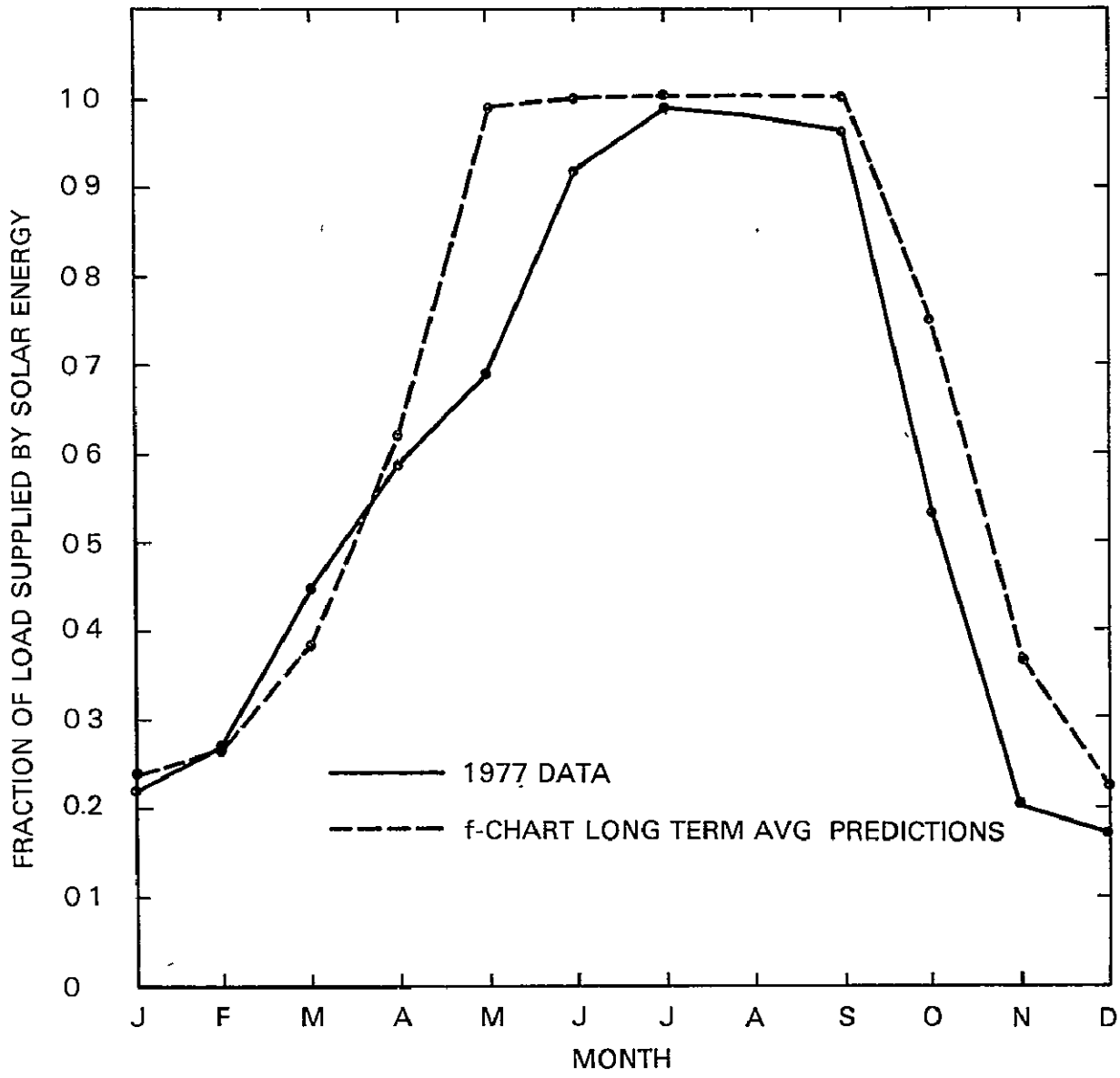

Figure 29. Comparison of Results to Theoretical Predictions

The system behavior is certainly qualitatively up to expectations. For example, January 1977 was more sunny than normal, but also much colder; these effects cancel each other, and thus the f-value for January was very nearly the predicted value. Similarly, November was nearly normal in temperature, but less than average in insolation, resulting in a lower-than-average value for f.

The performance of the system as a hot water heater is somewhat disappointing, as can be seen from the predicted and observed f values for the summer months. It is believed that this can be attributed to the slightly unusual recirculating system for heating service hot water. A more effective system would have a preheat hot water tank, of similar size to the REMCO heater, in series with this unit. Cold water would enter this preheat tank, be heated by solar loop water, then advance to the REMCO unit and the domestic user as required. The present recirculation system is suspected to result in significant thermal losses.

F. Operating Experience

Prior to March 1977, the Greenbelt Project solar energy system had been operating in what was essentially a test mode for check-out and improvement of the design. Several operating problems, such as that associated with collector freeze-up, were detected and solved during this period, as described elsewhere in this document. Of interest here is the system performance during 1977, which will serve as a baseline period for estimation of system reliability, extraordinary maintenance, and required operating electrical power.

The solar system was inoperative for six days during 1977, resulting in a system availability of 0.98 (system availability is the fraction of possible operating time during which the system actually performed acceptably). This somewhat low value is attributable to two problems of significance. First, the motor on the main solar loop circulation pump (P1) burned out early in the year. The pump motor was undersized for this application, and

a larger motor was used to replace the original. No problems with the replacement have been experienced.

The second system outage was due to a leaking collector panel in one of the lower collector banks. The problem was solved by replacing several inter-collector connecting hoses and subsequent system re-balancing. It is suspected that this problem was residual damage from the prior collector freezing episode, which occurred in the same region of the collector bank.

Inspection of these hoses and connections is recommended as a periodic (i.e., spring/fall) preventive maintenance item.

One of the costs incurred by installation and use of a solar energy system is the additional electrical energy used by the system's motors and controls. The additional electrical energy used in the solar research home averaged some 400 kwh per month, of which about 100 kwh could be atttributed to the instrumentation and data acquisition system. Thus, 300 kwh (or, say, $18 per month at current energy prices) was used by the solar energy system itself. On an annual basis, this cost reduces the net solar savings by some 30 percent, which of course is quite significant. Improvements of the system, to be described in Section V below, should reduce the electrical energy use chargeable to the solar system to an estimated 100 kwh per month.

V. Summary and Recommendations

In this document and its appendices, the origin, design, and performance of the Greenbelt Project experimental solar heating system has been described. The system was intended to serve as a demonstration project to

explore the economics and aesthetics of solar heating for retrofit applications in the Washington, D.C. area, especially for multi-family dwellings. The effort was unusual in that the research building was subject to continuous occupancy during design, construction, and prove-in of the system. Also, an identical building was available to serve as an experimental control, greatly facilitating solar system performance assessment.

The solar system, with 84.3 m^2 of active collector surface area, was found capable of supplying on the order of 40 percent of the heating and domestic hot water needs for the test building, representing an annual savings of somewhat more than $700 at current bulk rate fuel prices. Costs for the research system, because of its custom design and other factors, are not easily reduced to an expected initial cost for similar systems. As discussed in Appendix D, a reasonable estimate for the initial installed cost of such a system would be in the range of $15-18,000.

As noted in Appendix D, the present system is not of optimum size for economic purposes. Such an optimum system would have a collector area of about 50 m^2 for this application, at a cost of some $11,000. Even this economically optimum system, however, will not prove to be an outstandingly advantageous investment at current fuel costs (particularly the bulk oil rates charged to Greenbelt Homes). It should be noted here that these economic conclusions are limited to the Greenbelt Homes situation. Factors such as tax rates, availability of capital, and individual energy costs could change both the optimum system sizing and the overall profitability of solar heating systems for different applications. Even for the Greenbelt application, a rise in fuel costs of, say, 10-15 percent without an equivalent rise in

solar system costs would make the installation of solar heating systems desirable.

Just as the presently-installed solar system is not economically optimal, so it is not technically optimal. Hands-on operating experience has led to the following design change recommendations which will result in better solar system operation:

A. Currently, the collectors are mounted in two tiers, forming one face of a gable-roof configuration. To minimize pumping power requirements, the upper collector tier should be mounted at the same elevation as the lower. Sufficient roof space is available so that shading should not be a problem.

B. During collector-bypass mode operation, greatly reduced pumping power is required, since the solar fluid does not have to be pumped up to the level of the collectors. Use of a variable speed pump motor on pump P1, or even two separate pumps, should be used, one pump or speed for each solar loop mode. The pump is currently sized for the collection mode and is thus greatly oversized for the bypass mode—thus wasting electrical energy.

C. After the initial start-up period, no problems with collector piping corrosion were experienced. Nevertheless, use of a copper collector and piping system should be investigated, since a twenty year system life will probably be required for economic viability.

D. Solar space heating was inhibited by the load heat exchanger configuration employed. Specifically, the cast iron radiators, while ideal for boiler-heated water, are undersized for solar applications, in which the

heating fluid temperatures are somewhat lower. Finned hot water baseboard units are recommended.

E. A domestic hot water preheat tank should be used rather than the present recirculation scheme. This will save electrical energy as well as facilitating more effective solar water heating.

F. Any future solar system design for the present application should consider solar cooling as well as heating, since this is expected to be at least as cost-effective as solar heating. Also, the system should be designed economically optimal according to the prevailing economic conditions and the situation of the potential solar system owner.

In sum, the Greenbelt Project Solar Heating Program has proved to be quite successful in achieving its original goals. Solar space and hot water heating has been demonstrated to be technically realizable for retrofit application to multi-family dwellings. Although not currently economical for the Greenbelt Homes situation, solar heating is close enough to being economically viable to warrant periodic reexamination as energy and solar equipment costs change. Finally, much was learned about both the technical and the economic aspects of solar energy retrofit installations for multi-family dwellings.

VI. References

1. Trewartha, G., An Introduction to Climate, 4th Ed., McGraw-Hill, New York, 1968.
2. National Oceanic and Atmospheric Administration, Climate of the States, NOAA Water Information Center, Port Washington, New York, 1974.

3. U.S. Department of Commerce, Climatic Atlas of the U.S., DOC/ESSA, Environmental Data Service, 1968.

4. Power Systems Division, Lewis Research Center, "Standardized Performance Tests of Collectors of Solar Thermal Energy — A Selectively Coated, Steel Collector with One Transparent Cover," NASA TMX-71870, 1976.

5. ASHRAE Guide and Data Book, Applications Volume, Chapter 59, American Society of Heating, Refrigerating, and Air Conditioning Engineers, 1974.

Appendix A — Data Acquisition and Handling System

Introduction

The Greenbelt Project presented a unique opportunity to gather data pertaining to a retrofitted solar heating/domestic hot water system for a multi-family dwelling with a virtually identical building available to serve as a control for the experiment. Accordingly, the research home was outfitted with an array of thermocouples and other measuring devices, and necessary corresponding transducers were installed in the control building. The flow path of the gathered data is shown in Figure A.1.

Data Acquisition System

The characteristics of the major data acquisition equipments are summarized in Table A.1. Data from various measuring points was automatically sampled; other data was manually read. The sampling frequency was pre-set—half hourly between the hours of 8:00 a.m. and 4:30 p.m., hourly at other times and on weekends—using a digital data logger (Doric Scientific Digitrend Model 210) located in the solar home mechanical room. Millivolt inputs (from thermocouples, pyranometer, and valve and pump on/off indicators) are internally converted to digital signals and linearized and scaled in the case of temperatures by the Digitrend 210. Permanent output was via a printer and paper tape.

Key temperatures throughout the solar system, storage tanks, solar home living space, and control building were monitored using ASTM Type T (copper-constantan) thermocouples. The locations of the thermocouples in the energy system are shown in Figure A.2, while the collector array temperature measurement points are detailed in Figure A.3.

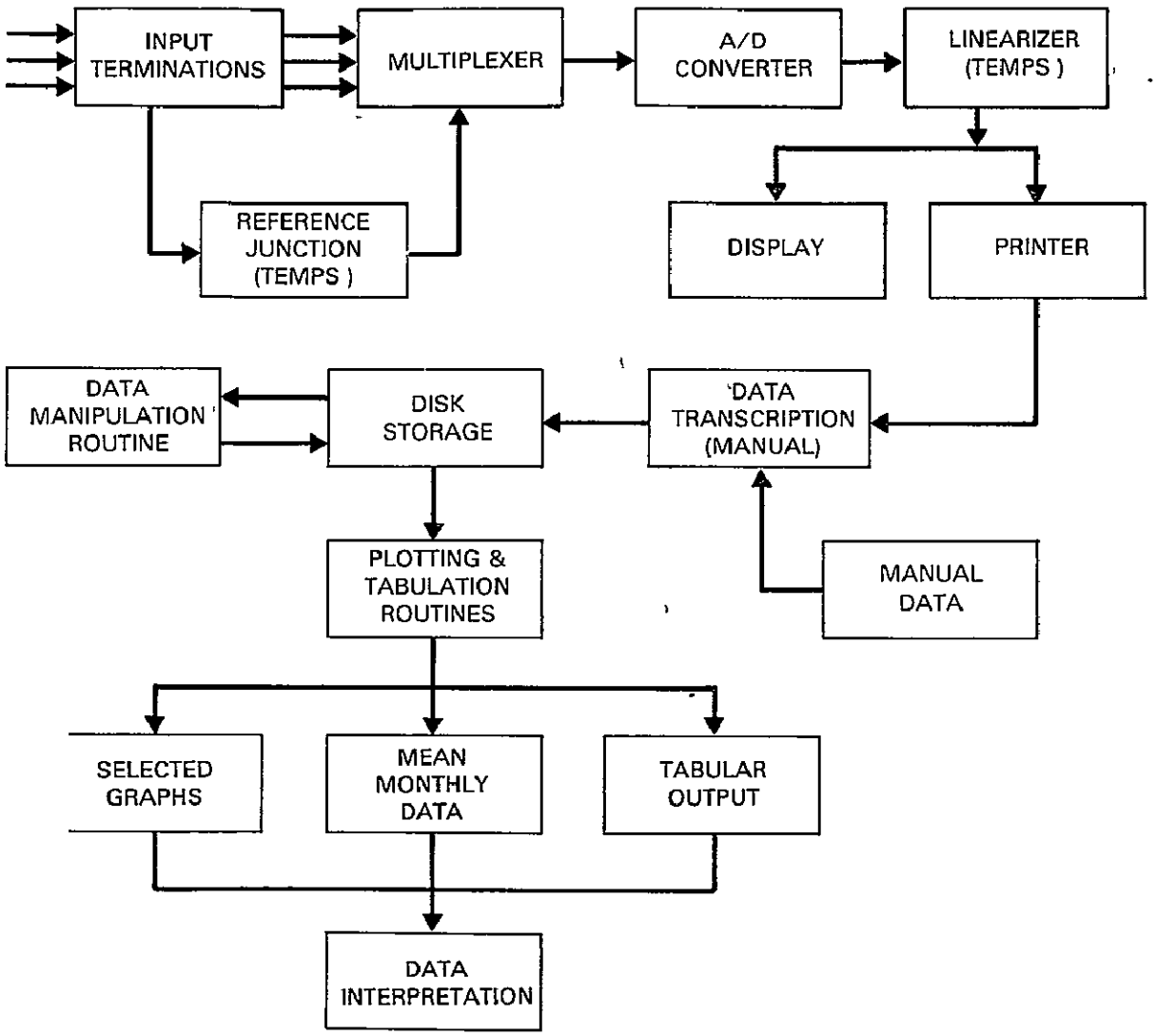

Figure A.1. Data Flow Diagram

FOLDOUT FRAME 1

ORIGINAL PAGE IS
OF POOR QUALITY

ORIGINAL PAGE IS
OF POOR QUALITY

FOLDOUT FRAME 2

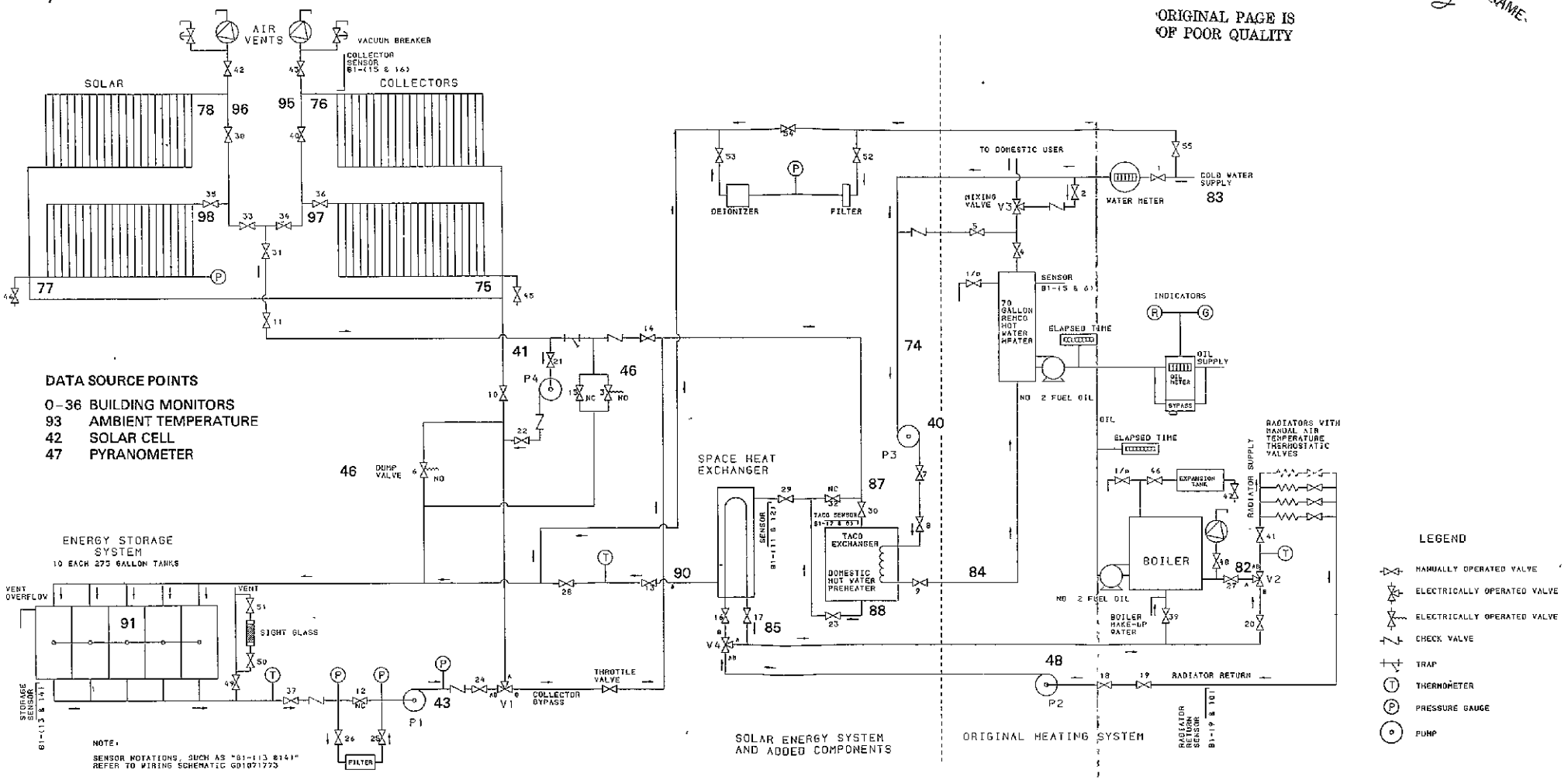

Figure A.2. Temperature Monitoring Points

Table A.1. Data Acquisition Equipment

Data Logger	
Manufacturer	Doric Scientific
Model number	Digitrend 210
Temperature range	-190 to 400°C
Calibration accuracy	±0.3°C
Millivolt range	±200 mv
Calibration accuracy	±0.00 4 mv
Number of channels	100
Channel scan rate	2 channels/sec.
Pyranometer	
Manufacturer	Eppley Laboratories, Inc.
Model	Pyroheliometer Model 150
(Calibrated 12/76)	
Thermocouples	
Manufacturer	Copper-Constantan
Type	(ASTM Type T)
Flowmeter (collector array)	
Manufacturer	Bell & Gossett
Model	Thermoflo TF1-1 1/4
Range	10-40 g pm
Integrating fuel meter	
Manufacturer	Flowtron Industries
Model	PM-100
Range	0-35 gallons/hour
Accuracy	±0.25%

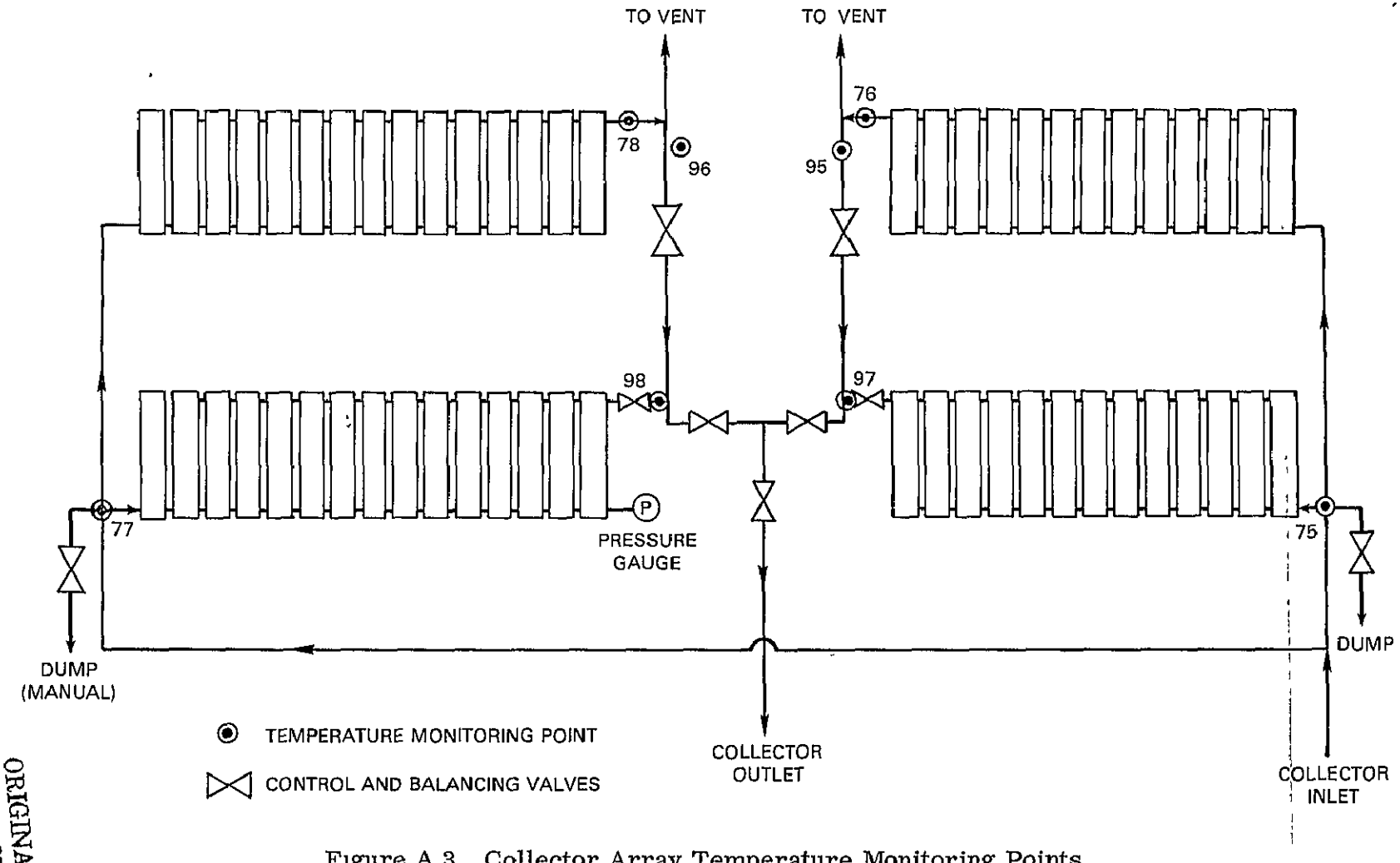

Figure A.3. Collector Array Temperature Monitoring Points

The incident solar radiation intensity was monitored using both a pyranometer and a silicon solar cell. The primary insolation transducer is the pyranometer, an Eppley Pyroheliometer Model 50 (calibration: 11.08 mV = 1000 W/m^2, calibrated against a pyranometer of known characteristics) mounted at 54° to the horizontal (collector tilt angle). The uncalibrated silicon solar cell is used as a back-up device rather than a primary source of input energy data.

The solar collector loop flow rate during collector mode operation was measured intermittently using a Bell & Gosset hydronic flowmeter and found to be in the range 57-68 1/min (15-18 g pm). This is an example of manually monitored data used in calculating energy system performance characteristics. Note that greater accuracy in collector flow rate determination is not really required since system performance is only weakly dependent on this quantity.*

Radiator loop flow rates were also not measured directly; the required data for use in the data analysis program was supplied by GHI engineers based on their knowledge of the conventional heating system. This lack of accurate data does not pose a severe problem because system energy flows can often be calculated using other measured quantities.

Fuel consumption was monitored using a Flowtron Industries integrating fuel meter outfitted with a custom power supply. This meter was read manually; the manufacturer claims an accuracy of ±0.25% for the device. Domestic hot water consumption was obtained using a conventional water meter.

*Beckman, W. A., S. A Klein, and J. A. Duffie, Solar Heating Design, Wiley, New York 1977, p. 66.

The location, nature, and channel designation of all automatically recorded data are shown in Table A.2.

Table A.2. Thermocouple Locations

Channel Number	Location	
00	Reference Calibration Voltage (214.4 ± .2)	
01	2-D Downstairs Radiator Supply Line	
02	2-D Downstairs Radiator Return Line	
03	2-D Downstairs Room Air Temperature	
04	2-D Upstairs Radiator Supply Line	
05	2-D Upstairs Radiator Return Line	
06	2-D Upstairs Room Air Temperature	Solar Heated Bldg.
07	2-C Downstairs Room Air Temperature	
09	2-A Downstairs Radiator Supply Line	
10	2-A Downstairs Radiator Return Line	
11	2-A Downstairs Room Air Temperature	
12	2-A Upstairs Room Air Temperature	
17		
18		
21	2-E Downstairs Radiator Supply Line	
22	2-E Downstairs Radiator Return Line	
23	2-E Downstairs Room Air Temperature	
24	2-E Upstairs Radiator Supply Line	
25	2-E Upstairs Radiator Return Line	
26	2-E Upstairs Room Air Temperature	
27	2-F Downstairs Room Air Temperature	Control Bldg.
28	2-G Upstairs Room Air Temperature	
29	2-H Downstairs Radiator Supply Line	
30	2-H Downstairs Radiator Return Line	
31	2-H Downstairs Room Air Temperature	
32	2-H Upstairs Room Air Temperature	
33	2-F Downstairs Radiator Supply (Future)	
34	2-F Downstairs Radiator Return (Future)	
35	2-G Upstairs Radiator Supply (Future)	
36	2-G Upstairs Radiator Return (Future)	
37	Available for future connection	
38	Available for future connection	
40	Pump 3 (0 mV = off, 25 mv = on) Digitrend prints out with on/off trigger	

Table A.2. (Continued)

Channel Number	Location
41	Pump 4
42	Solar Cell (25 mv = 1000 w/m^2)
43	Valve 1 (5 mV = fill, 0 mV = By-Pass)
45	Valve 4 (5 mV = through Heat Exchanger, 0 mV = By-Pass) Digitrend prints out with a 5/0 mV trigger
46	Dump Valves 3 and 6 (0 mv = Closed, 5 mV = Open)
47	Pyranometer (11.08 mV = 1000 w/m^2)
48	Pump 2 (0 mV = off; 25 mV = on)
73	Remco Output Temperature
74*	Taco Heat Exchanger Inlet (Domestic Side)
75*	Rt. Collector Array Inlet Temp.
76	Upper Rt. Collector Outlet Temp.
77	Left Collector Array Inlet Temp. Outside Pipe Temp.
78	Upper Left Collector Outlet Temp.
82*	Radiator Supply Water Temp.
83	Cold Water Supply
84	Taco Heat Exchanger Outlet Temp. (Domestic Water Side)
85*	Space Heat Exchanger Outlet Temp. (Radiator Side)
86*	Radiator Return Water Temperature
87*	Taco Heat Exchanger Inlet (Solar Side)
88*	Taco Heat Exchanger Outlet (Solar Side)
89*	Space Heat Exchanger Inlet (Solar Side)
90*	Space Heat Exchanger Outlet (Solar Side)
91	Storage Tank Temperatures
93	Ambient Air Temp.
95	Upper Rt. Collector Outlet (in well)
96*	Upper Left Collector Outlet
97	Right Lower Collector Outlet Temp.
98	Left Lower Collector Outlet Temp.

*Thermocouple placed inside piping 5/20/77.

Data Handling and Manipulation

As previously noted, the flow path of the gathered data is shown in Figure A-1. The paper tape output from the data logger, gathered daily, was transcribed to data coding forms and subsequently input to a Hewlett-Packard 9830 Desk Calculator and entered into floppy-disk storage.

At convenient intervals, the data was retrieved and manipulated to give both graphical and tabular output using specially prepared BASIC language programs. The usual form of output for daily data was automatically generated plots of significant system performance parameters. Monthly data is primarily tabular.

Appendix B — Data Analysis Relationships

Introduction

The purpose of this Appendix is to detail the relationships by which the raw data taken during the course of the experiment has been reduced to allow a performance assessment of the solar energy system to be made. When combined with economic considerations, this system performance data can then be used to assess the reasonableness of the "solar solution."

It is useful at the outset to define "performance." A suitable definition for the performance of the system might be "the efficacy with which the system fulfills its intended function." A performance assessment consists of the qualification of those operating parameters related to system function. For purposes of this section, only thermal performance is of concern, i.e., technical performance as opposed to that ultimate arbiter of success—economics. A thermal performance calculation is really an energy flow inventory.

System Performance Variables

Tabular and graphical data, discussion of system performance, and related conclusions resulting from this study are contained in Section IV of this report. The relationships used to reduce the raw data to parameters directly or indirectly indicating system and subsystem thermal performance are to be presented here. In order to facilitate this presentation, a listing of the primary and subsidiary variables of importance as well as the equations that are used to calculate them will be made. Potential uncertainties in the data will also be noted.

In many cases, instantaneous, daily, and monthly total values for the performance variables could be identified. Instantaneous rate data is not really pertinent to solar system evaluation. Daily data is useful in the diagnosis of problems in system operation and design, but is too voluminous for convenient performance comparisons. The primary data to be used for both technical and economic performance analyses are mean monthly values of the various system energy flows.

Primary performance variables include*:

a. Insolation, I. This of course is a measure of the rate at which solar energy is made available to the system, on a per-unit-area-of-collector basis. Insolation in the present study is directly measured with a pyranometer, as described in Appendix A. Overall insolation measurement accuracy was estimated to be ±2 percent.

b. Available solar energy, Q_s. This is an integrated value of the solar energy flux incident on the collectors. If A is the collector active area, the daily value of the available solar energy is

$$Q_s = \int I\,A\,dt, \qquad \text{(B.1)}$$

Where the integral is carried out numerically over 24 hours of sampled data. Monthly values of Q_s are obtained by summing the daily totals. An estimate of the integration error due to the use of Simpson's Rule is ±2 percent, so that Q_s is known to ±4 percent.

* Superscript dots indicate energy flow rates. Energy quantities are expressed in J (SI system) or in BTU (British Engineering System). Efficiencies and effectiveness are dimensionless.

c. Collected solar power, $\dot{Q}_c$. This is a measure of the rate at which solar energy is collected. An instantaneous energy balance on the collector array results in an equation for $\dot{Q}_c$ in terms of the collector fluid flowrate, specific heat, and temperature drop:

$$\dot{Q}_c = \dot{m}_s C_p \Delta T_c \tag{B.2}$$

Here $\dot{m}_s$ is the mass flow rate of the solar loop fluid through the collectors, C_p is the collector fluid specific heat, and ΔT_c is the fluid temperature difference between collector inlet and outlet. For actual data reduction, $\dot{Q}_c$ is calculated only when valve V_1 is in the bypass mode, the energy collection rate is taken to be zero.

Uncertainty in the collector mass flow rate is taken as ±5 percent, mainly due to the infrequent readings taken of this variable. However, pump P_1 operates in a throttled condition, so that $\dot{m}_c$ should not greatly fluctuate. Errors in fluid temperature measurement are expected to be of the order of ±3 percent, and thermal properties are taken to be known exactly. Then the error in $\dot{Q}_c$ is about ±6 percent.

d. Collected solar energy, Q_c. This is the time-integrated value of the collected solar power,

$$Q_c = \int \dot{Q}_c \, dt, \tag{B.3}$$

and is evaluated using the solar power data calculated as above. Considering the integration error, the uncertainty in Q_c is then estimated to be ±8 percent.

e. Integrated collector efficiency, η_c. This parameter is a direct measure of the time-averaged behavior of the collection subsystem. In terms of previously

defined variables,

$$\eta_c = \frac{Q_c}{Q_s} \tag{B.4}$$

With the previously mentioned uncertainties in Q_c and Q_s, the calculated collector efficiency is estimated to have a maximum uncertainty of ±10 percent. Thus, if η_c is computed as 70 percent, $0.63 < \eta_c < 0.77$.

f. Space heating load, or instantaneous radiator energy, $\dot{Q}_{SH}$. This is a measure of the rate at which energy must be supplied to the living space to achieve the required interior temperatures. The space heating load is dependent on radiator thermostat settings and outside ambient conditions (temperature, wind velocity and direction, insolation) but can be easily be estimated using monitored data by use of the equation

$$\dot{Q}_{SH} = \dot{m}_R C_P \Delta T_R \tag{B.5}$$

Here $\dot{m}_R$ is the radiator circulation flowrate. C_P is the specific heat of the radiator fluid (water), and ΔT_R is the temperature drop from radiator supply to radiator return. $\dot{Q}_{SH}$ is thus seen to be the heat rejected at the radiators.

In actuality, thermal losses throughout the system contribute to offsetting the space heating load. This fact, along with uncertainties in radiator flowrate and temperature measurement, results in an uncertainty in calculated values of $\dot{Q}_{SH}$ of 10 percent.

g. Space heating energy requirement, Q_{SH}. This is simply the time integrated value of $\dot{Q}_{SH}$,

$$Q_{SH} = \int \dot{Q}_{SH}\, dt \tag{B.6}$$

Daily values for Q_{SH} are calculated, using a Simpson's Rule integration routine, from the raw data. Monthly values are obtained by summing the daily values. The uncertainty in Q_{SH} is estimated to be ±12 percent.

h. Domestic hot water load, Q_{DHW}. A significant fraction of the energy demand for a residence can be attributed to the heating of hot water for domestic use. In the present system, hot water at a pre-set temperature (57°C (135°F)) is supplied to the residence; this constant temperature is achieved by use of an automatic mixing valve. A formal equation for

$$\dot{Q}_{DHW} = \dot{m}_w C_p \Delta T_w \qquad (B.7)$$

in which $\dot{m}_w$ is the hot water mass flowrate, C_p is the specific heat of water, and ΔT_w is the temperature difference through which mains water is raised before being delivered to the residence. Note that this equation assumes negligible losses during the water's time of residence in the hot water tank.

For the present work, however, an instantaneous value for $\dot{m}_w$ was not obtained; monthly values for the hot water consumption were measured with a standard water meter. This allowed the computation of Q_{DHW}.

i. Domestic hot water energy requirement, Q_{DHW}. Only monthly values for the energy consumed in heating water for domestic use were obtained. This was calculated with the equation

$$Q_{DHW} = m_w C_p (T_{HW} - T_C) \qquad (B.8)$$

in which m_w is the measured mass of water heated for domestic use, T_{HW} is the pre-set hot water temperature, and T_C is the mains water temperature. For the uncertainties involved in obtaining Q_{DHW}, see item 11 below.

j. Space heating energy supplied by solar system, $Q_{SH,S}$. This is a daily or monthly quantity indicating the contribution of the solar system to the space heating load. The solar system can supply energy to the radiator water only when, (a) valve V_4 allows boiler water to flow through the space heat exchanger, and (b) pump P_1 is operative, causing solar system water either from storage or from the collectors to flow through the space heat exchanger. Since the state of V_4 is noted on the data output, calculation of $Q_{SH,S}$ is facilitated. The appropriate equation is

$$Q_{SH,S} = \int \dot{m}_s C_p \Delta T_{SH} \, dt \qquad (B.9)$$

Here $\dot{m}_s$ is the flowrate in the solar loop, and ΔT_{SH} is the fluid temperature difference across the space heat exchanger on the solar side.

The integrand is taken to be non-zero only when conditions (a) and (b) above are met, and the integral is carried out over a single day. Monthly values are obtained by summing $Q_{SH,S}$ for each day of the month. Losses in the heat exchanger are taken to contribute to the heating of the building and so can be ignored. Estimated uncertainty in this variable is ±8 percent.

k. Domestic hot water energy supplied by solar systems, $Q_{DHW,S}$. Exact calculation of the solar contribution to the overall energy requirement for domestic water heating is not a straightforward exercise with the data points obtained and the data acquisition system used in this experiment. Solar water flows through the TACO (domestic hot water-solar water) heat exchanger whenever pump P_1 operates. We can then write

$$Q_{DHW,S} = \int \dot{m}_s C_p \Delta T_T \, dt - Q_L \qquad (B.10)$$

where $\dot{m}_s$ is the mass flow of solar water, ΔT_T is the temperature drop of this water across the TACO exchanger, and Q_L is the energy lost in the TACO exchanger.

The integral is carried out over those times when pump P1 is operating. The loss term accounts for energy given up in the TACO exchanger when there is no circulation on the DHW side as well as conventional losses when the exchanger is operative. In this analysis we ignore the loss term—as we have ignored parasitic losses from the hot water heater in the use of equation (B.8)—and recognize that during the heating season such losses contribute to meeting the space heating load in any case.

The solar energy supplied to the domestic hot water subsystem may be further broken down to gauge the magnitude of the error involved in neglecting the loss term. Solar energy is supplied in two ways: either by direct preheating of cold water being supplied to the hot water heater (when domestic hot water is being used in the residence) or by supplying make-up energy to hot water in the tank when pump P3 operates and forces it to flow through the TACO exchanger. Thus,

$$Q_{DHW,S} = Q_P + Q_R \tag{B.11}$$

that is, the total domestic hot water energy supplied by solar energy is the sum of that used to preheat mains water allotted for domestic hot water use and that supplied when P3 operates and recirculates domestic hot water.

Since the data recorder has been set to annotate the activation or deactivation of pump P3, Q_R is easily calculated as

$$Q_R = \int \dot{m}_s C_p \Delta T_T \, dt \tag{B.12}$$

Here again $\dot{m}_s$ is the mass flow rate of solar water (which of necessity flows through the TACO exchanger whenever P1 operates), while ΔT_T is the temperature drop of the solar water across the TACO exchanger. The integral in (B.12) is carried out only when both P1 and P3 are operating, and daily and monthly values of Q_R are obtainable.

Q_p is then the difference between $Q_{DHW,S}$ and Q_R, again presuming negligible losses.

Due to the approximations inherent in this analysis (caused by data acquisition limitations), the results for $Q_{DHW,S}$, Q_P, Q_R, and Q_{DHW} are estimated to have a possible error of ±25 percent.

l. Net solar energy supplied to storage, Q_{ST}. In order to assess the performance of the storage subsystem, an energy balance on this portion of the solar system must be made. Energy is added to the storage subsystem only when valve V_1 is in the collection mode, and can be computed from

$$Q_{ST} = \int \dot{m}_s C_p (T_{SHE} - T_{ST}) \, dt \qquad (B.13)$$

where the integrand is non-zero only when V1 is in the collection mode, T_{SHE} is the solar water temperature on exit from the space heat exchanger, and T_{ST} is the current storage tank temperature. Note that losses in the intervening pipes are presumed negligible. Estimated uncertainty in Q_{ST} is ±10 percent.

m. Useful energy supplied from storage, $Q_{ST,U}$. Useful energy can be supplied from storage only when valve V1 is in the bypass mode, and the energy given up can be calculated if flow rates and temperature drops through the space heat exchanger and the TACO exchanger are known.

Four situations can be envisioned: (a) V1 is in the bypass mode, but V4 is also in the bypass mode and domestic hot water is not being circulated; (b) V1 is in the bypass mode with only a domestic hot water load; (c) V1 is in the bypass mode and there is only a space heating load; (d) V1 is in the bypass mode and the solar fluid is giving up energy to both space heating and hot water loads. Detailed calculations differentiating these system operating modes are not possible with the data gathered.

The assumption will be made that all the heat losses in the storage use mode contribute to the space heating load at times when a net space heating load exists, and are negligible at other times. The former proviso is reasonable, while the latter is somewhat questionable.

With this assumption we can calculate $Q_{ST,U}$ as

$$Q_{ST,U} = \int m_s C_p \Delta T \, dt \qquad (B.14)$$

where the integral is taken to be non-zero only when V1 is in the bypass mode. The temperature drop to be used in (B.14) is, for purposes of analysis, the decrease in temperature of the solar water between the TACO exchanger inlet and the space heat exchanger outlet.

An alternative to the use of (B.14) is consideration of the net heat lost by storage when VI is in the bypass mode,

$$Q_{ST}' = \Sigma m_{ST} C_P (T_{ST1} - T_{ST2}) \qquad (B.15)$$

Here m_{ST} is the mass of water in the storage subsystem, T_{ST1} is the storage temperature when V1 switches to the bypass mode, and T_{ST2} is the storage temperature when V1 returns to the collection mode. The sum is carried out

C-2

for all periods of bypass mode operation in a twenty-four hour period (for daily data). The daily data are summed to give monthly totals. Q_{ST}' will be greater than $Q_{ST,U}$ by the amount of energy lost in the pumping process from storage to the heat exchangers and back again, as well as parasitic losses from the storage subsystem while V1 is in the bypass mode.

Due to the approximations made in calculating $Q_{ST,U}$, the overall error could be as large as ±25 percent.

n. Energy gain of storage, U_{ST}. This variable provides a balancing of the energy flows to and from the storage subsystem during a period of interest, and is given by

$$\Delta U_{ST} = m_s C_p (T_f - T_i) \qquad \text{(B.16)}$$

where m_s is the mass of water used as the storage medium, T_f is the storage water temperature at the end of the period of interest (day or month), and T_i is the storage temperature at the start of the period.

Uncertainties in ΔU_{ST} are primarily due to temperature measurement uncertainty; ΔU_{ST} is presumed to be known to ±4 percent.

o. Percentage of space heating load supplied by solar energy system, f_{SH}. This primary performance variable indicates the capacity of the solar system to provide space heat for the residence. As an equation,

$$f_{SH} = \frac{Q_{SH,S}}{Q_{SH}} \times 100 \qquad \text{(B.18)}$$

Note that a high value of f_{SH} does not necessarily imply that the solar system is economically optimal. Estimated uncertainty is ±14 percent.

p. Percentage of domestic hot water load supplied by solar system, f_{DHW}. This variable is analogous to f_{SH}, except that it pertains to the domestic hot water load. In equation form,

$$f_{DHW} = \frac{Q_{DHW,S}}{Q_{DHW}} \times 100 \qquad (B.19)$$

The uncertainty in f_{DHW} can be judged from the individual component uncertainties as ±28 percent. Both f_{DHW} and f_{SH} can be reported as daily or monthly percentages.

q. Building equipment effectiveness, E_o. An estimate of the overall thermal effectiveness of all heat transfer equipment in the solar building is supplied by this parameter, the ratio of the total heat load of the residence to the total energy supplied to the energy system. In equation form,

$$E_o = \frac{Q_{SH} + Q_{DHW}}{Q_c + m_f (HV)_f} \qquad (B.20)$$

The terms Q_{SH}, Q_{DHW}, and Q_c have all been defined previously. The mass of fuel burned in the period of interest is denoted by m_f, while the heating value of the fuel is $(HV)_f$. The estimated uncertainty in E_o is on the order of ±30 percent.

r. Solar system equipment effectiveness, E_{ss}. This is a measure of the heat transfer efficiency of the solar equipment other than the collection subsystem. In equation form,

$$E_{ss} = \frac{Q_{SH,S} + Q_{DHW,S}}{Q_c} \qquad (B.21)$$

The uncertainty in this effectiveness is ±30 percent.

s. Fuel savings in solar building. This, of course, is the "bottom line" in the thermal performance considerations for the Greenbelt Project. The existence of a monitored control building for this experiment can be seen to be highly advantageous for calculation of this ultimate performance index; if no control were used, the fuel savings would be computed from the net calculated heating load and the known amount of auxiliary fuel used. Since the numerical value of the load is only known to, say, ±15 percent, a more exact accounting of the net fuel savings is gained by comparing the actual fuel use of the solar residence and the control building. Any gross discrepancy in the loads of the subject buildings can be ascertained from the recorded temperatures and metered hot water use, and so can easily be accounted for in the final fuel savings figure.

Economic viability of the solar alternative is easily gauged through consideration of the net fuel savings and system costs. The technical performance of all the major subsystems (collection, heat transfer, and energy storage subsystems) is readily discernable by examination of the other 19 factors.

Appendix C — Theoretical Prediction of System Thermal Performance

To the consumer of solar energy systems, the key parameter is usually economic performance, that is, the net return on his solar investment over the operating life of the system. Central to the calculation of such economic performance data, of course, is an estimate of the expected thermal performance of the system—the net useful energy supplied.

Straightforward methods of solar heating system design have only recently been developed. In fact, such methods were not widespread at the time that the Greenbelt Project solar heating system was being designed. For this reason, the considerations used to determine the size and configuration of the solar components to be used (as briefly described in Section II) were fairly crude; as will be seen, however, the resulting design is really quite satisfactory.

Rational calculations for the thermal performance of a given system in a given location generally require two important pieces of information: (1) the amount of solar radiation that can be collected each month in the particular location of interest, considering both local insolation values and long-term collector efficiency values, and (2) reasonable estimates of the building heat load, consisting of both the space heating load and the hot water demand. (Note that we are not considering solar cooling for the building.) The latter information can readily be provided from climatological information and building construction details; the insolation can also be ascertained to reasonable accuracy from available data. However, there is as yet no a priori method for judging long-term

collector efficiencies, since these depend strongly on climatic conditions, system configuration and design, and heating loads.

One method for obtaining thermal performance predictions is the use of computer simulations to determine optimum system sizing. These simulation programs use detailed average weather data to calculate solar energy delivery, building loads, and auxiliary energy requirements over an entire year or heating season. It has been found that such calculations must be performed on an hourly basis [C.1]*, rather than on a monthly, weekly, or even daily basis. As might be expected, the programs used require considerable time and effort for accurate results to be obtained.

Recently, however, at the University of Wisconsin, a relatively simple and quite accurate calculation scheme has been developed for residential and small commercial structures based on hundreds of computerized hourly-basis simulation runs [C.2, C.3, C.4, C.5]. This method, which is thoroughly described in a recent monograph [C.6], was used to predict the thermal performance of the Greenbelt project solar heating system and to generate data for the optimum system sizing to be described in Appendix D. It must be cautioned that these results are for "average" long-term operation and cannot be directly compared to any given year's performance results due to varying weather and load conditions.

A primary input into the calculations is the characterization of the solar collectors to be employed. The net collected energy for a collector depends on the

*Designations in square brackets are keyed to References at the end of this Appendix.

absorber plate temperature (related to the coolant fluid temperature) and losses due to convection and radiation. If the entire collector were at the coolant fluid inlet temperature T_i at a given instant, an energy balance would yield

$$\dot{Q}_u = I_T A(\tau\alpha) - U_L A(T_i - T_a) \qquad (C.1)$$

in which $\dot{Q}_u$ is the rate of energy collection, I_T is the incident solar flux, $(\tau\alpha)$ is the product of the cover plate(s) transmissivity and the absorber plate absorptivity, U_L is the loss coefficient, and T_a is the ambient temperature. The temperature T_i is used in equation (C.1) because it is a single, unambiguous temperature which may be applied to characterize the thermal state of the collector.

Since in an actual situation the absorber plate and other portions of the collector will be at a temperature different from T_i, equation (C.1) will not be correct; a correction factor F_R is applied to the equation, yielding

$$\dot{Q}_u = F_R A \ (\tau\alpha) I_T - U_L (T_i - T_a) \qquad (C.2)$$

The factor F_R is known as the collector heat removal efficiency factor, and is a characteristic of the given collector design.

It is usual to indicate collector performance by the collector efficiency η, given by

$$\eta = \frac{\dot{Q}_u}{A I_T} \qquad (C.3)$$

the ratio of useful energy collected to the solar energy incident on the collector.

In collector tests, the useful energy collected is determined for a known incident solar flux by performing an energy balance on the flowing coolant,

$$\dot{Q}_u = A G C_p (T_i - T_o) \qquad (C.4)$$

in which G is the collector mass flowrate per unit collector area, C_p is the coolant specific heat, and T_o is the (measured) coolant outlet temperature. The collector efficiency can then be determined for various mass flow rates.

Dividing equation (C.2) by the rate of solar energy supply, AI_T, we obtain

$$\eta = F_R(\tau\alpha) - F_R U_L \frac{T_i - T_a}{AI_T} \qquad (C.5)$$

which is seen to be linear in the quantity $\frac{T_i - T_a}{AI_T}$. Therefore, if the efficiency is plotted versus this variable, the collector parameters $F_R(\tau\alpha)$ and $F_R U_L$ can be determined for the particular collector design as the η-axis intercept and the negative of the slope, respectively.

For the Miromit 110 collectors used in the Greenbelt Project, the collector efficiency curve as determined by the NASA Lewis Research Center [C.7] for the design flowrate of 48.8 kg/hr · m^2 is shown in SI units as Figure C.1. From the curve it can be seen that the intercept is

$$F_R(\tau\alpha)_n = 0.70 \qquad (C.6)$$

The subscript "n" is appended to the transmissivity-absorptivity product because this quantity varies with the incident angle of the radiation. A correction can be applied to this value to account for variations in solar position, which changes depending on the season. A reasonable approximation to this variable correction factor, over the entire year, is to use

$$\overline{F_R(\tau\alpha)} = 0.94\, F_R(\tau\alpha)_n = 0.658 \qquad (C.7)$$

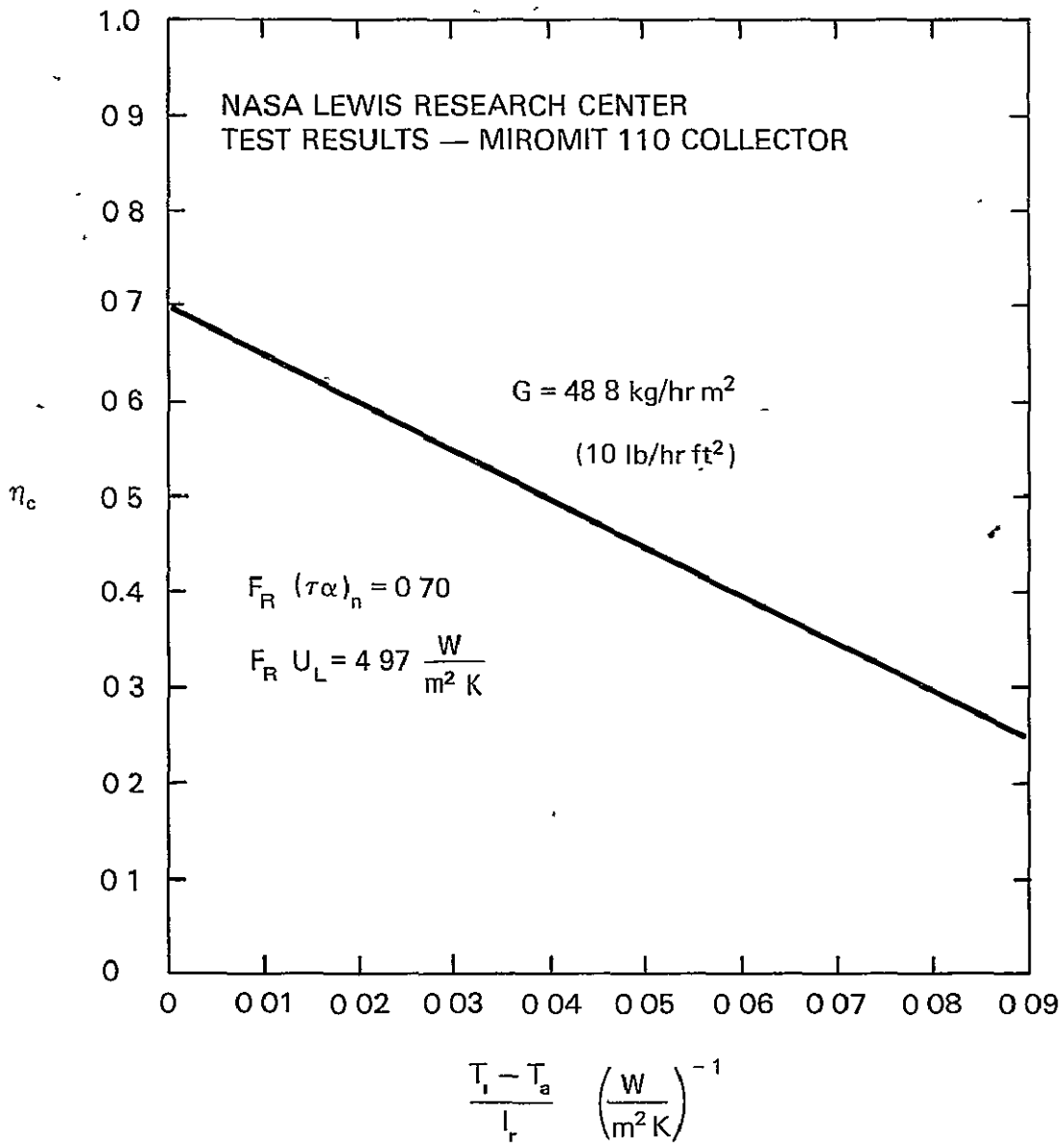

Figure C.1. Greenbelt Project Collector Performance

The slope of the Miromit 110 collector efficiency curve yields

$$F_R U_L = 4\ 97\ W/m^2K \qquad (C.8)$$

which is a typical value for a selective surface collector with a single glass cover plate.

These two collector parameters will be seen to enter in an important way into the thermal performance calculation. Before such a calculation may be made, however, some estimate of the typical heating loads to be expected must be made. Average solar radiation data must also be available.

The space heating load (on a monthly basis) is easily estimated using the degree-day method as

$$L_s = (UA) \times (DD) \tag{C.9}$$

where (DD) is the number of heating degree days to be expected in a given month, and the (UA) product is a characteristic of the building in question, the design heating load divided by the design temperature difference.

For the 4-unit Greenbelt Project buildings, U values for walls, ceilings, foundation, doors, and windows were obtained from standard handbooks for the construction methods and materials employed. When multiplied by the various component areas as shown in Table 6, the (UA) building characteristic can be determined. Changing to SI units and allowing for a somewhat conservative estimate of system thermal performance, there results

$$(UA) \simeq 1500 \text{ W/°C} \tag{C.10}$$

For this study, the domestic hot water load was calculated on a monthly basis by assuming a hot water use rate of 100 liters/day (25 gal/day) for each person. Ten persons were presumed to occupy a typical four-unit Greenbelt Community building. The equation used to estimate hot water usage is

$$L_w = N \times n \times mC_p \times (T_w - T_m) \tag{C.11}$$

Table C.1. Parameters Used in Thermal Performance Analysis

Month	Days	$\overline{H_T}$ MJ/m^2 · day	Heating °C-days	Space Heating Load (GJ)	Mains H_2O Temp. (°C)	DHW Load (GJ)	Total Load (GJ)
Jan	31	14.14	502	65.06	13	5.72	70.78
Feb	28	15.28	439	56.89	13	5.16	62.05
Mar	31	16.98	363	47.04	14	5.59	52.63
Apr	30	17.28	171	22.16	14	5.41	27.57
May	31	16.95	46	5.96	15	5.46	11.42
Jun	30	17.04	0	0	15	5.28	5.28
Jul	31	16.31	0	0	15	5.46	5.46
Aug	31	16.70	0	0	15	5.46	5.46
Sep	30	18.18	23	2.98	14	5.41	8.39
Oct	31	17.54	134	17.36	14	5.59	22.95
Nov.	30	14.92	307	39.78	13	5.53	45.31
Dec.	31	13.41	483	62.60	13	5.72	68.32
Totals	365		2486	319.8	—	65.8	385.6

Here N is the number of days in the month in question, n is the number of occupants, m is the mass of water used in the month by each occupant, C_p is the specific heat of water, T_w is the design hot water delivery temperature, and T_m is the mains water supply temperature.

The total monthly heating load is then the sum of L_s and L_w. Table C.1 lists the calculated heating loads for the Greenbelt project solar heated building, as well as the appropriate solar radiation data. Note that the insolation values

were calculated using Silver Hill, Maryland data from reference [C.6], rather than the data of Table 2, as being more typical for suburban Maryland and in any case more conservative than the Table 2 data. (So as not to overpredict the solar system performance and thereby draw overly optimistic conclusions, conservatism is applied throughout these calculations. It can be seen that the loads indicated in Table C.1 are about 11 percent higher than those used in the original design calculations.) About 17 percent of the total load is seen to be due to domestic hot water use, which is reasonable for a residential structure of this type.

The f-chart thermal performance calculation method is embodied in a simple correlation based on numerous computer simulation runs. The correlation gives, for each month, the fraction of building heating needs which can be expected to be supplied by solar energy (f), and is developed as a function of two nondimensional variables [C.6]:

$$f = 1.029\,Y - 0.065\,X - 0.245\,Y^2 + 0.0018\,X^2 + 0.0215\,Y^3 \qquad (C.12)$$

Here X is a dimensionless loss parameter, related to the collector energy loss–building heat load ratio:

$$X = F_R U_L (T_{ref} - \bar{T}_a) \times \Delta t \times \frac{A}{L} \qquad (C.13)$$

The reference temperature, T_{ref}, used to develop equation (C.12) was 100°C; $\bar{T}_a$ is the average outside ambient temperature during the month in question, and Δt is the temporal length of the month.

The dimensionless parameter Y, termed the "solar parameter," is related to the ratio of the total incident solar energy to the building heating load:

$$Y = F_R(\tau\alpha) \times \bar{H}_T \times N \times \frac{A}{L} \qquad (C.14)$$

The variable $\bar{H}_T$ is the monthly average daily total solar radiation incident on the tilted collectors, and is listed in Table C.1.

The correlation, when applied to the installed Greenbelt Project solar energy system (collector area: 84.3 m^2), results in the thermal performance shown in Figure C.2. It can be seen that the solar-supplied energy is more or less constant throughout the year (except in summer, when excess solar energy is available) but the fraction of the monthly load supplied by solar varies from about 22.4 percent in December to 100 percent in the summer months. In order to

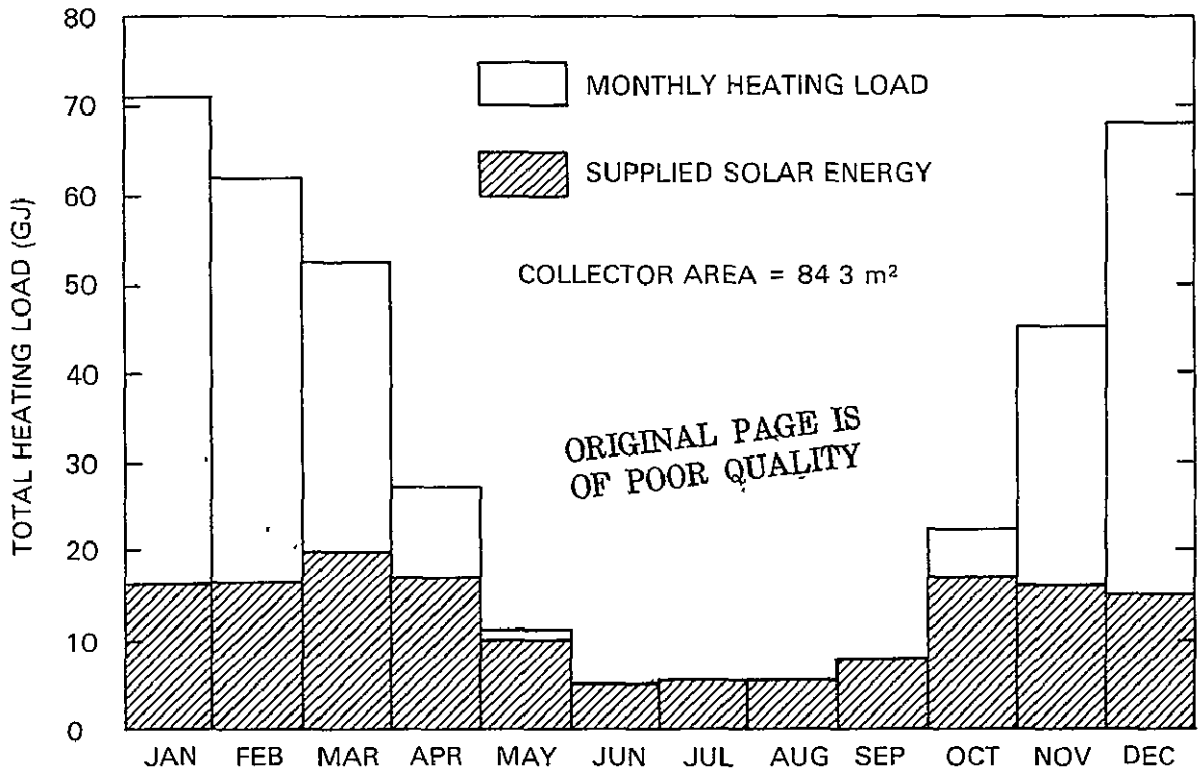

Figure C.2. Installed System Thermal Performance

calculate the fraction of the yearly heating load supplied by the solar system, the following formula is used:

$$\bar{f} = \frac{1}{L_{tot}} \sum_{i} f_i L_i \qquad (C.15)$$

Here the summation is carried out over each of the twelve months of the year, and L_{tot} is the total yearly heating load. For the installed system, $\bar{f}$ = 40 percent.

A complete listing of f values is shown in Table C.2. Also shown in this table is the maximum collectable solar energy, Q_{max}, and the solar heat delivered,

Table C.2. Installed System Thermal Performance

Month	Days	Maximum Collectable Energy (GJ)	Total Heating Load (GJ)	f	Solar Heat Delivered	η_{ss}
Jan	31	36.95	70.78	0.232	16.42	0.444
Feb	28	36.07	62.05	0.265	16.44	0.456
Mar	31	44.37	52.63	0.381	20.05	0.452
Apr	30	43.70	27.57	0.626	17.26	0.395
May	31	44.30	11.42	0.993	11.34	0.256
Jun	30	43.09	5.28	1.00	5.28	0.123
Jul	31	42.62	5.46	1.00	5.46	0.128
Aug	31	43.64	5.46	1.00	5.46	0.125
Sep	30	45.98	8.39	1.00	8.39	0.182
Oct	31	45.84	22.95	0.747	12.14	0.374
Nov	30	37.73	45.31	0.366	16.58	0.439
Dec	31	35.04	68.31	0.224	15.30	0.437

Q_{sol}. The efficiency of the solar system in supplying useful energy to the residence can be defined as

$$\eta_{ss} = \frac{Q_{sol}}{Q_{max}} \tag{C.16}$$

This parameter is also shown in Table C.2. Note that the solar system efficiency is not really pertinent when applied to the summer months, when excess solar energy is available. At peak load, the solar system is seen to be about 45 percent efficient in utilizing the incident solar energy.

When economics is considered, it has been found unreasonable to design a solar system capable of supplying 100 percent of the energy demand of buildings. In practice, there is some optimum mix of solar heat and auxiliary heat which is highly dependent on local meteorological conditions and costs; solar system costs are largely collector area dependent. In order to find the optimum collector area for a given heating "job" in a given location, the variation of the fraction of energy supplied by the solar system with collector area is required.

For the building and weather characteristics of the Greenbelt Community solar heated residence, the f-chart algorithm was applied for various collector areas between 0 and 100 m^2. The resulting annual-load-fraction-supplied-by-solar versus collector area curve is shown as Figure C.3. This curve is a classic manifestation of the law of diminishing returns; a 100 percent increase in collector area (from 50 to 100 m^2) gives only a 16 percent increase in supplied energy. The expected solar system thermal performance, as indicated in Figure C.3, will be used in the economic analyses of Appendix D.

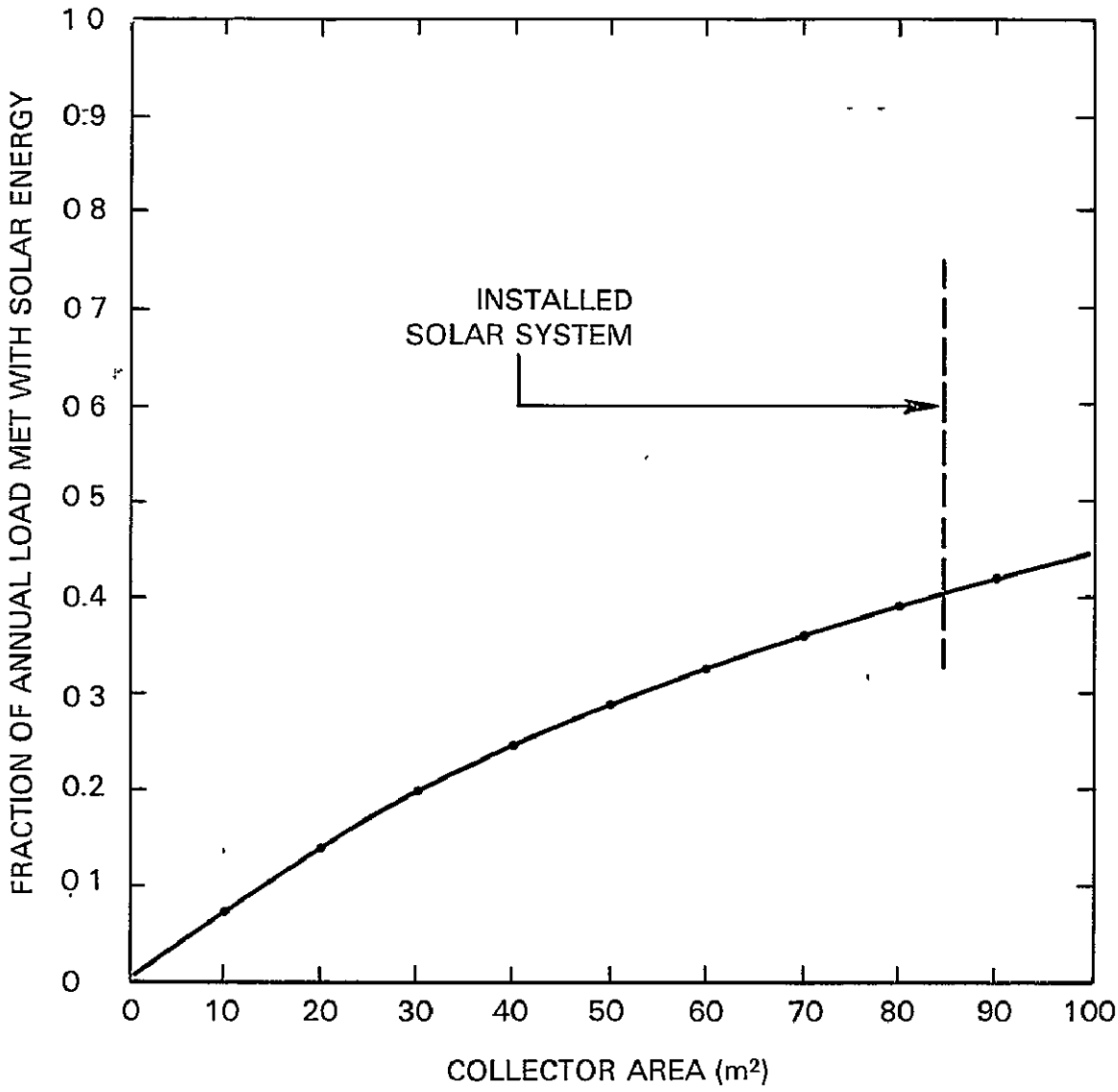

Figure C.3. Variation of f with Collector Area

Although relatively detailed economic considerations will be treated in the appendix to follow, it is perhaps interesting to conclude this section on an economic note. It is clear that any realistic economic model must include the expected increase in fuel costs, system life, and prevailing interest rates to estimate the justifiable investment in a solar system of a given size.

Kreider and Kreith [C.8] have calculated such justifiable investments and presented the results as an easily-interpreted set of curves. For a current fuel cost of $6/GJ, the average monthly fuel savings of the installed Greenbelt solar heating system for the first year would be $77; at an interest rate of 7 percent, an expected system lifetime of 20 years, and a 10 percent inflation rate in the cost of fuel, Kreider and Kreith indicate a justifiable initial expenditure of $23,000—which may be a reasonable estimate of the current cost of solar systems for the Greenbelt community if installed in sufficient quantity. (Taxes, maintenance, but even more significantly, general inflation are not included in this analysis.)

References for Appendix C

C.1 Buchberg, H. and J. R. Roulet, "Simulation and Optimization of Solar Collection and Storage for House Heating," Solar Energy 12, 31 (1968).

C.2 Klein, S. A., "A Design Procedure for Solar Heating Systems," Doctoral Dissertation, University of Wisconsin, Madison (1976).

C.3 Klein, S. A., W. A. Beckman, and J. A. Duffie, "A Design Procedure for Solar Heating Systems," Solar Energy 18, 113 (1976).

C.4 Beckman, W. A., J. A. Duffie, and S. A. Klein, "Simulation of Solar Heating Systems," Applications of Solar Energy for Heating and Cooling a Building, Ch. 9, ASHRAE, New York (1976).

C.5 Klein, S. A., W. A. Beckman, and J. A. Duffie, "A Design Procedure for Solar Air Heating Systems," 1976 ISES American Section Conference, Winnipeg, Manitoba (1976).

C.6 Beckman, W. A., S. A. Klein, and J. A. Duffie, Solar Heating Design, Wiley, New York (1977).

C.7 Power Systems Division, "Standardized Performance Tests of Solar Thermal Energy — A Selectively Coated, Steel Collector with One Transparent Cover," NASA TMS-71870, January 1976.

C.8 Kreider, J. F. and F. Kreith, Solar Heating and Cooling, McGraw-Hill, New York (1977).

Appendix D — Economic Considerations in Solar System Design

In general, it is not economical to design a solar heating system to supply 100 percent of the energy needs of a building. Because of the reduced space heating loads during certain months of the year, such a system would be drastically oversized during all but a few months; equipment with an uneven load factor distribution is generally uneconomical. Hence, solar heating systems invariably include an auxiliary source of energy to supply that portion of the load which cannot be met by direct or stored solar energy.

The design of solar heating systems is an outstanding example of an apparently technical decision process which must in fact have a strong coupling to the economics of capital expenditures. The interaction of the thermal engineering and economics of solar systems is intimately related to the diminishing energy returns as collector area is increased.

It will be seen in this Appendix that there exists an optimum solar heating system sizing (i.e., total collector area) which depends on costs and inflation rates, as well as the details of the tax position of the solar consumer and predicted fuel price escalation.

Presented first is a simple exposition of life-cycle costing, which will be used to assess the economics of various solar investment alternatives. Following this discussion is a simplified break-even analysis for the installed system. Economic optimization of solar system sizing for Greenbelt Community application is then considered under simplified economic assumptions. A more

realistic set of assumptions, specific to the situation of the Greenbelt Project, is next applied to both a space heating/hot water installation and a solar system for the heating of hot water only. Finally, a brief discussion of the reasonableness and importance of the various assumptions is presented.

a. Life-Cycle Costing

The engineering economic analysis of systems of the type being discussed here is most frequently conducted based on the life-cycle cost method. Fundamental to such considerations is the time value of money—a dollar today is intrinsically of more worth than a dollar tomorrow. Some basic familiarity with this idea and simple economics terminology is assumed in what follows. In life cycle cost analyses, expenses and savings at future times are compared by examining their present worth given the prevailing discount rate—the best interest rate available to the consumer for an alternative investment.

A useful visual aid in the discussion of the real savings and costs of an investment is the cash flow diagram. Such a diagram is presented in Figure D.1 for a building solar heating system. Mortgage payments, taxes, maintenance costs, fuel savings, and tax savings are considered in this diagram. Payments, represented by arrows, are presumed to occur at the end of each year of the system's lifetime. Upward pointing arrows indicate income to the investor, while downward directed arrows are disbursements. System lifetime is "n" years for purposes of the figure.

In all that follows, we consider only the additional costs accrued because of the choice of a solar system. In most cases, the auxiliary heating system is virtually identical to that which would be installed if the "solar decision" were not

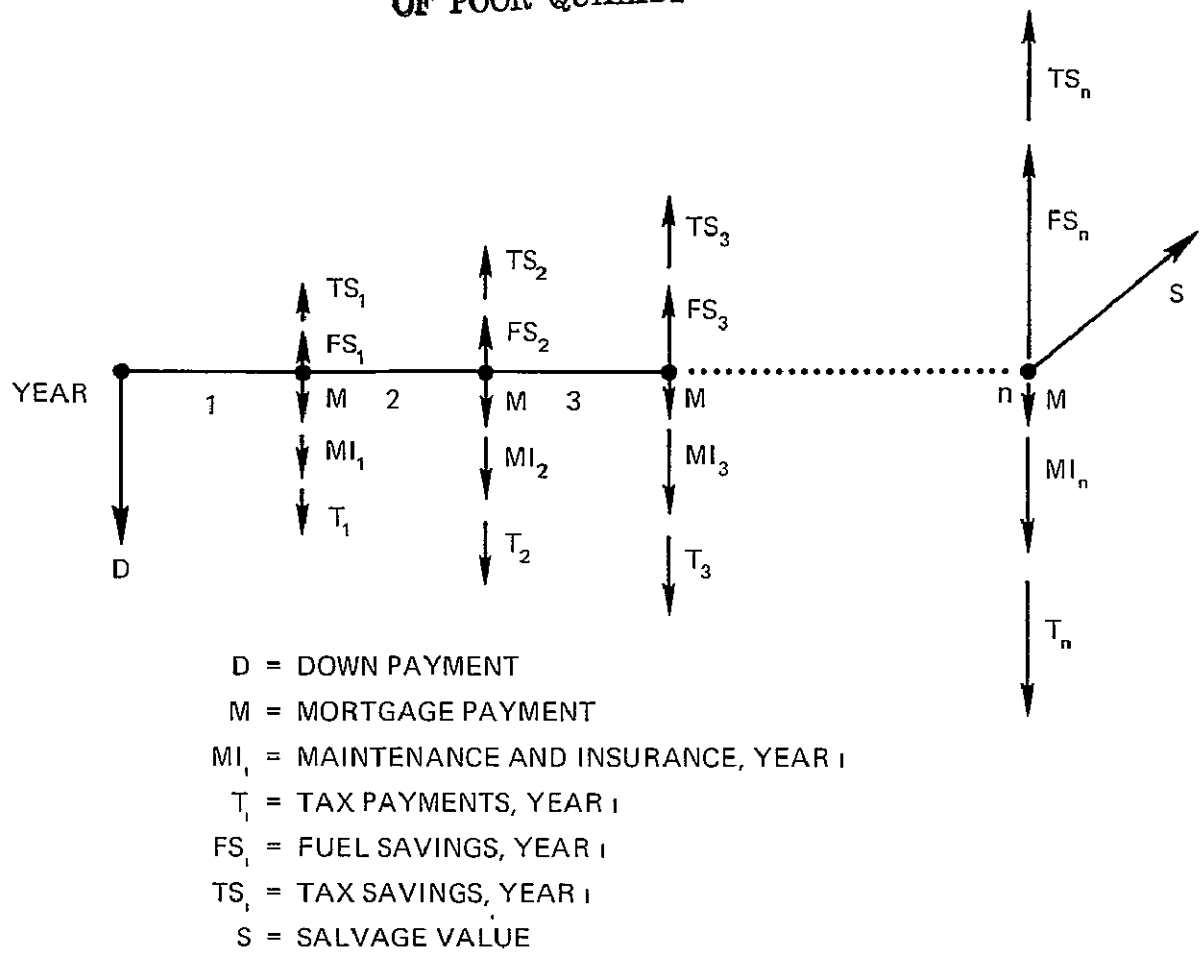

Figure D.1. Solar System Cash Flow Diagram

made. (This is especially true if the system is a retrofit—as for the Greenbelt Project.) The "investment" to be analyzed, then, is the additional cost associated with collectors, piping, storage, and preheat tanks, as well as solar system pumps and heat exchangers.

Costs shown in Figure D.1 include: (1) the down payment, (2) annual mortgage payments, (3) additional maintenance and insurance costs associated with the solar components, and (4) increases in property taxes due to the more expensive heating plant. Savings shown on the cash flow diagram are, (1) fuel savings,

(2) tax savings associated with mortgage interest payments, and (3) the salvage value of the solar components after year "n".

If the total cost of the solar portion of the heating system is C and D is the down payment, the annual mortgage payment for m years at an interest rate j is

$$M = (C - D)\left(\frac{a}{p}\right)^{j}_{m} \qquad (D.1)$$

Here the rightmost term in brackets is standard economic notation for the annuity which must be payed for m years at an interest rate j which is equivalent to one dollar at the present time. Letting M* be the present worth of all mortgage payments, with a discount rate of i, we have

$$M^* = (C - D)\left(\frac{a}{p}\right)^{j}_{m}\left(\frac{p}{a}\right)^{i}_{m} \qquad (D.2)$$

The rightmost term is the present worth at an interest rate i of a one dollar annuity to be paid for m years. (All such fractions can be determined from interest tables or simple formulas found in most economics texts or mathematical handbooks.*)

It is usual to estimate the additional maintenance and insurance charges attributable to the solar components as a fixed percentage of the solar system cost, applicable over the equipment operating life. This is subject to the general inflation rate, however. If r is the inflation rate, and MI_1 is the first year's maintenance and insurance charge, we have

*c.f. Smith, G W., Engineering Economy, 2nd ed., Iowa State University Press, Ames, 1973

$$MI_2 = (1 + r)\, MI_1, \tag{D.3}$$

and

$$MI_3 = (1 + r)^2\, MI_1 \tag{D.4}$$

while for year p,

$$MI_p = (1 + r)^{p-1}\, MI_1 \tag{D.5}$$

Reducing all such payments to their present worth, we have

$$MI^* = MI_1 \left(\frac{P}{f}\right)^1_1 + MI_2 \left(\frac{P}{f}\right)^1_2 + \quad + MI_n \left(\frac{P}{f}\right)^1_n, \tag{D.6}$$

in which the multipliers represent the present value of a future sum at a given discount rate.

An alternative expression for equation (D.6) is

$$MI^* = MI_1 \left(\frac{P}{c}\right)^r_n, \tag{D.7}$$

where $\left(\frac{P}{c}\right)^r_n$ represents the present worth of an annual payment inflating at a rate r.

The tax payment for year 1 is simply the added worth of the solar system multiplied by the local tax rate. Tax payments are presumed to be subject to general inflation; the present worth of all such payments is then

$$T^* = T_1 \left(\frac{P}{c}\right)^r_n \tag{D.8}$$

Next we consider savings due to the installation of a solar energy system. If FC is the total fuel cost (year 1) that would be incurred without the solar system,

then the solar system fuel savings for year 1 is given by

$$FS_1 = f \cdot FC \tag{D.9}$$

(Here f represents the fraction of the heating load supplied by solar energy.)

It is quite likely, in view of the depletion of fossil fuel reserves and current energy politics, that fuel prices will increase at a rate somewhat greater than the general inflation rate. If this rate is denoted by "k", the present worth of all fuel savings is

$$FS^* = FS_1 \left(\frac{p}{c}\right)_n^1 \tag{D.10}$$

Tax savings arise from several sources, depending on the particular tax situation of the solar investor. For a residential building, the first year's tax savings is the product of the investor's income tax rate and the sum of the first year property tax payment and mortgage interest payment. A simple formula for the present worth of all such savings, TS*, considering inflation, is not available, but TS* is easily calculated sequentially. Tax savings for commercial buildings would be comprised of the above savings plus additional savings due to depreciation, extra maintenance and insurance, and other additional costs.

The salvage value of the solar components will presumably be negligible; in fact, it may be negative—it may cost something to remove the equipment after year n. If salvage is considered,

$$S^* = S \left(\frac{p}{f}\right)_n^1 \tag{D.11}$$

The cash flow diagram shown in Figure D.1 does not consider miscellaneous payments such as one-time tax credits or other government solar incentives.

Of importance to the investor is the net life cycle cost savings, reduced to the present value of money. In terms of the variables already discussed, the net savings is

$$NS = FS^* + S^* + TS^* - M^* - MI^* - T^* \qquad (D.12)$$

b. Installed System Break-Even Analysis

The installed system, with 84.3 m^2 of collector area, can now be examined economically. For this analysis, we make several assumptions: (a) the system is paid for in cash and can be installed for $20,000, (b) no excess property tax is paid, hence (c) no tax savings result from installing the solar system.

In general, local tax rates, fuel prices, and the cost of money will have a more-or-less large effect on the resultant economic conclusions. Since mortgage interest payments and local property taxes are deductible income tax expenses, the tax savings (on both interest payments and local taxes) tend to counterbalance the local taxes paid. In the absence of specific details, however, an analysis based on the assumptions above can lead to definite insights as to the financial reasonableness of "going solar."

For the present work, a fuel cost in year one of $7.5/GJ is assumed. This is consistent with an effective fuel oil cost of 50¢/gallon and a heating plant efficiency of 45 percent. Additional solar system maintenance and income charges are taken to be 1 percent of system worth. A discount rate of 8 percent is

assumed; salvage is ignored.. Fuel costs are assumed to inflate at a rate of 10 percent, while a general inflation rate of 6 percent is presumed.

The results of these considerations are shown in Table D.1. Of most interest is column 6, the cumulative solar savings in current dollars. It can be seen that the break-even point for the system is in its 21st year of operation. Many experts believe that a 20 year solar system life is reasonable. We see, therefore, that the presently installed Greenbelt Project solar heating system is on the verge of being economical (under these assumptions). An 11 percent rate of increase of fuel costs, rather than the assumed 10 percent, or a lower discount rate, would tip the scale in favor of solar energy on an economic basis. Life cycle cost analyses always suffer from the necessity of predicting future price hikes and inflation rates; there is no substitute for prescient planning.

c. Optimization of System Sizing—Simplified Economic Analysis

It will be seen in this sub-section that, under the previous assumptions, the installed system is over-sized. In fact, a smaller solar system will lead to positive net solar savings over a 20 year system life—such a system would be economically advantageous.

It is at this point in the economic considerations that the thermal performance predictions of the previous Appendix become important. For this analysis, a solar system fixed cost* of $2,000 is assumed, with additional costs (at $200/m^2 of collector area) depending on system size. As before, an 8 percent discount rate, a 1 percent maintenance/insurance cost rate, a 10 percent fuel price

*Pumps, some piping, and equipment room components

Table D.1. Simplified Economic Analysis of Installed System

1 Year	2 Fuel Savings	3 Insurance & Maint.	4 Yearly Savings	5 Present Worth of 4	6 Cumulative Solar Savings
1	1041	200	841	779	-19221
2	1145	212	933	800	-18421
3	1260	225	1035	822	-17593
4	1386	238	1148	844	-16755
5	1524	262	1262	859	-15896
6	1677	278	1393	878	-15018
7	1844	294	1550	904	-14114
8	2029	312	1717	928	-13186
9	2232	331	1901	951	-12235
10	2455	351	2104	975	-11260
11	2700	372	2328	999	-10261
12	2970	394	2576	1023	-9238
13	3267	418	2843	1045	-8193
14	3594	443	3151	1073	-7120
15	3954	463	3491	1100	-6020
16	4349	497	3852	1124	-4896
17	4784	527	4257	1151	-3745
18	5262	559	4703	1177	-2568
19	5789	592	5197	1204	-1364
20	6367	628	5793	1231	-133
21	7004	666	6338	1259	+1126

inflation rate, and a 6 percent general inflation rate is presumed. Energy costs were taken to be $6.75/GJ (the current residential oil rate at 48 percent efficiency).

Under these conditions, the net life-cycle savings for solar systems between 0 and 100 m^2 were calculated using the f values of Appendix C. Solar systems from 11 to 100 m^2 are seen to be economically viable, with the optimum solar collector area on the order of 48 m^2.

Next, we calculate the net rate of return on the solar investment in a 48 m^2 system for a Greenbelt Community building. This is done by assuming several discount rates and repeating the previously described life cycle cost calculations.

This exercise results in the curve shown in Figure D.3, giving net solar savings for the 48 m^2 system as a function of the discount rate. The rate of return on the solar system investment is the discount rate at which there is zero net solar savings, and is seen to be about 10.2 percent.

Thus, as an investment, the 48 m^2 solar system yields a 10.2 percent annual interest rate. If alternative investments at higher interest rates are unavailable, the solar alternative is economically justifiable.

d. Detailed Economic Analysis for the Greenbelt Situation

The economic assumptions specific to the Greenbelt cooperative differ from those described in the previous sections in several aspects. In this subsection, analyses and conclusions for solar system installations under these more appropriate assumptions are described.

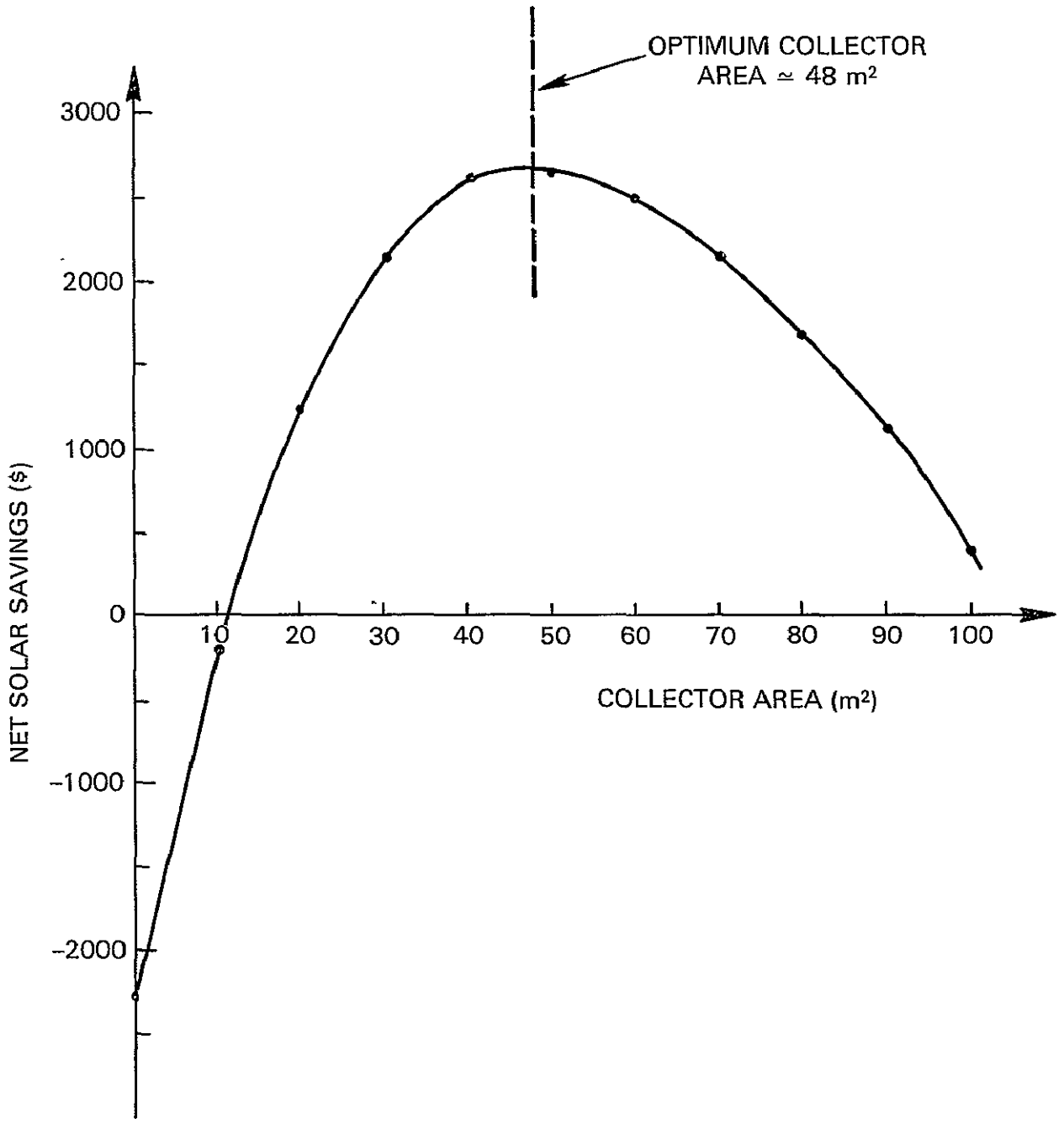

Figure D.2. Collector Area Optimization (Simple Case)

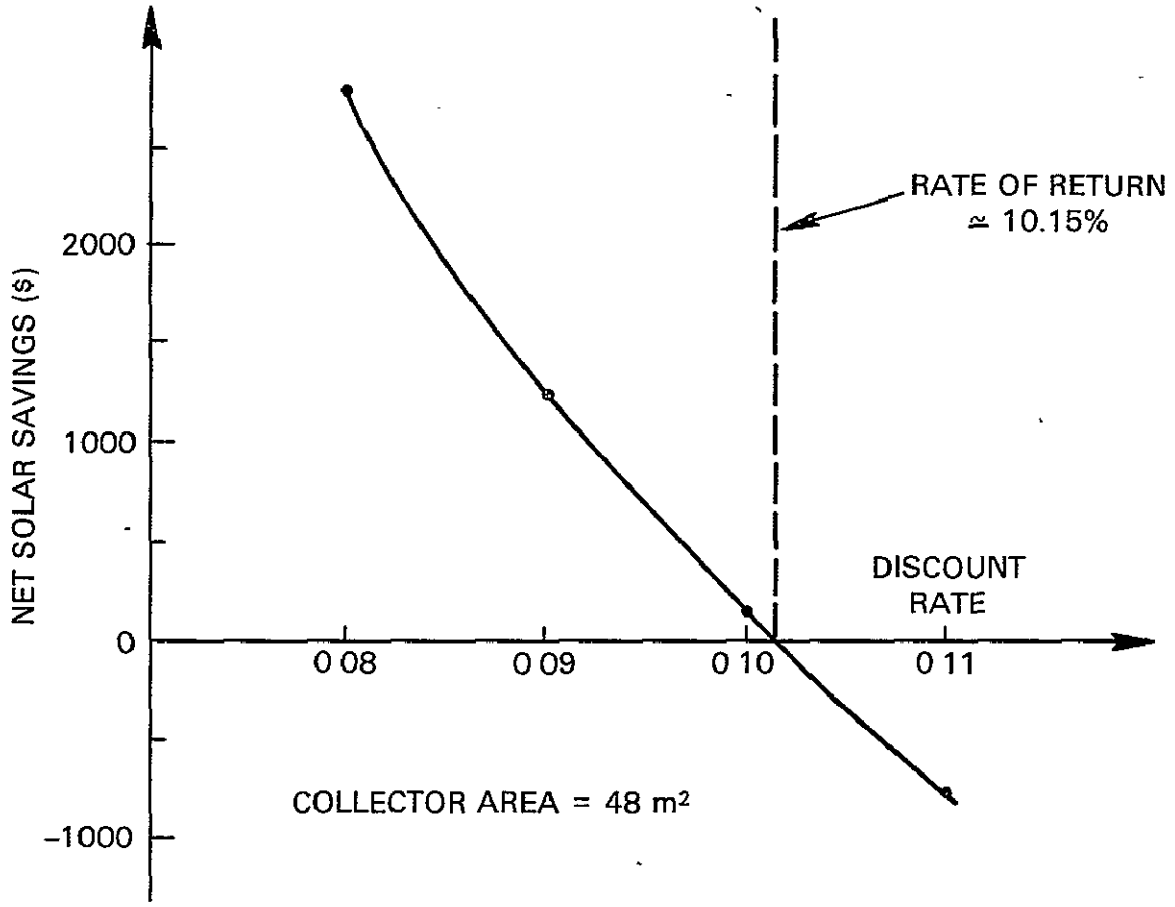

Figure D.3. Rate of Return Analysis (Simple Case)

We begin by examining the tax liability attributable to the solar installation. The standard Prince George's County tax rate and assessment policy was assumed to be applied to the value added by a solar energy system.

Lumping this property tax with maintenance and insurance costs resulted in a negative cash flow equal to 3.5 percent of the solar system value for these costs. It is unlikely that the full solar system cost would be paid at installation; amortization at 9 percent for 20 years was assumed with a 20 percent down payment.

Finally, oil is purchased at a bulk rate of 40¢/gallon by GHI. This is substantially less than the current local residential rate of slightly more than 48¢/gallon; coupled with an assumed heating plant efficiency of 48 percent, the GHI rate led to the minimum first year energy cost of $5.6/GJ employed for the analyses. (This compares to the local effective electricity cost of about $12.40/GJ—oil heating still has quite significant economic advantages!) Fuel costs were presumed to escalate at 10 percent per year, with general inflation at 6 percent. System life was taken to be 20 years.

For the space heating/domestic hot water system analysis, the thermal performance was assumed to be that of Appendix C. Collector-area-dependent costs were presumed to be $200/m^2, with a fixed solar system cost of $2000; as a reference point, these assumptions result in an installed cost of $18,860 for the 84.3 m^2 demonstration system described in the body of this report. This is a reasonable estimate of the installed cost of a standardized system of this type.

The result of the calculations is shown in Figure D.4. The net solar savings, under the economic assumptions detailed above, is shown for collector areas between 0 and 100 m^2 for several assumed energy costs in the range $5.6-$10/GJ. At $5.6/GJ, the system is seen to be uneconomical for all collector areas at a discount rate of 8 percent. (As it turns out, at this first year energy cost rate, the system is uneconomical for all discount rates.)

Examination of Figure D.4 reveals that an 8 percent rate of return is obtained on a solar system of approximately 40 m^2 at a $7.75/GJ first year fuel cost.

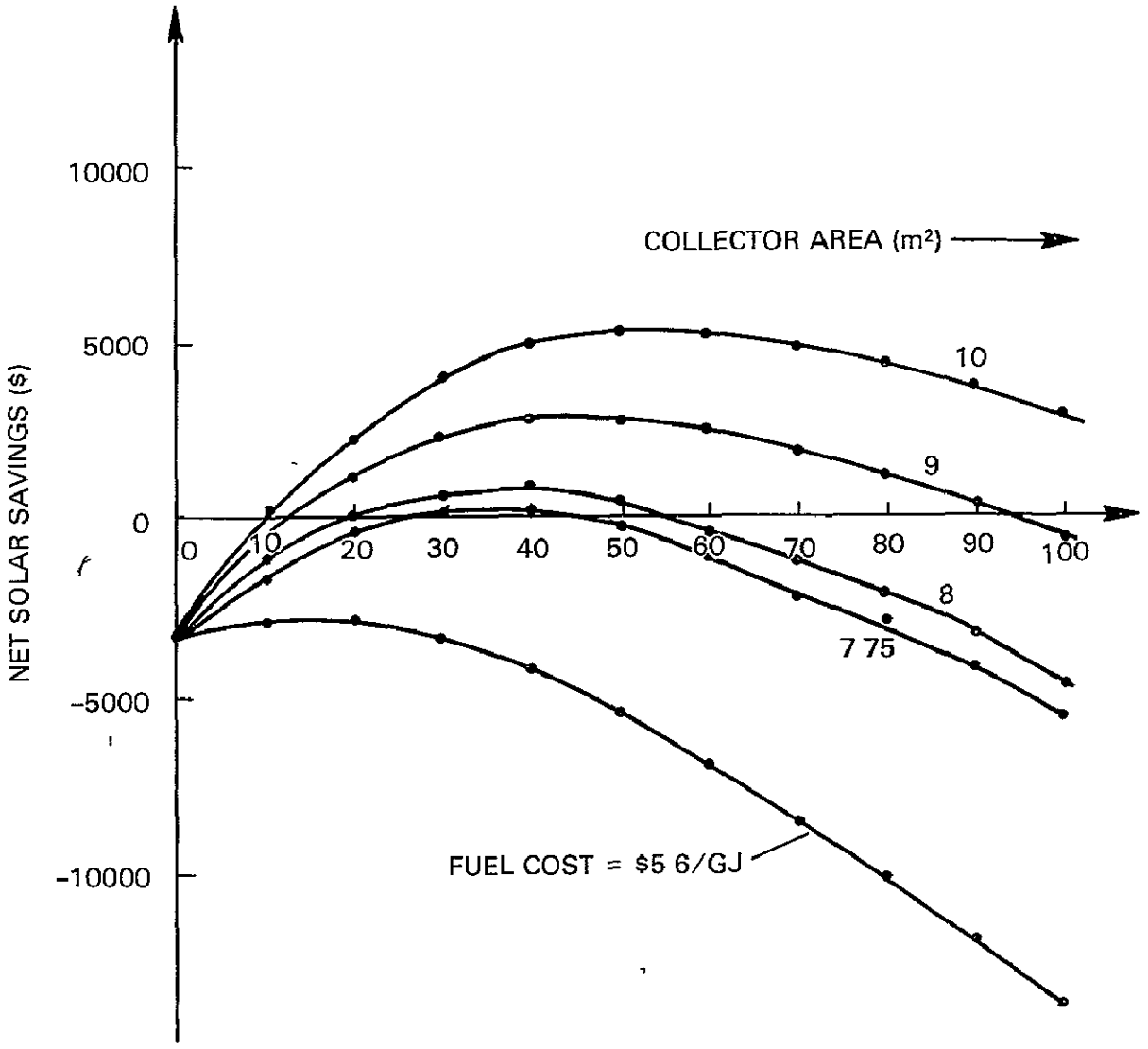

Figure D.4. Total Heating System Economic Performance
(Discount Rate = 8%)

This is the breakeven fuel cost and corresponds to a fuel oil cost of 57¢/gallon with a heating plant efficiency of 50 percent. (Fuel oil costs are related to energy costs for various heating plant efficiencies in Figure D.5.) It should be noted that under the assumptions of this analysis, solar heating systems are undeniably and significantly more economical than pure electric systems.

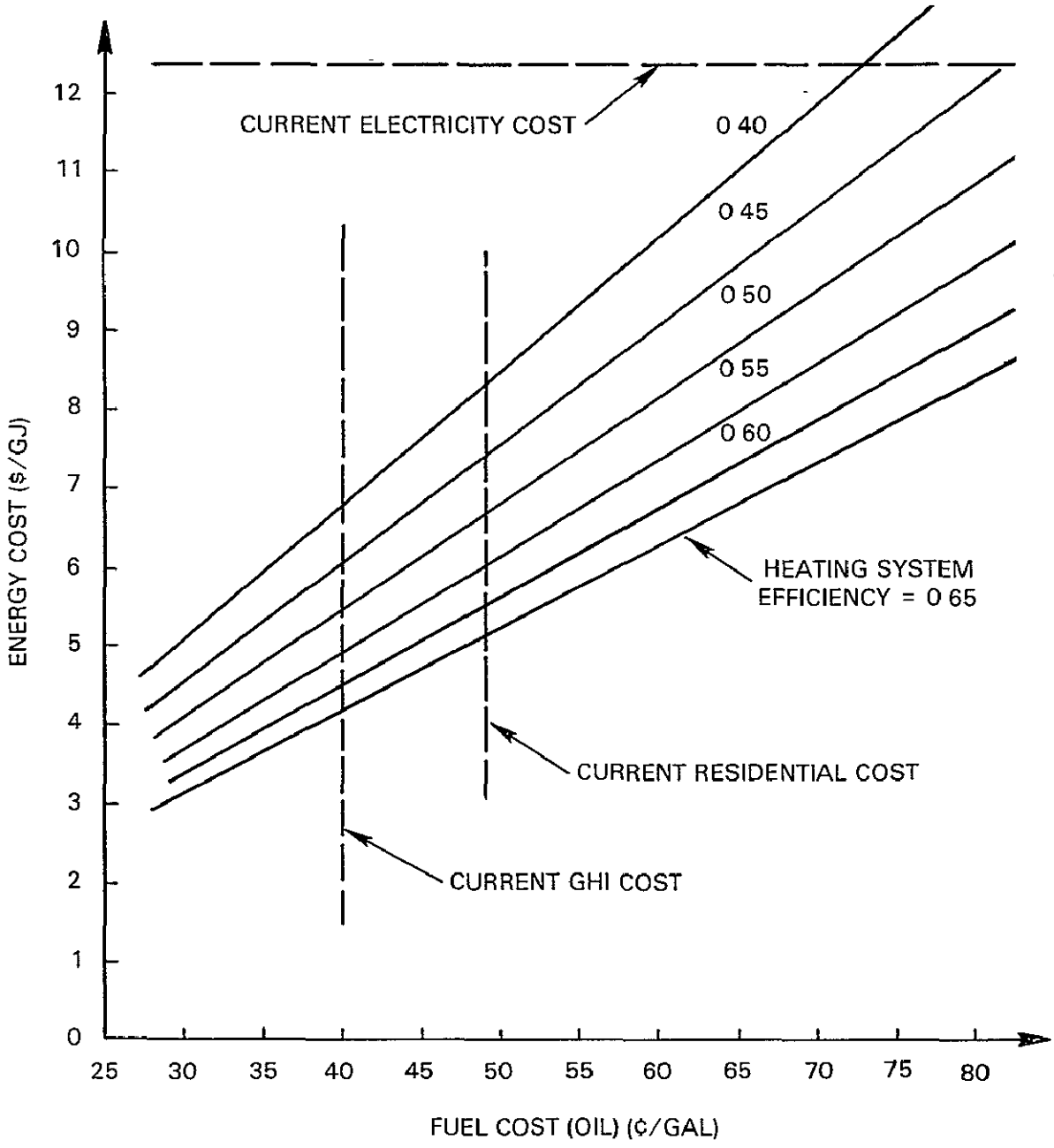

Figure D.5. Energy Cost Relationships

It is well known that, at the present time, solar domestic hot water-only systems are slightly more economically viable than total heating systems. It therefore is appropriate to examine such a system for Greenbelt Community application in view of the somewhat disappointing projected economic performance of a total system.

The standard f-chart design method described in Appendix C was derived for space-heating systems with domestic hot water loads of 20 percent or less.

A correction factor to the dimensionless loss factor X has been found to result in successful predictions of solar hot water system performance. The corrected value of X is given by the equation

$$X_c/X = (11.6 + 1.18\ T_w + 3.86\ T_m - 2.32\ \bar{T}_a)/(100 - \bar{T}_a) \qquad (D.13)$$

in which T_w is the hot water delivery temperature, T_m is the cold water supply temperature, and $\bar{T}_a$ is the monthly-average ambient temperature. Values of f, the fraction of the hot water heating load supplied by the solar system, were calculated for the Miromit collector under Greenbelt meteorological conditions; this thermal performance data was then used to estimate economic performance. The results are shown in Figure D.6.

Because of the decreased complexity of a hot water-only system, the area-dependent solar system cost was taken as $\$175/m^2$ with a \$1000 fixed cost. As with the total solar system, the domestic hot water system was found to be uneconomical at the current bulk-rate energy cost of \$5.6/GJ for all collector areas considered. (Note that the abscissa in Figure D.6 is in number of collectors—each collector has 1.51 m^2 of effective area.)

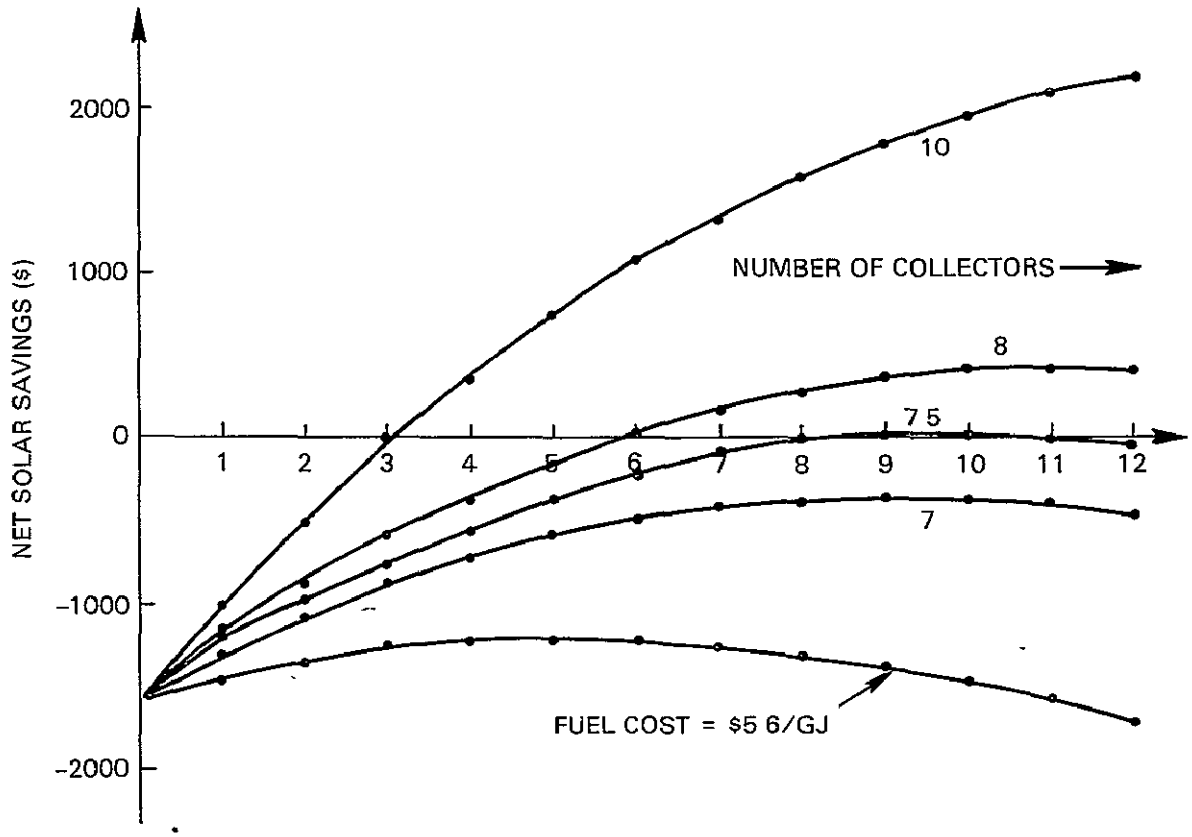

Figure D.6. Hot Water-Only Solar System Economic Performance (Discount Rate = 8%)

The break-even first year fuel cost for a solar domestic hot water system is seen to be $7.50/GJ, thus validating the presumption that such a system would be somewhat more economical than a combined space heating/hot water system under the assumptions of the present analysis.

e. Discussion of Key Assumptions and Conclusion

The future of solar systems as an alternative to conventional residential heating systems is highly dependent on economics. Somewhat different economic assumptions in the analyses of this Appendix could have led to more favorable (or more disappointing!) results. A brief critical examination of the assumptions is therefore quite appropriate.

1. Solar system costs. A $200/m^2 collector-area-dependent cost and a $2000 fixed cost was assumed for the combined space heating/service hot water systems, while corresponding costs for the domestic hot water-only systems were $175/m^2 and $1000. How realistic were these assumptions?

Collector-area-dependent costs assumed in recent published work are in the range $100-$200/m^2. Without a significant technological breakthrough (such a breakthrough is highly unlikely in the field of flat plate solar collectors), an installed collector cost of $100/m^2 is probably a lower limit.* An estimate of the mass-production costs involved with single cover plate, selective surface collectors** leads to an installed cost of $135/m^2 when adjusted to 1978 dollars.

When one considers the additional costs involved with the storage system for space heating applications, and secure installation frames, a $200/m^2 cost for the Greenbelt application does not seem unreasonable (although this value is most likely somewhat conservative and was so chosen intentionally). For the domestic hot water-only systems, a $175/m^2 cost was chosen primarily because a separate energy-storage system is not required in this case.

Fixed costs are somewhat more difficult to estimate. The $2000 figure was chosen primarily in response to prevailing assumptions in the literature for these costs, which cover the basic piping, required heat exchangers, the auxiliary water tank, pumps, and controls. For the service hot water system analysis, the

*c.f. Kreider, J F. and F Krieth, Solar Heating and Cooling, McGraw-Hill, New York, 1977, p. 86.

**Altman, M. et al , "Conservation and Better Utilization of Electric Power by Means of Thermal Energy Storage and Solar Heating," NSF/RANN/SE/GI27976/PR73/5, University of Pennsylvania, Philadelphia, 1973.

fixed cost was chosen as $1000, in recognition of the vastly reduced requirements for pumps and controls and the elimination of the intermediate heat exchanger connecting the solar loop with the conventional heating system.

Again, it should be noted that the assumed costs are reasonable but probably slightly conservative.

2. General inflation rate. For these analyses, an inflation rate of 6 percent per year was assumed. Recent economic history certainly justifies this assumption; if anything, a slightly higher value should be used (the Washington area inflation rate was 7.8 percent for 1977).

3. Cost of fuel. Predictions of future energy costs are obviously susceptible to substantial error. Starting with present price levels, a fuel cost inflation rate of 10 percent was assumed—4 percent higher than the general inflation. Is this scenario realistic?

Based on the events of the recent past, a 10 percent average fuel cost escalation seems reasonable, but political and economic factors will become more and more important as the final years of the fossil fuel age pass.

Important considerations when postulating future oil pricing include: (a) the 50-100 year world supply of oil at present consumption levels, (b) possible currency fluctuations which could influence the price of oil, and (c) the huge balance of payments deficit currently being incurred by the U.S. in trade with the oil-producing nations.

With regard to item (a), it is likely that in the next decade a significant oil price increase will occur in response to the dwindling supply and increased production costs. Currency fluctuations are a response to the health of the national economy and are difficult to predict. Finally, the $40 billion trade deficit due to oil imports which we are currently experiencing probably will not be allowed to continue. An increase in duties on imported oil to make domestically-produced energy more competitive and economically desirable is not inconceivable.

In light of these and other considerations, the assumed cost inflation factor for energy does not seem unreasonable.

4. Taxes, maintenance, and insurance. A 2.5 percent annual effective property tax rate for Prince George's County is not far from reality. It is not clear at this time, however, how the value added by the installation of a solar system will be assessed.

An additional 1 percent annual charge for maintenance and insurance was also assumed. Such a charge is more or less standard for economic analyses of solar residential heating systems, although both maintenance and insurance aspects of solar implementation are still an open question.

5. System life. Solar systems are still too new to have generated definitive data on typical solar system reliability. A 20 year life is perhaps optimistic; a 15 year system life is a commonly accepted conservative value. The piping system will not wear out in a service life of 20 years. Collector panels, however, may need to be overhauled. Pumps and controls should last for 15 years.

It is interesting to speculate on the solar system economic viability under a scenario in which the solar system is completely overhauled at 15 years of service.

In this Appendix it has been demonstrated that solar heating systems (both total and domestic hot water only) are nearly economical in the Washington area for a Greenbelt Community-type application. Under the assumptions discussed above, purchase of these systems cannot be unequivocally recommended at the present time.

However, if systems are available for somewhat less than the assumed prices, if fuel costs escalate to anticipated levels, or if suitable government solar energy incentives are enacted, the economic picture could easily be reversed. For example, if oil prices rise at the assumed rate, solar installations will be economical within 5 years.

Finally, if solar air conditioning systems now under development and demonstration prove technically viable, a combined heating/cooling/service hot water system should prove to be at least as economically sound as the solar heating systems discussed.* Such a complete system, as well as non-conventional solar systems (e.g., solar assisted heat pumps) should be considered when the uses of solar energy in retrofit space conditioning systems for multi-family dwellings are subsequently examined.

*Lof, G O. G , and R A Tybout, "Design and Cost of Optimal Systems for Residential Heating and Cooling by Solar Energy," Solar Energy 16, p. 9, 1974.

BIBLIOGRAPHIC DATA SHEET

1. Report No.	2. Government Accession No.	3. Recipient's Catalog No.
TM 79612		

4. Title and Subtitle	5 Report Date
Greenbelt Community Project: Solar Energy Retrofit for a Multi-Family Dwelling	June 1978
	6. Performing Organization Code
7. Author(s) E. W. Hymowitz, R. J. Hannemann, L. L. Millman, J. E. Pownell	8. Performing Organization Report No.
9 Performing Organization Name and Address Goddard Space Flight Center Greenbelt, Maryland 20771	10. Work Unit No
	11 Contract or Grant No.
	13 Type of Report and Period Covered Technical Memorandum
12. Sponsoring Agency Name and Address Same as above.	14 Sponsoring Agency Code

15. Supplementary Notes

R. J. Hannemann is an Assistant Professor in Dept. of Mech. Engrg. at U. of Md., College Park. Other authors are GSFC affiliated.

16. Abstract

As a result of the energy crisis of 1973-74 a cooperative project was initiated between Goddard Space Flight Center and the nearby community of Greenbelt, Maryland. The purpose was to design, install and operate an experimental solar heating system on a group of four tandem town houses. The system was successfully developed and is now operating. This report describes the design, installation, system operation and performance as well as the important consideration's for judging the economic feasibility of solar heating systems.

17. Key Words (Selected by Author(s))	18. Distribution Statement
Solar Energy Greenbelt Project	

19. Security Classif. (of this report)	20. Security Classif. (of this page)	21 No. of Pages	22. Price*
Unclassified	Unclassified	146	

*For sale by the National Technical Information Service, Springfield, Virginia 22151